The Pennsylvania State University
The Graduate School
Department of Physics

ISOLATED HORIZONS IN NUMERICAL RELATIVITY

A Thesis in
Physics
by
Badri Krishnan

Submitted in Partial Fulfillment
of the Requirements
for the Degree of

Doctor of Philosophy

August 2002

We approve the thesis of Badri Krishnan.

Date of Signature

Abhay Ashtekar Eberly Chair in Physics Thesis Adviser Chair of Committee	
Pablo Laguna Professor of Physics Professor of Astronomy and Astrophysics	
Lee Samuel Finn Professor of Physics	
Steinn Sigurdsson Assistant Professor of Astronomy and Astrophysics	
Jayanth Banavar Professor of Physics Head of the Department of Physics	

Abstract

The isolated horizon framework is applied to numerical relativity. This framework describes black holes which are in equilibrium in a spacetime which is otherwise fully dynamical. We introduce isolated horizons in a way which is directly applicable in numerical evolutions. In particular, we present and numerically implement a coordinate invariant method for calculating the mass and angular momentum of isolated horizons. We also show how isolated horizons can be used to study the local geometry of a black hole and extract invariant gravitational waveforms. We apply some results from the isolated horizon framework to calculate the binding energy between two black holes. This will be useful in comparing different initial data sets which represent similar physical situations. Finally, we also present a method for studying the physics of dynamical black holes. In particular, we derive balance laws relating the flux of matter fields/radiation with the change in the physical parameters of the black hole such as angular momentum and mass.

Table of Contents

List of Tables

List of Figures

Acknowledgments

I would like to thank all the members and visitors of the Center for Gravitational Physics and Geometry and the Center for Gravitational Wave Physics who have made Penn State a great place for doing physics. In particular I thank Chris Beetle, Martin Bojowald, Dan Cartin, Saurya Das, Amit Ghosh, Bruno Hartmann, Sean Hayward, Gaurav Khanna, Pablo Laguna, Jerzy Lewandowski, Keith Lockitch, Hugo Morales, Claudia Moreno, Dario Nunez, Alejandro Perez, Olivier Sarbach, Steinn Sigurdsson, Manuel Tiglio and Jacek Wiśniewski. I am grateful to Karen Brewster and Randi Neshteruk for their very professional help regarding administrative matters.

Thanks to all the people with whom I have had countless discussions and (usually) fruitful collaborations over the past few years: Olaf Dreyer, Sam Finn, David Garrison, Bernard Kelly, Erik Schnetter, Deirdre Shoemaker, Ken Smith, Patrick Sutton, Josh Willis and especially Steve Fairhurst. A special thanks to Piotr Puzynia and Marco Zagermann for many interesting scientific discussions.

My deepest thanks go to my advisor Abhay Ashtekar for his patience, excellent advice and for sharing his knowledge and scientific insights with me.

Most importantly, thanks to my parents and grand-parents for all their love and support over the years.

Chapter 1

Motivation

The last few years have seen many promising developments in simulations of black hole spacetimes in numerical relativity. The stability of numerical codes has seen steadily improving and it quite likely that we will very soon be able to answer important physical questions in regimes where the physical processes are highly dynamical and the gravitational field very strong. However, by its very nature, a numerical simulation of a spacetime is always tied down to a particular choice of coordinates, gauge conditions, dynamical variables etc. and it is often a non-trivial task to extract physics from a numerical evolution. This is especially true in dynamical situations where our intuition gained from idealized solutions involving the Kerr black hole is usually not directly applicable.

Historically, for very good reasons, most attention in mathematical relativity has focussed on idealized situations such as globally stationary spacetimes and has used concepts such as event horizons. This approach has led to many seminal results in black hole physics such as the laws of black hole mechanics, asymptotic properties of spacetimes, the uniqueness theorems etc. However, many of the techniques and results from these studies are not directly applicable to numerical evolutions. For example, consider the commonly used concept of an event horizon. An event horizon is a teleological notion: it can be constructed only after we have full knowledge of the spacetime and very often, due to practical limitations one cannot evolve all the way to future null infinity. It is therefore usually not feasible to find the event horizon numerically; almost all numerical simulations use the notion of apparent horizons which can be located on a single spatial slice. Similarly, the spacetimes we would like to study numerically are not the ones which have stationary or axial Killing vectors. Therefore, the definitions of conserved quantities such as mass and angular momentum in these idealized spacetimes cannot be carried over directly to more general situations. Yet another example is the study of gravitational radiation: the notion of null infinity is ideally suited for analytically studying the gravitational radiation waveforms and physical quantities such as the rate

of energy loss from a system. In numerical simulations, as mentioned earlier, it is usually not feasible evolve all the way to null infinity. Therefore, how should one extract gravitational radiation waveforms etc. invariantly from a completely general numerical evolution?

In order to address these questions, it is desirable to have a framework that combines the properties of apparent horizons with the powerful tools available at infinity. In the regime when the black hole is isolated in an otherwise dynamical spacetime, such a framework now exists in the form of isolated horizons [1, 2, 3, 4, 5]. In numerical simulations of, say, black hole collisions, the black hole would be isolated at early times when the black holes are well separated, or at late times when the final black hole has settled down, but radiation is still present in the spacetime. The aim of this thesis is to introduce the isolated horizon framework in a way that is directly useful in numerical relativity and implement some of the important results of this framework numerically.

An important part of this thesis is the computation of mass (M_Δ) and angular momentum (J_Δ) of an isolated black hole. One way to attribute a mass and an angular momentum to a black hole is to calculate the corresponding ADM quantities at infinity. The main difficulty is that the ADM mass and angular momentum refer to the whole spacetime. In a dynamical situation, such a spacetime will contain gravitational radiation and it is not clear how much of the mass or angular momentum should be attributed to the black hole itself and, if there is more than one black hole, to each individual black hole. Isolated horizons provide a way to identify a black hole quasi-locally, and allow for the calculation of mass and angular momentum. We show how to find isolated horizons numerically, and how to implement the isolated horizon formulae for J_Δ and M_Δ. We will show that one can just use the ADM formula for angular momentum but now applied at the apparent horizon. This is not an assumption, but a rigorous result obtained by calculating the Hamiltonian generating diffeomorphisms which reduce to rotational symmetries on the isolated horizon. This is completely analogous to what is done at infinity to obtain the ADM formulae for mass and angular momentum for asymptotically flat spacetimes. Indeed, the Hamiltonian analysis of isolated horizons is an extension of the ADM formalism to the case where the region of spacetime under consideration has an inner boundary in the form of an isolated horizon. The isolated horizon results for J_Δ and M_Δ are also convenient for practical reasons because their expressions only involve data defined on the apparent horizon. An important ingredient in the formula for J_Δ is an axial symmetry vector on the apparent horizon. Therefore

we also present and implement a numerical method for locating Killing vectors on the horizon.

Isolated horizons can also be used to study the local geometry of a black hole and extract dynamical information from the strong field region. This is done by constructing a preferred local coordinate system and null tetrad in a neighborhood of the horizon. The construction of this coordinate system is analogous to the construction of the Bondi coordinates near null infinity. The preferred null tetrad can be used to compute gravitational waveforms invariantly and it also enables us to compare the results of two different simulations using different coordinate systems, different initial conditions etc. We implement some of these ideas numerically.

Another potential application is in the construction of initial data sets for the binary black hole problem representing astrophysically interesting situations. We would like to model two black holes very far away from each other and having prescribed values of spin, mass, momentum etc. Since the two black holes are isolated, we expect the isolated horizon framework to be well suited to study them.

While isolated horizons have let to very important results in both the classical and quantum aspects of black hole physics, we eventually want to understand black holes in the fully dynamical regime. In particular, we would like to define black hole angular momentum, mass etc. in these situations and also describe how these physical quantities change when matter or radiation falls into the black hole. While this seems like a very difficult problem, it turns out that significant progress can be made by studying the constraint equations on the world tube of apparent horizons. This approach leads to a balance law for the black hole energy in the general case when the horizon has no symmetries, is arbitrarily distorted and arbitrary amounts of matter and radiation are crossing the horizon. We get equally general results for angular momentum except that we need the horizon to be axisymmetric in order to define angular momentum. Unlike in the analysis of isolated horizons, these results are based on geometric identities on the world tube of apparent horizons and not on a Hamiltonian formulation.

The rest of this thesis is organized as follows. Chapter 2 gives the relevant definitions of isolated horizons and describes their geometrical properties. In particular we give the formulae for M_Δ and J_Δ and briefly outline the Hamiltonian analysis used to define them. This chapter is mostly based on [3, 4]. In chapter 3 we first describe how isolated horizons can be identified in a numerical evolution and implement the formulae for M_Δ and J_Δ numerically. The computation of J_Δ requires us to locate a symmetry vector field on the horizon; a method of calculating symmetry vectors is described

and numerically implemented. This chapter is based on work in collaboration with Olaf Dreyer, Eric Schnetter and Deirdre Shoemaker [6]. Chapter 4 implements a method of finding a preferred null normal and a preferred foliation on the horizon. The method of finding the null normal is based on results obtained in [5] and the numerical implementation is in collaboration with Ken Smith. The results regarding the preferred foliations of the horizon are due to Jerzy Lewandowski and Tomasz Pawlowski. Chapter 5 discusses the application of isolated horizon ideas for studying binding energy in initial data using the Brill-Lindquist data as a test case. Chapter 6 is an attempt to study black holes in dynamical situations. The aim of this chapter is to obtain balance equations for the change in angular momentum and energy due to flux of radiation or matter fields across the horizon. Appendix A is a brief summary of the relevant parts of the Newman Penrose formalism; in particular we give the definitions of the curvature scalars and describe their transformation properties under tetrad transformations. Appendix B discusses the location of the apparent horizon in the Brill-Lindquist initial data describing two black holes. We obtain the location of the apparent horizon perturbatively in powers of m/d where m is the mass of the individual black hole(s) and d is the distance between them. This result is used in chapter 5. In appendix C, we give an exact solution found by Ernst describing a black hole immersed in a magnetic field. This example, is used in chapter 3 to demonstrate that the great-circle method of calculating angular momentum is not applicable in general.

Throughout this thesis, the spacetime metric is taken to have signature $(-,+,+,+)$, and we mostly use geometrical units where G and c are equal to unity. We will usually use the abstract index notation, but occasionally, especially for differential forms, the index free notation will also be used. The spacetime manifold will be denoted by $\mathcal{M}$, the Lorentzian spacetime metric by g_{ab} and ∇_a is the derivative operator compatible with g_{ab}. The Riemann tensor ${R_{abc}}^d$ will be defined by the equation $2\nabla_{[a}\nabla_{b]}\alpha_c = {R_{abc}}^d\alpha_d$ where α_a is an arbitrary co-vector. All manifolds and fields will be taken to be smooth.

Chapter 2

Isolated Horizons

This chapter describes the main results of the isolated horizon framework. Section 2.1 gives the basic definition and describes the relation between isolated and apparent horizons; this section is based on [6]. Section 2.2 describes the intrinsic geometry of non-expanding horizons. In particular, it discusses the induced metric, extrinsic curvature, surface gravity etc. of a non-expanding horizon; this section is mostly based on [3]. Section 2.3 describes the additional conditions that must be imposed on non-expanding horizons to study the mechanics of isolated horizons; this section is based on [3, 4, 5]. Finally, section 2.4 uses these additional conditions to define mass and angular momentum for isolated horizons. In this section, only the basic results and conceptual ideas are given; we refer the reader to [2, 3, 4] for details regarding isolated horizon mechanics.

2.1 Non-expanding horizons and apparent horizons

In this section we introduce non-expanding horizons (NEH). In order to motivate the definition from the perspective of numerical relativity, we also describe the close connection between apparent horizons (AH) and non-expanding horizons.

For completeness and to fix notation, let us start by reviewing the definition of apparent horizons. Let N^a be the unit timelike vector field orthogonal to a spatial slice Σ. Given a closed two-surface $S \subset \Sigma$, we have the unique unit outward-pointing spacelike normal R_a which is tangent to Σ. Let $\widetilde{q}_{ab}$ be the induced Riemannian two-metric on S and $\widetilde{\epsilon}_{ab}$ the area two-form on S constructed from $\widetilde{q}_{ab}$. We can construct a convenient basis for performing calculations at points of S in a natural way (see figure 2.1). First, define the outgoing and ingoing null vectors

$$\ell^a := \frac{1}{\sqrt{2}}(T^a + R^a) \quad \text{and} \quad n^a := \frac{1}{\sqrt{2}}(T^a - R^a)\,. \tag{2.1}$$

It is worth noting that any spacelike two-surface S determines uniquely, up to rescalings, two null vectors orthogonal to S. Any other choice of ℓ and n will differ from the one

made in equation (2.1) only by possible rescalings. We tie together the scalings of ℓ and n by requiring $\ell \cdot n = -1$.

Next, given two arbitrarily chosen spacelike orthonormal vectors e_1 and e_2 tangent to S, construct a complex null vector

$$m := \frac{1}{\sqrt{2}}(e_1 + ie_2). \tag{2.2}$$

It satisfies the relations $m \cdot m = 0$, $m \cdot \overline{m} = 1$, $\ell \cdot m = 0$, and $n \cdot m = 0$. Since ℓ and n satisfy $\ell \cdot n = -1$, we see that $(\ell, n, m, \overline{m})$ form a null tetrad at S. This is, of course, only one possible choice of null tetrad, and we must ensure that physical results are independent of this choice. The expansions of ℓ^a and n^a are defined as $\theta_{(\ell)} := \widetilde{q}^{ab}\nabla_a \ell_b$ and $\theta_{(n)} := \widetilde{q}^{ab}\nabla_a n_b$, respectively. Note that in order to find the expansions, we only need derivatives of ℓ and n along S, and there is no need to extend the null tetrad into the full spacetime. However, if in some numerical computations it is necessary to extend the null tetrad smoothly into the full spacetime; all calculations will be insensitive to this extension. The surface S is said to be an apparent horizon if it is the outermost outer-marginally-trapped-surface, i.e. it is the outermost surface on Σ with $\theta_{(\ell)} = 0$ and $\theta_{(n)} < 0$.

Consider now the world tube of apparent horizons H constructed by stacking together the apparent horizons on different spatial slices. As we shall show later in section 3.1, this world tube is generically spacelike; it is null when no matter or radiation is falling into the black hole. At late times, one expects the black hole to reach equilibrium when radiation and matter are no longer crossing the horizon. In this regime, the world tube H will be a null surface, and the two-metric $\widetilde{q}_{ab}$ on the apparent horizon S may now be used to construct a degenerate three-metric q_{ab} on the null surface H. Furthermore, from experience with numerical simulations and also from very general topological censorship results (see e.g. [7]), we know that at late times, the apparent horizons must have spherical topology. Therefore, at late times, the topology of H is $S^2 \times \mathcal{I}$. Finally, in this regime, the outward-normal ℓ constructed in equation (2.1) is a null normal to the world tube H, and most importantly, from the definition of an apparent horizon, the outward normal ℓ is always expansion free.

We will now argue that the isolated horizon framework is ideally suited to describe apparent horizons in the regime when the world tube H is null. For our purposes, the straightforward definition of a *non-expanding horizon* given below shall suffice. To carry out the Hamiltonian analysis in order to define mass and angular momentum, we

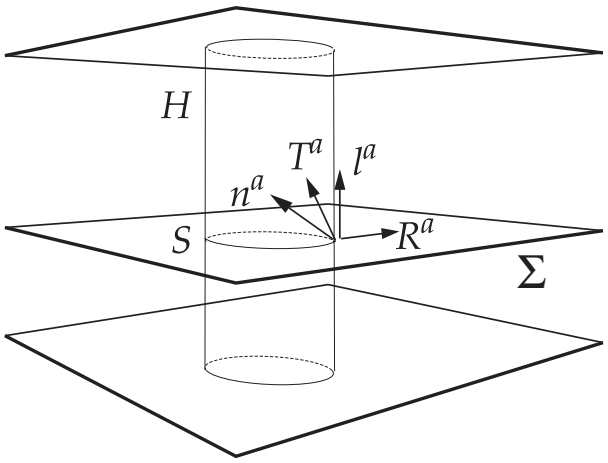

Fig. 2.1. The figure shows an apparent horizon S embedded in a spatial slice Σ. T^a is the unit timelike normal to Σ and R^a is the outward pointing unit spatial normal to S in Σ; ℓ^a and n^a are the outgoing and ingoing null vectors, respectively. The vector m^a (not shown in the figure) is tangent to S. H is the world tube of apparent horizons.

actually need to impose further conditions on non-expanding horizons, which we shall briefly describe towards the end of this section. The formulae for mass and angular momentum make sense even on non-expanding horizons.

Definition: A three dimensional sub-manifold Δ of a space-time $(\mathcal{M}, g_{ab})$ is said to be a non-expanding horizon (NEH) if it satisfies the following conditions:

(i) Δ is topologically $S^2 \times \mathcal{I}$ and null where $\mathcal{I}$ is an interval on the real line;

(ii) The expansion $\theta_{(\ell)} := q^{ab}\nabla_a \ell_b$ of ℓ vanishes on Δ, where ℓ is any null normal to Δ and q_{ab} is the degenerate metric on Δ;

(iii) All equations of motion hold at Δ.

Note that if condition (ii) holds for one null normal ℓ, then it holds for all. We will only consider those null normals which are nowhere vanishing and future directed. We are therefore allowed to rescale ℓ by any positive-definite function. If any matter fields are present with T_{ab} as the stress energy tensor, we also require that $-T^a_b \ell^b$ is future directed and causal for any future directed null normal ℓ. This energy condition is implied e.g. by the null energy condition which is commonly assumed.

Comparing the properties of the world tube H described earlier with conditions (i) and (ii) in the definition, we see that the NEH is precisely what we need to model the physical situation at hand; when the black hole is approximately isolated, the world tube H represents a non-expanding-horizon Δ. The motivation behind the conditions in the definition are thus rather straightforward from the perspective of apparent horizons.

Every spherical cross-section of Δ can be thought of as arising from the intersection of a spatial slice Σ with Δ. Such a cross-section is essentially an apparent horizon, because, as we just saw, the conditions in the above definition capture the essential properties of apparent horizons. A NEH is a notion in the full four-dimensional spacetime and does not refer to a time slicing in any way. If we were to choose another spatial slice $\tilde{\Sigma}$, then the apparent horizon would simply be a different cross-section of Δ. We are assuming here that $\tilde{\Sigma}$ is not very different from Σ, otherwise it might happen that there are no apparent horizons on $\tilde{\Sigma}$, or the apparent horizon may jump discontinuously from Σ to $\tilde{\Sigma}$. We require that the apparent horizons on Σ and $\tilde{\Sigma}$ lie on the same smooth null world-tube of apparent horizons.

There are however two differences between apparent horizons and cross sections of Δ: (i) Apparent horizons are required to be the *outermost* surfaces on a spatial slice

with the afore-mentioned properties. This is not true in general for cross sections of Δ; (ii) Since they are trapped surfaces, apparent horizons also satisfy the condition $\theta_{(n)} < 0$. Though this will most likely be true in actual numerical simulations, it turns out that this condition is not required to study the mechanics of isolated horizons. In fact, there exist exact solutions representing black holes which are isolated horizons but do not satisfy $\theta_{(n)} < 0$, e.g., the distorted black holes studied by Geroch and Hartle [8]. In these solutions the integral of $\theta_{(n)}$ over a cross section of the horizon is still negative even though $\theta_{(n)}$ is not necessarily negative everywhere. In the remainder of this thesis, we shall ignore these caveats and the phrases 'apparent horizon' and 'cross-section of Δ' will be used interchangeably.

2.2 Geometry of a non-expanding horizon

Although the conditions in the definition are quite weak, they have surprisingly rich consequences. While stating the results, it is convenient to use a null-tetrad $(\ell, n, m, \overline{m})$ which is *adapted to the horizon*; this means that ℓ is a (future directed) null normal to Δ. An example of such a null-tetrad is the one constructed in equations (2.1) and (2.2) but there is of course, an infinity of such tetrads. Physical quantities will be independent of which null-tetrad we choose.

2.2.1 Surface gravity and area

Definition of ω_a and surface gravity: Any null normal ℓ is expansion free and by definition. It is also automatically twist free because it is normal to a smooth surface. To show that the shear $\sigma_{(\ell)} := m^a m^b \nabla_a \ell_b$ also vanishes, use the Raychaudhuri equation for ℓ:

$$0 = -\mathcal{L}_\ell \theta_{(\ell)} \triangleq |\sigma_{(\ell)}|^2 + R_{ab}\ell^a\ell^b \tag{2.3}$$

where we have used the fact that ℓ is automatically twist free and the symbol '$\triangleq$' means that the equality holds only at points of Δ. From the energy condition it follows that $R_{ab}\ell^a\ell^b \triangleq 8\pi G T_{ab}\ell^a\ell^b \geq 0$. Since $|\sigma_{(\ell)}|^2$ is also positive, it follows from (2.3) that

$$R_{ab}\ell^a\ell^b = 0 \qquad \text{and} \qquad \sigma_{(\ell)} = 0\,. \tag{2.4}$$

Since ℓ is expansion, shear and twist free, it follows that there must exist a one-form $\omega_a^{(\ell)}$ associated with ℓ such that

$$\nabla_{\underleftarrow{a}} \ell^b \triangleq \omega_a^{(\ell)} \ell^b \tag{2.5}$$

where and arrow under a covariant index indicates the pullback of that index to Δ. Contracting this equation with ℓ^a we see that any null normal ℓ is also geodetic

$$\ell^a \nabla_a \ell^b = \ell^a \omega_a^{(\ell)} \ell^b = \kappa_{(\ell)} \ell^b \tag{2.6}$$

where $\kappa_{(\ell)} := \ell^a \omega_a^{(\ell)}$ is the *surface gravity* of Δ associate with the null normal ℓ. The 1-form ω will play an important role throughout this paper. It has an interesting geometrical interpretation. We can regard ω as a connection on the line bundle $T\Delta^\perp$ over Δ whose fibers are the 1-dimensional null normals to Δ. Under the rescalings $\ell \mapsto \tilde{\ell} = f\ell$, of the null normal ℓ, it transforms via:

$$\omega_a \mapsto \tilde{\omega}_a = \omega_a + \nabla_{\underleftarrow{a}} \ln f. \tag{2.7}$$

and surface gravity transforms as

$$\kappa_{(\ell')} := \ell'^a \omega_a^{(\ell')} = f\kappa_{(\ell)} + \mathcal{L}_\ell f \tag{2.8}$$

From (2.5) we also get

$$\mathcal{L}_\ell q_{ab} \triangleq \underleftarrow{\mathcal{L}_\ell g_{ab}} \triangleq 2\underleftarrow{\nabla_a \ell_b} \triangleq 0\,. \tag{2.9}$$

Thus, every null normal ℓ is a 'Killing field' of the degenerate metric on Δ. Although ℓ is a 'Killing field' of the intrinsic horizon geometry, the space-time metric g_{ab} need *not* admit a Killing field in any neighborhood of Δ. Robinson-Trautman metrics [9] provide explicit examples of this type.

Area two-form and the base space: The base space $\widehat{\Delta}$ associated with a NEH Δ is the space of integral curves of the null normals of Δ. It is obtaining by defining an equivalence relation on Δ which says that two points of Δ belong to the same equivalence class if they lie on the same null geodesic on Δ. We can thus define a projection $\pi : \Delta \to \widehat{\Delta}$ which maps a point on Δ to the geodesic on which it lies (see figure 2.2).

Every vector field X tangent to Δ satisfying $\mathcal{L}_\ell X \triangleq 0$ is projected to a vector $\widehat{X} := \pi_\star(X)$ and every co-vector $\widehat{\eta}$ on $\widehat{\Delta}$ is pulled back to a covector $\eta := \pi^\star(\widehat{\eta})$ which satisfies $\ell^a \eta_a \triangleq 0$ and $\mathcal{L}_\ell \eta \triangleq 0$. Conversely, every covariant tensor $\zeta_{a_1 a_2 \ldots a_n}$ defined

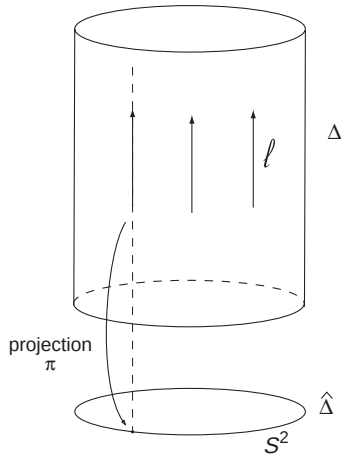

Fig. 2.2. Projective geometry of Δ. The space of integral curves of ℓ is $\widehat{\Delta}$ and π is the projection mapping.

intrinsically on Δ can be projected to yield a tensor on $\widehat{\Delta}$ if and only if the contraction of ℓ^a with any of the indices of $\zeta_{a_1 a_2 \ldots a_n}$ yields zero. There are also certain four-dimensional tensors which can be projected to $\widehat{\Delta}$, but we shall not need them in this thesis.

In particular, the degenerate metric q_{ab} can be projected to yield a non-degenerate Riemannian metric $\hat{q}_{ab}$ on $\widehat{\Delta}$. Associated with $\hat{q}_{ab}$ is a unique area two-form ${}^2\hat{\epsilon}_{ab}$ on $\widehat{\Delta}$ which, when pulled back to Δ gives a two-form ${}^2\epsilon_{ab}$ which satisfies $\ell^a\, {}^2\epsilon_{ab} \triangleq 0$ and $\mathcal{L}_\ell\, {}^2\epsilon_{ab} = 0$. The area of the NEH is then defined to be $A_\Delta := \int_S {}^2\epsilon$ where S is any cross section of Δ. The value of A_Δ is independent of which S we choose.

2.2.2 Derivative operator and extrinsic curvature of Δ

In the study of differential geometry with non-degenerate metrics, one of the basic results is the existence of a unique connection (or equivalently, a derivative operator). On our case, we have a manifold Δ with a degenerate metric q_{ab}. To what extent does q_{ab} fix a derivative operator? To answer this question, let $\mathcal{D}_a$ be a torsion-free derivative operator compatible with q_{ab} : $\mathcal{D}_a q_{bc} \triangleq 0$; let ∂_a be a fiducial torsion-free flat derivative

operator. There must then exist a tensor C^a_{bc} such that for any one-form η_a:

$$D_a\eta_b = \partial_a\eta_b + C^c_{ab}\eta_c\,. \tag{2.10}$$

Let us now try to repeat the standard proof which shows that C^a_{bc} exists and is unique in the non-degenerate case (see e.g. [10]). Since $\mathcal{D}_a$ is compatible with q_{ab}, we get

$$0 = \mathcal{D}_a q_{bc} \triangleq \partial_a q_{bc} + C^d_{ab}q_{cd} + C^d_{ac}q_{bd}\,. \tag{2.11}$$

permuting indices and taking appropriate linear combinations, we get

$$C^d_{ab}q_{dc} \triangleq \frac{1}{2}\left(\partial_c q_{ab} - \partial_a q_{bc} - \partial_b q_{ac}\right)\,. \tag{2.12}$$

Thus we see that q_{ab} uniquely determines $C^d_{ab}q_{dc}$. Since q_{ab} is degenerate with ℓ^a as its degenerate direction, if C^d_{ab} is a solution of (2.12), then so is $C^d_{ab} + \alpha_{ab}\ell^d$ for any symmetric tensor α_{ab}; there are infinitely many derivative operators compatible with q_{ab}. However, q_{ab} does uniquely determine the action of $\mathcal{D}_a$ on any one-form η_a satisfying $\ell^a\eta_a \triangleq 0$.

Another important situation in differential geometry is when a manifold Σ is smoothly embedded in a larger manifold $\mathcal{M}$ with non-degenerate metric g_{ab}. Let γ_{ab} be the non-degenerate induced metric on Σ. The important quantities here are the extrinsic curvature of Σ and the induced derivative operator on Σ. Can we define these quantities for a NEH? To answer this question, let us first review the general procedure for defining these quantities in the non-degenerate case (see e.g. [11]). Let $T(\mathcal{M})$ and $T(\Sigma)$ be the tangent bundles of $\mathcal{M}$ and Σ respectively. The key fact upon which the whole construction depends is that we can perform an orthogonal decomposition

$$T(\mathcal{M}) = N(\Sigma)\oplus T(\Sigma) \qquad \text{and} \qquad N(\Sigma)\cap T(\Sigma) = \{0\}\,, \tag{2.13}$$

where $N(\Sigma)$ is the *normal bundle* of Σ, the sections of which are the vector fields orthogonal to Σ. This is used to uniquely decompose any vector field ξ

$$\xi = \xi^\perp + \xi^\intercal \tag{2.14}$$

where $\xi^\perp$ is perpendicular to Σ and $\xi^\intercal$ is tangential to Σ. Let ∇ be the connection on $\mathcal{M}$ compatible with g_{ab} and let X, Y be vector fields tangential to Σ. We can then

decompose $\nabla_X Y$ using (2.13):

$$\nabla_X Y = (\nabla_X Y)^{\perp} + (\nabla_X Y)^{\mathsf{T}} . \tag{2.15}$$

Define a connection $\mathcal{D}$ on Σ by $\mathcal{D}_X Y := (\nabla_X Y)^{\mathsf{T}}$. It can be easily shown that $\mathcal{D}$ is compatible with γ_{ab} and using the Frobenius theorem, it can also be shown to be torsion free. The second fundamental form $\mathbf{K}$ of Σ is a linear mapping

$$\mathbf{K} : T(\Sigma) \otimes T(\Sigma) \to N(\Sigma) ; \qquad \mathbf{K}(X, Y) = (\nabla_X Y)^{\perp} . \tag{2.16}$$

Using the Frobenius theorem again, it is easy to show that $\mathbf{K}$ is symmetric ($\mathbf{K}(X, Y) = \mathbf{K}(Y, X)$). When the codimension of Σ is unity and if T^a is the unit timelike vector field normal to Σ, then $\mathbf{K}$ defines the extrinsic curvature tensor K by

$$K : T(\Sigma) \otimes T(\Sigma) \to \mathcal{C}^{\infty}(\Sigma) ; \qquad \mathbf{K}(X, Y) = K(X, Y)T \tag{2.17}$$

where $\mathcal{C}^{\infty}(\Sigma)$ is the space of smooth functions on Σ. It is again easy to show that this definition is equivalent to the definition used commonly in the general relativity literature: $K_{ab} = \gamma_a{}^c \gamma_b{}^d \nabla_c T_d$.

Returning now to the case of a NEH, we see that the crucial difference from the non-degenerate case is that the decomposition (2.13) is not valid. In particular, since Δ is a null surface, $N(\Delta) \subset T(\Delta)$; there exist non-zero vectors (the null normals), which are both tangent and perpendicular to Δ. Thus, for a general null surface, we cannot define the extrinsic curvature and the spacetime derivative operator need not induce a well defined derivative operator. In order to define a derivative operator, we have to choose a direction transverse to Δ, i.e. we have to choose a subspace $\tilde{N}_p(\Delta) \subset T_p(\mathcal{M})$ so that we can define a decomposition of the tangent bundle

$$T(\mathcal{M}) = \tilde{N}(\Delta) \oplus T(\Delta) \qquad \text{with} \qquad \tilde{N}(\Delta) \cap T(\Delta) = \{0\} \tag{2.18}$$

where $\tilde{N}(\Delta)$ is a vector bundle, which may be called the *transverse bundle*, the sections of which are vector fields everywhere transverse to Δ. This transverse direction could be chosen, for example, by choosing a foliation of Δ. We can then repeat the procedure described above and construct the induced connection and extrinsic curvature on Δ if we replace the normal bundle by the transverse bundle. For a general null surface, this construction will depend on the transverse distribution that we choose. Fortunately, the

properties of Δ guarantee the existence of a unique derivative operator $\mathcal{D}$ independent of this choice. To prove this, note that the only way the construction can be independent of the choice of $\tilde{N}(\Delta)$ is if $\nabla_X Y$ is always purely tangential to Δ so that there is no need to perform the decomposition using (2.18). From this perspective, for such a surface, since there is no component of $\nabla_X Y$ transverse to Δ, the second fundamental form (2.16) and therefore the extrinsic curvature, will be *identically zero*. The condition for $\mathcal{D}$ to be well defined is therefore

$$0 \triangleq \ell_b \left(X^a \nabla_a Y^b \right) \triangleq -X^a Y^b \nabla_a \ell_b \tag{2.19}$$

where X^a and Y^a are arbitrary vector fields tangent to Δ. This condition is equivalent to saying that any null normal ℓ must be both expansion and shear free. The vanishing of the expansion $\theta_{(\ell)}$ is part of the definition of a NEH and we have already shown that the shear of any null normal vanishes (eqn. (2.4)). Therefore $\mathcal{D}$ is a well defined derivative operator on Δ compatible with q_{ab}.

Another important notion in the study of non-degenerate submanifolds is the *shape operator* also known as the *Weingarten map* which is just the extrinsic curvature with one index raised: $K_a{}^b$. At any point p, it can be viewed as a mapping from the tangent space of Σ to itself and it carries all the information about the embedding of Σ in $\mathcal{M}$. For example, for a surface embedded in flat Euclidean space, its eigenvalues are the principal curvature, its determinant gives the Gauss curvature and its trace is the mean curvature. Can we find an analog of the shape operator for the null surface Δ? As we showed earlier, the extrinsic curvature of Δ is zero. However, by analogy with the non-degenerate case, we might define $\nabla_{\underleftarrow{a}} \ell^b$ as the shape operator of Δ. This will be used later to motivate the definition of a weakly isolated horizon.

It is convenient to express the action of $\mathcal{D}$ using the pullback notation:

$$\mathcal{D}_a X^b \triangleq \nabla_{\underleftarrow{a}} \tilde{X}^b \qquad \text{and} \qquad \mathcal{D}_a \eta_b \triangleq \nabla_{\underleftarrow{a}} \tilde{\eta}_{\underleftarrow{b}} \tag{2.20}$$

where an arrow under a covariant index denotes the pullback of that index to Δ; $\tilde{X}^b$ and $\tilde{\eta}_b$ are arbitrary extensions of X^b and η_b into the full spacetime. Note that $\tilde{X}^b$ is equal to X^b at points of Δ while $\tilde{\eta}_b$ need not be equal to η_b at Δ; only the pullback $\tilde{\eta}_{\underleftarrow{b}}$ is equal to η_b at points of Δ. In this notation it is very easy to see that $\mathcal{D}$ is compatible with q_{ab}

$$\mathcal{D}_a q_{bc} \triangleq \nabla_{\underleftarrow{a}} g_{\underleftarrow{bc}} = 0\,. \tag{2.21}$$

As discussed earlier, the action of $\mathcal{D}$ on a one-form η_a satisfying $\ell^a \eta_a = 0$ is determined by q_{ab}. The spacetime derivative operator ∇ fixes the action of $\mathcal{D}$ on the remaining one-forms. In fact, this extra information in $\mathcal{D}$ which does not come from q_{ab} is present in the one-form ω_a defined in (2.5) because $\mathcal{D}_a \ell^b \triangleq \omega_a \ell^b$.

If η_a is a one-form on Δ which is the pull-back of any one-form $\widehat{\eta}_a$ on the base space $\widehat{\Delta}$, then

$$\mathcal{D}_a \eta_b = \pi^\star \left(\widehat{\mathcal{D}}_a \widehat{\eta}_b \right) \tag{2.22}$$

which shows that $\mathcal{D}_a{}^2 \epsilon_{bc} = 0$.

Consider now a cross section of Δ denoted by S. Let n_a be a one-form (determined upto a scaling) which annihilates all vectors tangent to S. Since the null-normals give a preferred direction transverse to S, we can define the induced derivative operator and extrinsic curvature of $S \hookrightarrow \Delta$. Choose a null normal ℓ^a and fix the one-form n_a by requiring $\ell^a n_a \triangleq -1$. Then we can define a projection operator for S: $q_a{}^b = \delta^b_a + n_a \ell^b$ which can be used to project all tensors intrinsic to Δ onto S. The derivative operator $\widetilde{\mathcal{D}}$ on S is then the part of $\mathcal{D}$ determined by q_{ab} and the extrinsic curvature is $\widetilde{S}_{ab} := q_a{}^c q_b{}^d \mathcal{D}_c n_d$ which is the part of $\mathcal{D}$ not determined by q_{ab}.

2.2.3 Conditions on the Ricci and Weyl tensors

The second equation in (2.4) implies that the vector $-R^a{}_b \ell^b$ is tangential to Δ. The energy condition and the field equations imply this vector must also be future causal. This means that $R^a{}_b \ell^b$ must be proportional to ℓ^a and hence, $R_{\underleftarrow{a}\, b} \ell^b = 0$. In the Newman-Penrose formalism (see appendix A) this condition translates to:

$$\Phi_{00} \triangleq 0 \quad \text{and} \quad \Phi_{01} = \overline{\Phi}_{10} \triangleq 0. \tag{2.23}$$

Since this statement is equivalent to $R_{\underleftarrow{a}\, b} \ell^b = 0$, it is gauge invariant, i.e. it does not depend upon the specific choice of null normal ℓ and m.

To obtain properties of the Weyl tensor C_{abcd} at Δ, let us begin with the definition of the Riemann tensor, $[\nabla_a \nabla_b - \nabla_b \nabla_a] X^c = -2 R_{abd}{}^c X^d$. If we set $X^c = \ell^c$ and pull back the indices a and b, then using (2.5), we obtain:

$$[\mathcal{D}_a \omega_b - \mathcal{D}_b \omega_a] \ell^c \triangleq -2 R_{\underleftarrow{abd}}{}^c \ell^d \triangleq -2 C_{\underleftarrow{abd}}{}^c \ell^d \,. \tag{2.24}$$

The last equality follows from $R_{\underset{\leftarrow}{ab}}\ell^b \triangleq 0$. Thus, if v is any 1-form on Δ satisfying $v \cdot \ell \triangleq 0$, contracting the previous equation with v_c we get

$$C_{\underset{\leftarrow}{abd}}{}^c v_c \ell^d \triangleq 0\,.$$

Let us choose a null tetrad and set v to be m or $\overline{m}$. Then

$$\Psi_0 \triangleq 0 \qquad \text{and} \qquad \Psi_1 \triangleq 0\,, \tag{2.25}$$

where we have used the trace-free property of the Weyl tensor in the second equation (see appendix A for the definitions of Ψ_i $(i = 0 \ldots 4)$). It is also clear that equations (2.25) are independent of which null normal ℓ, and vector fields m and $\overline{m}$ we choose to construct the null tetrad; equation (2.25) is gauge invariant.

There is also an important relation between the one-form ω_a defined in (2.5) and the imaginary part of Ψ_2. To show this, contract (2.24) with n_c and use $\ell^a n_a = -1$. Then we have:

$$2\mathcal{D}_{[a}\omega_{b]} \triangleq C_{\underset{\leftarrow}{abd}}{}^c \ell^d n_c \triangleq C_{\underset{\leftarrow}{abcd}} \ell^c n^d\,. \tag{2.26}$$

Expanding the Weyl tensor in terms of the Ψ's, one obtains

$$\begin{aligned} C_{abcd}\ell^c n^d \;\triangleq\; & 4(\mathrm{Re}\,[\Psi_2])n_{[a}l_{b]} + 2\Psi_3 \ell_{[a}m_{b]} + 2\overline{\Psi}_3 \ell_{[a}\overline{m}_{b]} \\ & -2\overline{\Psi}_1 n_{[a}m_{b]} - 2\Psi_1 n_{[a}\overline{m}_{b]} + 4i(\mathrm{Im}\,[\Psi_2])m_{[a}\overline{m}_{b]}\,. \end{aligned} \tag{2.27}$$

Substituting this expression into (2.26), pulling back on the two free indices and taking into account (2.25) we obtain

$$d\omega \triangleq 2(\mathrm{Im}\,[\Psi_2])\,{}^2\epsilon\,. \tag{2.28}$$

This relation will play an important role in what follows. Note that, because Ψ_0 and Ψ_1 vanish on Δ, Ψ_2 is gauge invariant.

The gauge freedom we are concerned with here is the choice of null tetrads adapted to Δ. The allowed gauge transformations relating different choices are null rotations about ℓ:

$$\begin{aligned} \ell &\;\to\; \ell \\ m &\;\to\; m + \overline{c}\ell \\ n &\;\to\; n + cm + \overline{cm} + c\overline{c}\ell \end{aligned} \tag{2.29}$$

and spin-boost transformations:

$$\begin{aligned} \ell &\rightarrow A\ell \\ n &\rightarrow A^{-1}n \\ m &\rightarrow e^{2i\theta}m \end{aligned} \tag{2.30}$$

Here c, A and θ are arbitrary smooth functions on Δ. It turns out that Ψ_2 is always invariant under spin-boost transformations; under null rotations, it transforms as (see appendix A)

$$\Psi_2 \rightarrow \Psi_2 + 2c\Psi_1 + c^2\Psi_0\,. \tag{2.31}$$

Since Ψ_0 and Ψ_1 vanish at Δ, we see that Ψ_2 is in fact gauge invariant at the horizon: it does not depend on the choice of null tetrad as long as ℓ is one of the null generators of Δ. This property is important because it tells us that the value of Ψ_2 at the horizon does not depend on how we choose to foliate our spacetime. A different spatial slice $\tilde{\Sigma}$ will lead to a different $\tilde{\ell}$, $\tilde{n}$ and $\tilde{m}$. The two null tetrads will be related by a combination of the following transformations: a null-rotation about ℓ, a spin-boost transformation, or a multiplication of m by a phase. Whichever null-tetrad we use to calculate Ψ_2, we will get the same result. As we shall see, it is the imaginary part of Ψ_2 which is physically interesting for our purposes.

2.3 Weakly-Isolated and Isolated Horizons

As we have seen, the notion of non-expanding horizons describes the late time behavior of apparent horizons. However, in order to define the mass M_Δ and angular momentum J_Δ of Δ, one needs to go beyond this definition and introduce additional structures on the horizon. This is done via the definitions of *weakly isolated horizons* and *isolated horizons* [3, 4]. The Hamiltonian analysis which leads to the definitions of mass and angular momentum requires this extra structure. Fortunately, it turns out that the *formulae* for M_Δ and J_Δ do not depend on this extra structure and make sense even on non-expanding horizons.

In a NEH, the intrinsic metric q_{ab} is time independent since $\mathcal{L}_\ell q_{ab} \triangleq 0$. However, there is no restriction on the time derivatives of the extrinsic curvature of Δ or the intrinsic connection on Δ (by 'time derivative' we mean derivative along ℓ). Since Δ is a null surface, there is no natural notion of extrinsic curvature (though, as discussed in the previous section, for any given choice of the transverse bundle, the extrinsic curvature

vanishes identically). The closest thing to extrinsic curvature is the tensor $K_a{}^b$ defined via $K_a{}^b \triangleq \nabla_{\underleftarrow{a}} \ell^b$ for any t^a tangent to Δ. This tensor is known in the mathematics literature as the Weingarten map as discussed in the previous section; we immediately obtain $K_a{}^b \triangleq \omega_a \ell^b$. This implies that requiring $K_a{}^b$ to be time independent is equivalent to requiring $\mathcal{L}_\ell \omega_a \triangleq 0$. However, because of the transformation property of ω_a (see equation (2.7)), it is clear that this equation is not meaningful if all rescalings of ℓ are allowed. Note however that if we restrict ourselves to rescalings that are constant on the horizon, then ω_a is invariant. We thus need to restrict ourselves to an equivalence class of null normals $[\ell]$ the members of which are related to each other by a constant, positive non-zero rescaling. We can then associate a unique ω_a with $[\ell]$. The equation $\mathcal{L}_\ell \omega_a \triangleq 0$ is now perfectly meaningful if ℓ is a member of $[\ell]$ and we can make the following definition of a weakly isolated horizon (WIH)

Definition 2: A weakly isolated horizon $(\Delta, [\ell])$ consists of a non-expanding horizon Δ, equipped with an equivalence class $[\ell]$ of null normals to it satisfying

$$\mathcal{L}_\ell \omega \triangleq 0 \text{ for all } \ell \in [\ell]. \tag{2.32}$$

Strictly speaking, we should use the symbol $\omega_a^{(\ell)}$ instead of ω_a but this should not lead to any confusion because, when dealing with a WIH, we shall always use the ω_a associated with $[\ell]$. Given a NEH, we can always find such an equivalence class (as we shall see below, this equivalence class however, is not unique). Thus every NEH can be turned into a weakly isolated horizon. Fortunately, for numerical applications, the Hamiltonian analysis of weakly isolated horizons leads to formulae for mass and angular momentum and as we shall see in section 2.4, these formulae are insensitive to arbitrary rescalings of ℓ and thus they make sense even for non-expanding horizons.

The condition (2.32) is equivalent to the zeroth law of black hole mechanics which says that the surface gravity $\kappa_{(\ell)} := \ell \cdot \omega$ of a black hole is constant:

$$0 = \mathcal{L}_\ell \omega = \ell \cdot d\omega + d\,(\ell \cdot \omega) = d\kappa_{(\ell)} \tag{2.33}$$

where we have used (2.28) and $\ell \cdot {}^2\epsilon \triangleq 0$. Let us now determine the rescaling freedom in ℓ if the surface gravity is required to be constant. Start with the transformation law for surface gravity (2.8). For any ℓ, we can simply solve for f by requiring that $\kappa_{(\ell')}$ be constant on Δ. The solution is not unique. If $\kappa_{(\ell)}$ is constant, given any non-zero

function g satisfying $\mathcal{L}_\ell g \triangleq 0$ and a constant κ', let us set

$$f \triangleq g\, e^{-\kappa_{(\ell)}\, v} + \frac{\kappa'}{\kappa_{(\ell)}} \tag{2.34}$$

where v satisfies $\mathcal{L}_\ell v \triangleq 1$. Then, we obtain an $\ell' \notin [\ell]$ for which $\kappa_{(\ell')} \triangleq \kappa'$. This is the only freedom if both $\kappa_{(\ell)}$ and $\kappa_{(\ell')}$ are to be constant. Thus, each non-expanding horizon gives rise to an infinite family of weakly isolated horizons. More properties of weakly isolated horiozns are given in section 4.2.

We can introduce an even stronger definition. A weakly isolated horizon requires that ω_a be time independent. As mentioned earlier, ω_a can also be regarded as a component of the intrinsic connection D_a induced on Δ by the four dimensional connection ∇_a compatible with the four-metric. However, ω_a is just one component of D_a. In an *isolated horizon* (IH), we require that *all* components of D_a are time independent
Definition 3: An isolated horizon is a weakly isolated horizon $(\Delta, [\ell])$ such that

$$[\mathcal{L}_\ell, \mathcal{D}] \triangleq 0 \tag{2.35}$$

Generically, it turns out that this condition selects a preferred equivalence class $[\ell]$ from among the infinitely many equivalence classes for which $(\Delta, [\ell])$ is a WIH. In fact, it is also possible, though unlikely, that a horizon could be a WIH without being an isolated horizon.

2.4 Mass and Angular Momentum

In this section we discuss the formulae for mass and angular momentum of a WIH. We shall focus on vacuum spacetimes only. The detailed derivations of the results and inclusion of matter fields can be found in [3, 4].

2.4.1 Phase space and symplectic structure

In this thesis, we use a Hamiltonian framework to calculate conserved quantities such as angular momentum and mass. We therefore begin by describing the phase space we are interested in. Let $\mathcal{M}$ be the region of spacetime that we are interested in. The boundary of $\mathcal{M}$ consists of four components: the timelike cylinder τ_∞ at spatial infinity, two spacelike surfaces $M^\pm$ which are the future and past boundaries of $\mathcal{M}$ and and inner

boundary Δ which is a weakly isolated horizon with a preferred class of null normals $[\ell]$ (see figure (2.3)). The two spheres $S^{\pm}$ are the intersections of $M^{\pm}$ with Δ. We

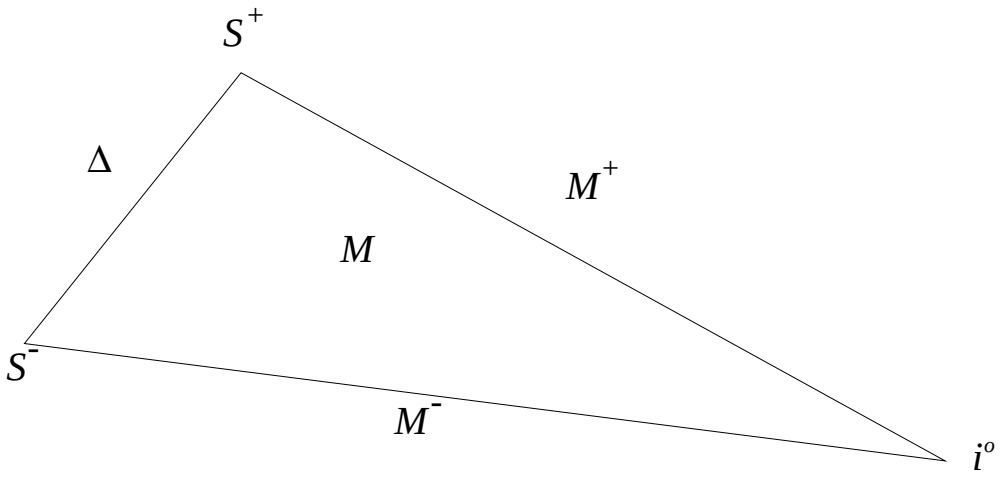

Fig. 2.3. The region of space-time $\mathcal{M}$ under consideration has an internal boundary Δ and is bounded by two partial Cauchy surfaces $M^{\pm}$ which intersect Δ in the 2-spheres $S^{\pm}$ and extend to spatial infinity i^o.

shall use a first order formalism in which the fundamental fields are the gravitational connection ${A_{aI}}^J$ and a tetrad e_a^I which satisfy appropriate boundary conditions (see [12] for a formulation in terms of metrics and extrinsic curvature). The lowercase latin indices refer to the spacetime wnd the uppercase letters refer to a fixed internal four dimensional Lorentzian vector space with internal metric η_{IJ} with signature $(-,+,+,+)$. A Lorentz connection ${A_{aI}}^J$ defines a derivative operator acting on internal indices

$$D_a k_I := \partial_a k_I + {A_{aI}}^J k_J \tag{2.36}$$

where ∂_a is an arbitrary flat fiducial derivative operator.

Fix a preferred internal null tetrad $(\ell^I, n^I, m^I, \overline{m}^I)$ at Δ. The allowed field configurations $({A_{aI}}^J, e_a^I)$ are those which satisfy the appropriate fall-off conditions at infinity

to ensure asymptotic flatness; and at Δ are such that (i) $\ell^a = \ell^I e^a_I$ is a member of the preferred equivalence class $[\ell]$ fixed at Δ and (ii) (Δ, ℓ) is a WIH.

It turns out (see [3] for details) that due to the zeroth law, the standard gravitational action is a viable action even in the presence of the internal boundary Δ:

$$S(e,A) = -\frac{1}{16\pi G}\int_{\mathcal{M}} \Sigma^{IJ} \wedge F_{IJ} + \frac{1}{16\pi G}\int_{\tau_\infty} \Sigma^{IJ} \wedge A_{IJ} \tag{2.37}$$

where

$$\Sigma_{IJ} := \frac{1}{2}\epsilon_{IJKL} e^K \wedge e^L \tag{2.38}$$

and

$$F_I{}^J = dA_I{}^J + A_I{}^K \wedge A_K{}^J \tag{2.39}$$

is the curvature of the derivative operator D_a.

Our phase space Γ, known as the covariant phase space, is the set of solutions to the field equations satisfying the boundary conditions specified above.

The symplectic structure is obtained by second variations of the action and leads to the following expression

$$\begin{aligned}\Omega\,(\delta_1, \delta_2) = \quad & -\frac{1}{16\pi G}\int_M [\delta_1\Sigma^{IJ} \wedge \delta_2 A_{IJ} - \delta_2\Sigma^{IJ} \wedge \delta_1 A_{IJ}] \\ & +\frac{1}{8\pi G}\oint_S [\delta_1({}^2\epsilon)\,\delta_2\psi - \delta_2({}^2\epsilon)\,\delta_1\psi]\end{aligned}$$

where δ_1 and δ_2 are tangent vectors to Γ (they are variations of the fields which preserve the boundary conditions and the field equations), M is a partial Cauchy surface in $\mathcal{M}$, and the function ψ is defined via the conditions

$$\mathcal{L}_\ell \psi \triangleq \kappa_{(\ell)} \qquad \text{and} \qquad \psi|_{S^-} = 0\,. \tag{2.40}$$

The field ψ is introduced to make the symplectic structure independent of which partial Cauchy surface M we choose to integrate over.

2.4.2 Angular Momentum

Physical observables and conserved quantities such as energy and angular momentum are usually associated with symmetries. Energy is the generator of time translations and angular momentum is the generator of spatial rotations. In the present case, using

the symplectic structure, we can explicitly calculate the generators of the appropriate symmetries. For general relativity, due to general covariance, we expect that the Hamiltonians which generate time translations and spatial rotations can be expressed as surface integrals; the volume integrals over the Cauchy surface M will vanish if the constraints are satisfied. In the present case, the surfaces we are concerned with are the sphere at infinity and the section of the horizon $S = M \cap \Delta$. Thus the Hamiltonians will consist of two terms: a term at infinity and a term at the horizon. The terms at infinity will reproduce the ADM formulae for energy and angular momentum. The terms at the horizon will define the energy and angular momentum of the weakly isolated horizon.

Let us begin with angular momentum (see [4] for details). We want to find the Hamiltonian which generates motion along a rotational vector field ϕ^a defined everywhere in $\mathcal{M}$. In other words, we want to find a phase space function H_ϕ such that Hamilton's equation is satisfied:

$$\delta H_\phi = \Omega(\delta, \delta_\phi)\,. \tag{2.41}$$

Here δ_ϕ is the infinitesimal variation associated with diffeomorphisms generated by ϕ^a and δ is an arbitrary variation in the phase space. What boundary conditions must we impose on ϕ^a so that we have a well defined Hamiltonian? At infinity, it must approach a fixed rotational Killing vector of the flat background metric at infinity. The KVF at infinity must be fixed for all asymptotically flat spacetimes so that we can meaningfully compare angular momentum along the same axis for different spacetimes.

On the horizon however, there is no fixed metric. In general, there need not even exist any rotational symmetry vectors on the horizon. We will fix a rotational vector field φ^a on the inner boundary Δ satisfying

1. $[\varphi, \ell] \triangleq 0$ for every $\ell \in [\ell]$,
2. φ^a vanishes on exactly two generators of Δ and
3. φ^a has closed circular orbits of affine length 2π.

Our phase space will consist of only those spacetimes for which φ^a is a rotational symmetry of the WIH $(\Delta, [\ell])$ (see [4] for a general discussion and classification of the symmetries of weakly isolated horizons). This means that φ^a must preserve the equivalence class $[\ell]$, the connection one-form ω_a and the metric q_{ab}:

$$\mathcal{L}_\varphi \ell \in [\ell]\,, \qquad \mathcal{L}_\varphi q_{ab} = 0\,, \qquad \mathcal{L}_\varphi \omega_a = 0\,. \tag{2.42}$$

A WIH $(\Delta, [\ell])$ with such a symmetry vector field will be denoted $(\Delta, [\ell], \varphi)$.

Our phase space Γ_φ is a submanifold of the covariant phase space Γ and consists of solutions to the field equations for which the inner boundary Δ is a WIH with a fixed axial symmetry φ^a. A direct calculation [4] leads to the following result

$$\delta H_\phi = \Omega(\delta, \delta_\phi) = -\frac{1}{8\pi G} \oint_S \delta \left[\left(\varphi^a \omega_a\right)^2 \epsilon \right] + \oint_{S_\infty} (\ldots) \tag{2.43}$$

where S_∞ is the sphere at infinity. As expected, the expression for δH_ϕ consists of two terms: a term at the horizon and a term at infinity. The term at infinity turns out to be the familiar ADM angular momentum and we define the angular momentum of the horizon to be the term at the horizon. This leads to the following expression for the horizon angular momentum

$$J_\Delta = -\frac{1}{8\pi} \oint_S (\omega_a \varphi^a)\, \mathrm{d}^2V = -\frac{1}{4\pi} \oint_S f \mathrm{Im}\left[\Psi_2\right]\, \mathrm{d}^2V, \tag{2.44}$$

where S is the apparent horizon and the function f is related to φ^a by $\partial_a f = \epsilon_{ba}\varphi^b$. In the second equality, we have used equation (2.28) and an integration by parts. Since Ψ_2 is gauge invariant, so is the angular momentum, and in particular, it does not depend on the scaling of ℓ and it thus makes sense even on a NEH. If, in a neighborhood of Δ, there was a spacetime rotational Killing vector ϕ^a which approaches φ^a at Δ, then the above formula for J_Δ would be equal to the Komar integral calculated for ϕ^a [4]. However, the formula in equation (2.44) is more general. As a practical matter, even if there were a Killing vector in the neighborhood of Δ, it is easier to use (2.44) rather than the Komar integral since that would require us to find the Killing vector in the full four-dimensional spacetime. It is also worth mentioning that if the vector field φ^a is not a symmetry of Δ but is an arbitrary vector field tangent to S, then J_Δ is still the Hamiltonian generating diffeomorphisms along φ^a. But in this case, there would be no reason to identify J_Δ with the angular momentum since conserved quantities such as mass and angular momentum are always associated with symmetries. However, the existence of the axial symmetry is the least that must be true if the horizon is to be close to Kerr in any sense. Note that angular momentum is a coordinate independent quantity; even if we use corotating coordinates to describe the black hole, the black hole still has the same angular momentum.

We want to apply the formula for J_Δ in a numerical simulation which evolves quantities such as the three-metric and extrinsic curvature defined on spatial surfaces.

Let Σ be one such spatial slice and let $S = \Delta \cap \Sigma$ be the relevant cross-section of Δ. Let us choose a ℓ^a for which surface gravity is constant and let n_a be the one-form orthogonal to S which satisfies $\ell^a n_a \triangleq -1$. We would like all our calculations to be based only on quantities defined on S. Recall that the vector field φ^a appearing in the formula for J_Δ is a *fixed* vector field on Δ. This was necessary for carrying out the Hamiltonian analysis. Since S is essentially an arbitrary cross-section of Δ, the fixed φ^a need not be tangent to S. However, the component of φ^a tangent to S defined by $\tilde{\varphi}^a := \varphi^a + (n_b \varphi^b)\ell^a$ is a Killing vector of the two-metric $\tilde{q}_{ab}$ induced on S. We could use $\tilde{\varphi}^a$ to calculate J_Δ but if we had a different foliation of Δ, then we would have a different cross-section S' which would give a different $\tilde{\varphi}'^a$. It is quite easy to see that J_Δ is independent of which $\tilde{\varphi}^a$ we use. Let S be given by $v = f(\theta, \phi)$ where (v, θ, ϕ) are coordinates on Δ; v is the affine parameter along ℓ. Then

$$n = -dv + df\,, \qquad \ell = \partial_v \tag{2.45}$$

and

$$\oint_S \left(\tilde{\varphi}^a \omega_a\right)\ {}^2\epsilon - \oint_S \left(\varphi^a \omega_a\right)\ {}^2\epsilon \triangleq \kappa_{(\ell)} \oint_S \left(\mathcal{L}_{\tilde{\varphi}} f\right)\ {}^2\epsilon \triangleq 0\,. \tag{2.46}$$

Thus in a given numerical simulation, we only need to find the symmetry vector $\tilde{\varphi}^a$ tangent to S. In the rest of this thesis, we shall therefore drop the distinction between φ^a and $\tilde{\varphi}^a$ and refer to the symmetry vector on S by φ^a.

We now describe a form of equation (2.44) which is much better suited for calculating J_Δ numerically. From equation (2.5), which is the defining equation for ω_a, we get

$$t^a \omega_a \triangleq -n_b t^a \nabla_a \ell^b \triangleq \ell^b t^a \nabla_a n_b \tag{2.47}$$

where t^a is any vector tangent to Δ. Assume that we have found the symmetry vector field φ^a on the horizon (the method we use for finding φ^a is described below). From equation (2.44), we are eventually interested in calculating $\varphi^a \omega_a$; since φ^a is tangent to Δ, setting $t^a = \varphi^a$ we get

$$\begin{aligned}
\varphi^a \omega_a &\triangleq \varphi^a \ell^b \nabla_a n_b = \frac{1}{2}\varphi^a (T^b + R^b)\nabla_a (T_b - R_b) \\
&\triangleq \frac{1}{2}\varphi^a (T^b \nabla_a T_b - T^b \nabla_a R_b + R^b \nabla_a T_b - R^b \nabla_a R_b) \\
&\triangleq -\varphi^a R^b \nabla_a T_b \triangleq -\varphi^a R^b K_{ab}
\end{aligned}$$

where we have used equation (2.1) along with the fact that T^a and R^a are orthonormal. In the last step, the definition of extrinsic curvature $K_{ab} = \gamma_a{}^c \gamma_b{}^d \nabla_c T_d$ has been used where $\gamma_{ab} = g_{ab} + T_a T_b$ is the three-metric on the spatial slice Σ. We have thus reduced the calculation of $\varphi^a \omega_a$ to finding a single component of the extrinsic curvature. The integration of this scalar over the apparent horizon yields the angular momentum:

$$J_\Delta = -\frac{1}{8\pi} \oint_S (\varphi^a R^b K_{ab}) \, \mathrm{d}^2 V \, . \tag{2.48}$$

This is our final formula for the angular momentum. This formula is remarkably similar to the formula for the ADM angular momentum computed at spatial infinity:

$$\begin{aligned} J^\phi_{ADM} &= \frac{1}{8\pi} \oint_{S_\infty} (K_{ab} - \gamma_{ab} K) \phi^a \, \mathrm{d}^2 S^b \\ &= \frac{1}{8\pi} \oint_{S_\infty} K_{ab} \, \phi^a \, \mathrm{d}^2 S^b \, . \end{aligned} \tag{2.49}$$

The $\gamma_{ab} K$ term does not contribute because ϕ^a is tangent to S_∞, which is the sphere at spatial infinity. Since the metric on S_∞ is just the standard two-sphere metric, we have no difficulty in choosing a ϕ^a and we can calculate J_{ADM} about any axis. In contrast, since the metric on the apparent horizon S is distorted, finding ϕ^a is more complicated. Finally, as mentioned earlier, the similarity between equations (2.48) and (2.49) is not surprising because both quantities are surface terms of Hamiltonians generating diffeomorphisms along the appropriate rotational symmetry vector fields; J_Δ is the surface term at the inner boundary while J_{ADM} is the surface term at infinity.

2.4.3 Energy and mass

Conceptually, the calculation of the energy of a WIH is similar to the calculation of angular momentum. We need to find the generator of diffeomorphisms along a time evolution vector field t^a. At infinity, t^a must approach a time translation vector field. At the horizon, we assume that

$$t^a \triangleq A_{(\ell,t)} \ell^a - \Omega_{(t)} \varphi^a \tag{2.50}$$

where $A_{(\ell,t)}$ and $\Omega_{(t)}$ are constants on Δ. Unlike for angular momentum where we required that ϕ^a approach a *fixed* rotational vector φ^a on Δ, in this case t^a is not fixed

on Δ; the constants $A_{(\ell,t)}$ and $\Omega_{(t)}$ may depend on the dynamical fields $({A_{aI}}^I, e^I_a)$; they are functions on phase space. In the terminology of numerical relativity, t^a, unlike φ^a, is a *live* vector field.

Now,using the symplectic structure, we wish to calculate the one-form on phase space defined by

$$X^t(\delta) := \Omega(\delta, \delta_t) \tag{2.51}$$

where δ is an arbitrary variation in phase space (or equivalently a tangent vector to the phase space Γ_φ) and δ_t is the variation due to diffeomorphisms along t^a. Once again, $X^t(\delta)$ will consist of a surface term at infinity and a surface term at the horizon. A direct calculation yields

$$X^t(\delta) = -\frac{\kappa_{(t)}}{8\pi G}\delta A_\Delta - \Omega_{(t)}\delta J_\Delta + \delta E^t_{\rm ADM} \tag{2.52}$$

where $\kappa_{(t)} := A_{(\ell,t)}\ell^a\omega_a$ is the surface gravity associated with the restriction of t^a to Δ, A_Δ is the area of Δ and $E^t_{\rm ADM}$ is the ADM energy associated with t^a. The first two terms in the RHS of this equation are associated with the horizon while the $E^t_{\rm ADM}$ term is associated with an integral at infinity. We would like to say that the terms at the horizon give the energy of the WIH while the term at infinity gives the ADM energy. However, at this point, we see an important difference from the angular momentum calculation: the right hand side of equation (2.43) is an exact variation which means that H^ϕ is well defined. However, in equation (2.52), it is not guaranteed that the right hand side is an exact variation; in other words, δ_t need not be a Hamiltonian vector field in phase space. We want to look for a function on phase space E^t_Δ (which will be called the energy of the WIH) satisfying

$$\delta E^t_\Delta = \frac{\kappa_{(t)}}{8\pi G}\delta A_\Delta + \Omega_{(t)}\delta J_\Delta\,. \tag{2.53}$$

To study the existence of E^t_Δ, note that quantities such as A_Δ, J_δ and other geometrical quantities characterizing e.g. the distortion of the horizon etc. can be used as coordinates in phase space. The condition for the existence of E^t_Δ is the integrability condition

$$\frac{\partial\kappa_{(t)}}{\partial J_\Delta} = 8\pi G\frac{\partial\Omega_{(t)}}{\partial A_\Delta}\ . \tag{2.54}$$

Equations (2.53) and (2.52) tell us that among the infinite number of coordinates in phase space, E^t_Δ,$\kappa_{(t)}$ and $\Omega_{(t)}$ can depend only on A_Δ and J_Δ. This is a restriction

on the time evolution vector field t^a. Such a vector field t^a for which E^t_Δ exists will be called a *permissible* time evolution vector field. It is interesting to note that equation (2.53) is just the first law of black hole mechanics for E^t_Δ. Therefore, t^a is permissible if and only if the first law holds.

Each permissible live t^a defines a horizon energy E^t_Δ. The same thing is true at infinity. However, at infinity, due to the presence of a universal flat metric, we can fix a preferred time translation vector field t^a_0 and use it to define a preferred ADM energy which is then called the ADM mass of the spacetime. At the horizon we only have a equivalence class $[\ell]$ and there is apriori no reason for t^a to be equal to some fixed vector field at the horizon. Nevertheless, one way to fix a value of E^t_Δ is by choosing a suitably regular function $\kappa_0(A_\Delta, J_\Delta)$ and requiring that the surface gravity $\kappa_{(t)}$ be equal to κ_0 for all spacetimes under consideration. We can then solve equation (2.54) for $\Omega_{(t)}$ and thereby uniquely fix the vector field t^a at Δ [5]. Then E^t_Δ will be uniquely determined upto addition of a constant in phase space because eqn. (2.53) only determines δE^t_Δ and not E^t_Δ itself. By equation this constant must be zero because there is no energy scale that one can construct from G and c alone [2]. By this procedure, given $\kappa_0(A_\Delta, J_\Delta)$, we can find E^t_Δ. It is natural to choose κ_0 to have the same dependence on area and angular momentum as in the Kerr family:

$$\kappa_0(A_\Delta, J_\Delta) = \frac{R^4_\Delta - 4J^2_\Delta}{2R^3_\Delta \sqrt{R^4_\Delta + 4J^2_\Delta}}\,. \tag{2.55}$$

With this choice of surface gravity, we get a unique energy E^t_Δ. The resulting function E^t_Δ will be called the mass of the WIH and will be denoted by M_Δ. It will have the same dependence on the area and spin as in the Kerr solutions:

$$M_\Delta = \frac{1}{2R_\Delta}\sqrt{R^4_\Delta + 4J^2_\Delta} \tag{2.56}$$

where R_Δ is the area radius of the horizon: $R_\Delta = (A_\Delta/4\pi)^{1/2}$. Note that even though we have used properties of the Kerr solutions to fix this mass, this formula is valid for *all* vacuum spacetimes which admit an axi-symmetric WIH as an inner boundary. The Kerr black holes have been used as reference solutions to obtain this result.

Under some physically reasonable assumptions on fields near future time-like infinity (i^+), one can show that $M_\Delta - M_{ADM}$ is equal to the energy radiated across future null-infinity if the isolated horizon extends all the way to i^+ [2]. Thus, M_Δ is the

mass left over after all the gravitational radiation has left the system. This lends further support for identifying M_Δ with the mass of the black hole.

Chapter 3

Numerical computation of M_Δ and J_Δ

In this chapter we numerically implement the formulae for M_Δ (equation (2.56)) and J_Δ (equation (2.48)) described in the previous chapter. This chapter is almost entirely based on [6].

To calculate J_Δ and M_Δ in a typical numerical evolution, we must go through the following steps:

1. Find the world tube H of apparent horizons;
2. Check that H is a null surface;
3. If H is indeed null, then find the symmetry vector φ^a on an apparent horizon S and
4. Calculate the integral in equation (2.48) to calculate J_Δ and use it to calculate M_Δ from (2.56).

In the first step, to find H, we need to find apparent horizons on each spatial slice using an apparent horizon tracker. For the purposes of this thesis, we shall assume that this has been done and that we know the location of the AH, the two-metric on the AH, the extrinsic curvature interpolated to the location of the AH and the outward normal R^a.

If steps 2 and 3 have been carried out, then the final step is quite easy. The implementation of step 2 is carried out in section 3.1 and section 3.2 deals with step 3.

3.1 Isolated horizons and trapping horizons

Our strategy to find non-expanding horizons is to locate apparent horizons on each spatial slice and then to check whether the world tube H obtained by stacking these horizons together is a NEH. What remains to be checked is whether the tube is a null surface. By definition, a surface is null if the metric h_{ab} induced on this surface has a degenerate direction, i.e. if there exists a vector X^a tangent to H such that $h_{ab}X^b = 0$; therefore, one possible method to check whether H is isolated is to construct the induced metric h_{ab} on H and see if it has a zero eigenvalue. To construct h_{ab} numerically, we

have to know the two-metric $\widetilde{q}_{ab}$ on at least two different time slices. Furthermore, in a numerical simulation, H will never be exactly isolated because of numerical errors, and it is not clear how this method can quantify how close the horizon is to being exactly isolated. Fortunately, there is a much simpler method which only requires data on a single time slice and also provides a quantitative measure of how close H is to being perfectly isolated. This method is based on the shear $\sigma^{(\ell)}_{ab}$ of ℓ, which is the symmetric trace-free part of the projection of $\nabla_a \ell_b$ onto the apparent horizon S. The tensor $\sigma^{(\ell)}_{ab}$ has two independent components, and is conveniently written in terms of a single complex number $\sigma_{(\ell)} := m^a m^b \nabla_a \ell_b$, where m is defined in equation (2.2). To calculate $\sigma_{(\ell)}$ conveniently, we simply decompose ℓ using equation (2.1):

$$\begin{aligned} \sigma_{(\ell)} &\triangleq m^a m^b \nabla_a \ell_b \\ &\triangleq \frac{1}{\sqrt{2}} m^a m^b \nabla_a T_b + \frac{1}{\sqrt{2}} m^a m^b \nabla_a R_b \,. \end{aligned} \tag{3.1}$$

The first term is just a component of the extrinsic curvature K_{ab}, while the second term can be calculated on the spatial slice by calculating the connection associated with the three-metric γ_{ab}. We shall now prove the following important result concerning $\sigma_{(\ell)}$:

The world tube of apparent horizons is a NEH if and only if $\sigma_{(\ell)} \triangleq 0$ (We extend the notation '$\triangleq$' to also mean that the equality holds only at points of H).

To prove this statement, we need to consider the general case when H is not null. This has been studied in great detail by Hayward [13]. In Hayward's terminology, the surface H is essentially a *future outer trapping horizon*. This means that H is foliated by a family of marginally trapped surfaces (which in our case are the apparent horizons) satisfying the relations $\theta_{(\ell)} \triangleq 0$, $\theta_{(n)} < 0$ and $\mathcal{L}_n \theta_{(\ell)} < 0$. These are physically very reasonable conditions, and all black holes found in simulations are expected to satisfy them.

The proof of this statement, adapted from [13], is then quite simple: let z^a be a vector tangent to H and orthogonal to the foliation whose leaves are the apparent horizons. Such a vector field may be considered to define time evolution at the horizon. It is easy to see that, up to a rescaling, z^a can be expressed as a linear combination of ℓ^a and n^a

$$z^a \triangleq \ell^a - \alpha n^a \tag{3.2}$$

where α is a smooth function on H. The rescaling freedom in z will be inconsequential for our purposes. The surface H is null, spacelike, or timelike if and only if α is zero, positive, or negative respectively. We will now show that $\alpha \geq 0$. From the definition of apparent horizons we know that the expansion $\theta_{(\ell)}$ vanishes everywhere on the horizon, therefore $\mathcal{L}_z \theta_{(\ell)} \triangleq 0$. This in turn gives

$$\alpha \triangleq \frac{\mathcal{L}_\ell \theta_{(\ell)}}{\mathcal{L}_n \theta_{(\ell)}} \,. \tag{3.3}$$

Even though $\theta_{(\ell)}$ and $\theta_{(n)}$ are so far defined only on H, in equation (3.3) (and also in the very definition of a trapping horizon) we are taking the derivatives of these quantities along ℓ and n which are not necessarily tangent to H. To make sense of this equation we need to extend ℓ and n in a neighborhood of the surface S. This can easily be done by using the unique geodesics determined by these vectors.

The Raychaudhuri equation for ℓ then leads to

$$\mathcal{L}_\ell \theta_{(\ell)} \triangleq -|\sigma_{(\ell)}|^2 - \Phi_{00} \tag{3.4}$$

where $\Phi_{00} = \frac{1}{2} R_{ab} \ell^a \ell^b$. If we assume that the spacetime is vacuum, then $\Phi_{00} = 0$, and therefore $\mathcal{L}_\ell \theta_{(\ell)} \triangleq -|\sigma_{(\ell)}|^2$, which along with equation (3.3) gives

$$\alpha \triangleq -\frac{|\sigma_{(\ell)}|^2}{\mathcal{L}_n \theta_{(\ell)}} \,. \tag{3.5}$$

This immediately implies that $\alpha \triangleq 0$ (which is equivalent to H being null) if and only if $\sigma_{(\ell)} \triangleq 0$. This is what we wanted to show. More generally, since $\mathcal{L}_n \theta_{(\ell)} < 0$, this shows that $\alpha \geq 0$, which means that Δ is spacelike when the shear is non-zero.

As a side remark we also show that H is null if and only if the *area element* on the apparent horizons ϵ_{ab} is preserved in time. To show this we need the equations

$$\mathcal{L}_\ell \epsilon_{ab} \triangleq \theta_{(\ell)} \epsilon_{ab} \triangleq 0 \qquad \text{and} \qquad \mathcal{L}_n \epsilon_{ab} \triangleq \theta_{(n)} \epsilon_{ab} \,. \tag{3.6}$$

It then follows that

$$\mathcal{L}_z \epsilon_{ab} \triangleq \mathcal{L}_\ell \epsilon_{ab} - \mathcal{L}_{\alpha n} \epsilon_{ab} \triangleq -\alpha \theta_{(n)} \epsilon_{ab} \tag{3.7}$$

therefore $\alpha \triangleq 0$ if and only if $\mathcal{L}_z \epsilon_{ab} \triangleq 0$, which is what we wanted to prove. This implies that if $\alpha \triangleq 0$, then the area of cross-sections of Δ is constant. However, the converse

is not necessarily true, because ϵ_{ab} could be changing in such a way that its integral is constant; the area can be constant globally without being constant locally. Thus, in principle, we can have situations in which the area is constant without the horizon being isolated. However, constancy of area is still a very useful first check to see when the horizon reaches equilibrium. Finally, as a side remark we note that since $\alpha \geq 0$ and $\theta_{(n)} < 0$, we get $\mathcal{L}_z A_\Delta \geq 0$, which is the area increase law.

In this paper we are interested in the case when $\sigma_{(\ell)}$ vanishes (up to numerical errors). In order for the horizon to be isolated we should have

$$s := \oint_S |\sigma_{(\ell)}|^2 \, \mathrm{d}^2V = 0 \tag{3.8}$$

where d^2V is the natural area measure on S constructed from q_{ab}. The quantity s is dimensionless since $\sigma_{(\ell)}$ has dimensions of inverse length. For the horizon to be numerically isolated, we require that s converges to zero appropriately when the numerical resolution is increased. We want to point out that as it stands, the quantity s can not be used as a general measure of how isolated a given horizon is, since it is not gauge invariant. A simple rescaling of ℓ changes $\sigma_{(\ell)}$ and thus s. However, if we are only concerned with given apparent horizons embedded in given spatial slices, and if we agree to use equation (2.1) for defining ℓ thereby removing the boost freedom, then the horizon will be close to being isolated if the condition

$$s \ll 1 \tag{3.9}$$

is satisfied. While this is not a satisfactory solution for identifying the small parameter, it is useful in practice. The complete solution to this problem will require the notion of an *isolated horizon* which selects a preferred null normal. A method for selecting a preferred null normal is described in section 4.2.

3.2 Finding the Killing vector

First of all, we should point out that in some numerical simulations (especially simulations with built-in axi-symmetry) the axial symmetry vector is already known. In that case, one can go ahead and find the angular momentum using equation (2.48). However, we are also interested in the more general case, when there is an axial symmetry, but the coordinates used in the simulation are not adapted to it. In this section, we describe a general numerical method for finding φ^a. Our method of finding Killing

vectors on the apparent horizons is based on the Killing transport equation, which we now describe. This method does not depend on the fact that we are on an apparent horizon, and it is possible that this procedure could find Killing vectors efficiently in more general situations. We first describe the general method.

Let ξ^a be a Killing vector on $(S, \widetilde{q}_{ab})$, and define the two-form $L_{ab} = \nabla_a \xi_b$. This is a two-form because of the Killing equation $\nabla_{(a}\xi_{b)} = L_{(ab)} = 0$. It is then not difficult to prove the following (see e.g. [10])

$$\begin{aligned} v^a \nabla_a \xi_b &= v^a L_{ab} \\ \text{and} \qquad v^a \nabla_a L_{bc} &= R_{cba}{}^d \xi_d v^a \,. \end{aligned} \tag{3.10}$$

The reason for inserting an arbitrary vector v^a will soon become clear. Instead of viewing these as equations for a Killing vector, let us instead think of them as equations for an arbitrary vector ξ^a (or a one-form ξ_a) and an arbitrary two-form L_{ab}. If we start with a one-form $\xi_a^{(p)}$ and a two-form $L_{ab}^{(p)}$ at a point p on the manifold, then the above equations can be solved along any curve $\gamma(t)$ (with v^a as its tangent) starting at p to give a unique one-form η_a and a unique two-form α_{ab} at any other point on the curve. This procedure is analogous to parallel transport, but the differential equation used in the transport is not the geodesic equation, but instead equation (3.10) above, and instead of transporting a vector, these equations transport a one-form and a two-form. Viewed this way, equations (3.10) are often referred to as the *Killing transport equations* [14]. We are thus led to consider the vector space V_p consisting of all pairs $(\xi_a^{(p)}, L_{ab}^{(p)})$ for an arbitrary one-form $\xi_a^{(p)}$ and an arbitrary two-form $L_{ab}^{(p)}$ at a point p. For any curve $\gamma(t)$ which starts at p and ends at q, the equations in (3.10), being linear, give us a linear mapping between V_p and V_q. If $(\xi_a^{(p)}, L_{ab}^{(p)}) \in V_p$ actually comes from a Killing vector and its derivative, then it will be mapped to $(\xi_a^{(q)}, L_{ab}^{(q)}) \in V_q$, which comes from the same Killing vector.

If we consider closed curves starting and ending at the point p, then the Killing transport for a curve $\gamma(t)$ gives us a linear mapping $M_p(\gamma) : V_p \to V_p$. A Killing vector corresponds to an eigenvector of $M_p(\gamma)$ with eigenvalue equal to unity for any closed curve γ. In our case, S is a topological two-sphere which means that V_p is a three dimensional vector space and, if we choose a basis, $M_p(\gamma)$ can be represented as a 3×3 matrix (if S is an n dimensional manifold, then $M_p(\gamma)$ is a $\frac{1}{2}n(n+1)$ dimensional matrix). Finding the Killing vector at p then reduces to an eigenvalue problem for a 3×3 matrix. For a constant curvature two-sphere, as in the Schwarzschild horizon, this matrix will just be

the identity matrix for any point p. For an axially symmetric sphere, such as the one in a Kerr spacetime, there will be precisely one such eigenvector. Having found ξ^a and L_{ab} at one point, we can again use equation (3.10) to find it everywhere on the sphere, using various other curves. Finally, the Killing vector is normalized by requiring its integral curves to have affine length 2π (it can be shown that the integral curves must in fact be closed). Since we are only free to rescale the Killing vector by an overall constant, we only have to perform the normalization on one integral curve. This normalization is valid for rotational Killing vectors. If we were dealing with, say, translational or stationary Killing vectors, the appropriate normalization condition would be to require the vector to have unit norm at infinity.

To make this procedure concrete, let us write down the equations explicitly in spherical coordinates. The Riemannian two-metric q_{ab} on the apparent horizon S in arbitrary spherical coordinates (θ, ϕ) is:

$$\widetilde{q} = \widetilde{q}_{\theta\theta}\, d\theta \otimes d\theta + \widetilde{q}_{\phi\phi}\, d\phi \otimes d\phi + \widetilde{q}_{\theta\phi}\, (d\theta \otimes d\phi + d\phi \otimes d\theta)\,. \tag{3.11}$$

The horizon may be arbitrarily distorted; $\widetilde{q}_{ab}$ does not have to be the standard two-sphere metric. Note that on a sphere, any two-form L_{ab} can be written uniquely as $L_{ab} = L\epsilon_{ab}$, where L is a function on S, and ϵ_{ab} is the area two-form on S; $\epsilon = \sqrt{\det \widetilde{q}}\, d\theta \wedge d\phi$ where $\det \widetilde{q} = \widetilde{q}_{\theta\theta}\widetilde{q}_{\phi\phi} - \widetilde{q}^2_{\theta\phi}$ is the determinant of q_{ab}. Any one-form ξ_a can be expanded as $\xi = \xi_\theta d\theta + \xi_\phi d\phi$. The covariant derivative of a one-form ξ_a is expressed in terms of the Christoffel symbols ${\Gamma_{ab}}^c$ as

$$\nabla_a \xi_b = \partial_a \xi_b - {\Gamma_{ab}}^c \xi_c\,. \tag{3.12}$$

The Riemann tensor of q_{ab} has only one independent component

$$R_{abcd} = \frac{1}{2} R \epsilon_{ab}\epsilon_{cd}\,. \tag{3.13}$$

Now we must choose a closed curve in order to find the Killing vector at a single point. The equator ($\theta = \pi/2$) is a convenient choice for the curve since it avoids the coordinate singularity at the poles. The tangent vector v^a is then simply ∂_ϕ. The equations (3.10)

then become

$$\begin{aligned}
\frac{\partial \xi_\theta}{\partial \phi} &= \Gamma_{\theta\phi}{}^{\theta}\xi_\theta + \Gamma_{\theta\phi}{}^{\phi}\xi_\phi - L\sqrt{\det q}\,, \\
\frac{\partial \xi_\phi}{\partial \phi} &= \Gamma_{\phi\phi}{}^{\theta}\xi_\theta + \Gamma_{\phi\phi}{}^{\phi}\xi_\phi\,, \\
\frac{\partial L}{\partial \phi} &= \frac{1}{2}R\sqrt{\det q}\left(q^{\theta\theta}\xi_\theta + q^{\theta\phi}\xi_\phi\right)\,.
\end{aligned} \tag{3.14}$$

(In these formulas we do not sum over repeated indices.) These are three coupled, linear, first-order differential equations in $(\xi_\theta, \xi_\phi, L)$. The same equation holds for any line of latitude (θ = constant). The second-order Runge-Kutta method was used to solve these equations. The initial data required for this equation are the values of $(\xi_\theta, \xi_\phi, L)$ at, say, $\phi = 0$. The solution of the equation will be $(\xi_\theta, \xi_\phi, L)$ at $\phi = 2\pi$. We are eventually interested only in (ξ_θ, ξ_ϕ), but the function L is necessary to transport the data. The solution to these equations can be written in terms of a matrix $\mathbf{M}$:

$$\begin{pmatrix} \xi_\theta \\ \xi_\phi \\ L \end{pmatrix}_{(\phi=2\pi)} = \mathbf{M} \begin{pmatrix} \xi_\theta \\ \xi_\phi \\ L \end{pmatrix}_{(\phi=0)}\,. \tag{3.15}$$

To find the matrix $\mathbf{M}$, we start with the initial data sets $(1,0,0)$, $(0,1,0)$ and $(0,0,1)$. The solutions will give the first, second and third columns respectively of $\mathbf{M}$. Next we find the eigenvalues and eigenvectors of $\mathbf{M}$. The eigenvector with unit eigenvalue is what we want. In principle, we should verify that *every* closed curve starting and ending at the point $(\theta = \pi/2, \phi = 0)$ gives the same eigenvector. However, as in any numerical method, we only do this for a small number of curves. The eigenvector obtained in this way is the only possible candidate for a Killing vector. Numerically, no eigenvalue is exactly equal to unity; therefore, in practice, we choose the eigenvalue closest to unity (see the next section). For the horizon to be axisymmetric or close to Kerr in any sense, this eigenvalue should be very close to unity. If this is not the case, then this proves that the horizon is not close to Kerr in any sense. All eigenvalues will be unity in the spherically symmetric case.

Having found the eigenvector at the point $\phi = 0$, we then transport it to every grid point on the sphere. The curves used to transport the eigenvector are the lines of latitude and longitude. Transport along constant θ curves is done by equations (3.14),

while for the constant ϕ curves we use:

$$\begin{aligned}
\frac{\partial \xi_\theta}{\partial \theta} &= \Gamma_{\theta\theta}{}^{\theta}\xi_\theta + \Gamma_{\theta\theta}{}^{\phi}\xi_\phi\,, \\
\frac{\partial \xi_\phi}{\partial \theta} &= \Gamma_{\theta\phi}{}^{\theta}\xi_\theta + \Gamma_{\theta\phi}{}^{\phi}\xi_\phi + L\sqrt{\det q}\,, \\
\frac{\partial L}{\partial \theta} &= -\frac{1}{2}R\sqrt{\det q}\left(q^{\phi\theta}\xi_\theta + q^{\phi\phi}\xi_\phi\right)\,.
\end{aligned} \tag{3.16}$$

(Again, no summation over repeated indices.) Finally, having found $(\xi_\theta, \xi_\phi, L)$ at each grid point, we now need to normalize the Killing vector $\xi = (\xi_\theta, \xi_\phi)$ so that its integral curves have affine length 2π. To do this, we need to follow the integral curves of ξ^a:

$$\frac{d\theta}{dt} = \xi^\theta(\theta,\phi) \qquad \text{and} \qquad \frac{d\phi}{dt} = \xi^\phi(\theta,\phi) \tag{3.17}$$

and normalize the affine parameter t so that its range is $[0, 2\pi]$. Numerically, we only have to make sure that ξ^a does not vanish at the starting point. While solving equation (3.17) numerically, we will need the value of ξ^a at points not included in the grid. We use a second order interpolation method for this purpose. This finally gives us the normalized symmetry vector φ^a, which is used to calculate J_Δ from equation (2.48).

3.3 Numerical results

Using the results of sections 3.1 and 3.2, we can now refine the steps outlined in the beginning of this chapter for calculating J_Δ and M_Δ such that we only require data on a *single* spatial slice:

1. Find the apparent horizon S on a single spatial slice;
2. Check that the quantity s defined in equation (3.8) vanishes on S upto numerical errors or is much smaller than unity;
3. Find the Killing vector φ^a on S satisfying $\mathcal{L}_\varphi \tilde{q}_{ab} \triangleq 0$;
3. calculate J_Δ and M_Δ using equations (2.48) and (2.56).

In step 3, we should also check that φ^a preserved ω_a and the equivalence class $[\ell]$. These are easy to check in practice and we shall only focus on the non-trivial check $\mathcal{L}_\varphi \tilde{q}_{ab} \triangleq 0$. The numerical results are given below.

In this section, we apply our approach to finding the Killing vector and our ability to identify an isolated horizon. In order to validate our approach for identifying Killing

vectors on S, we first test our method using analytic data (γ_{ij}, K_{ij}) in a simple case for which the location of S and its Killing vectors are also known; we consider the boosted Kerr-Schild solution [15] with the basic parameters of mass $M = 1$, spin $a = 1/2$, and a boost in the z-direction. The notion of a boost is well defined for metrics in the Kerr-Schild form because of the presence of a flat background metric. By boosting the black hole, we impose a coordinate distortion on the horizon, while retaining its physical properties. For these test cases, we know that the horizon is isolated; and we take advantage of only needing to compute quantities intrinsic to a two-sphere and use spherical coordinates. The following steps were used to test the numerical code maintaining second order accuracy at each step:

1. From the Kerr-Schild data, calculate analytically the apparent horizon two-metric q_{ab}, the normal R_a, and the components of the extrinsic curvature K_{ab} at the location of the apparent horizon. Discretise these quantities using a spherical grid on the apparent horizon.

2. Using the discretised data, find the unnormalized Killing vector, ξ^a, at a single point (in our case we choose this point to be $(\theta = \pi/2, \phi = 0)$) through the procedure described in the previous section, applying the Runge-Kutta method.

3. Solve both equations (3.14) and (3.16) to find ξ^a everywhere on the apparent horizon.

4. Normalize the Killing vector, ϕ^a, using interpolation and a Runge-Kutta method for equations (3.17).

5. Calculate J_Δ via equation (2.48), using R^a given by the apparent horizon and ϕ^a determined by steps 1–4.

The first step is easy if we have the analytic expressions for the relevant quantities. In the second step, we have to find the matrix $\mathbf{M}$ described in equation (3.15) and find its eigenvector with eigenvalue closest to unity. One can ask whether there is any ambiguity in choosing the right eigenvalue; is it possible that more than one eigenvalue is close to unity? In the spherically symmetric case ($a = 0$), all eigenvalues are equal to unity and it is immaterial which one we choose; the angular momentum will be zero. When a is sufficiently large, one eigenvalue is much closer to unity in magnitude as compared to the other two. In our case, it turns out that the matrix $\mathbf{M}$ has one real eigenvalue λ and two complex eigenvalues $\lambda_{Re} \pm i\lambda_{Im}$. Figure 3.1, a plot of the real and imaginary parts

of the eigenvalues as a function of a (for the un-boosted Kerr-Schild hole) , demonstrates the unambiguous nature of the eigenvalue for large values of a. The ambiguity may arise when a is very small. In figure 3.2, we plot both functions for a smaller range of a. Both plots were generated for a resolution of $d\phi = \pi/80$. The figures show that the correct eigenvalue is typically easy to identify, because the other eigenvalues diverge from unity rather rapidly and also, at least in this case, the 'wrong' eigenvalues are complex while the correct eigenvalue is real.

Having found the correct eigenvector and therefore the Killing vector at a single point, we then find it at every other grid point and use it to calculate J_Δ. Figure 3.3 plots the values of the angular momentum of the black hole found using equation (2.48) versus different values of the boost parameter for the Kerr-Schild data. Three different resolutions are plotted, showing a second-order convergence rate towards the known analytical value of $J_\Delta = 0.5$ as expected. Although there is a slight loss in accuracy as the boost approaches the speed of light, the angular momentum loses only 1% in accuracy for the least resolved case in figure 3.3 when the boost parameter is increased from 0 to 0.8. We obtained similar results for boosts in other directions.

A more realistic situation is to compute J_Δ and M_Δ during a numerical simulation of a black-hole spacetime, in which the spacetime data will be given on a spatial grid. To test our method in this case, we again use boosted Kerr-Schild data, but this time we start with numerical data discretised on a Cartesian mesh on a spatial slice; this mesh will not coincide with the spherical mesh on the apparent horizon. We use an apparent horizon finder to locate the apparent horizon S and its unit spacelike normal R^a, and construct a spherical grid on the apparent horizon. Let dx and $d\phi$ be the grid spacing of the Cartesian and spherical grid respectively. We want the two grids to be of similar spacing, i.e. we choose $d\phi$ such that $d\phi \approx dx/R$ where R is the coordinate radius of the apparent horizon. The data are then interpolated onto the spherical grid, an additional source of error. We extract the two-metric q_{ab} numerically from the data, use it to find the Killing vector field φ^a, and apply our formula for angular momentum. We present a series of test cases involving the black hole in boosted Kerr-Schild data. One is static, and three others have a spin of 1/2 about the z-axis, with one of the spinning holes boosted perpendicular to the spin along the x-axis, another parallel to the spin along the z-axis. Table 3.1 lists the different scenarios. Due to the additional complexity of having the data in a mesh that is not the one on S where the calculation is done, we have to deal with two different numerical grids. We refined both the Cartesian grid and the spherical grid intrinsic to the apparent horizon to perform convergence tests. All runs

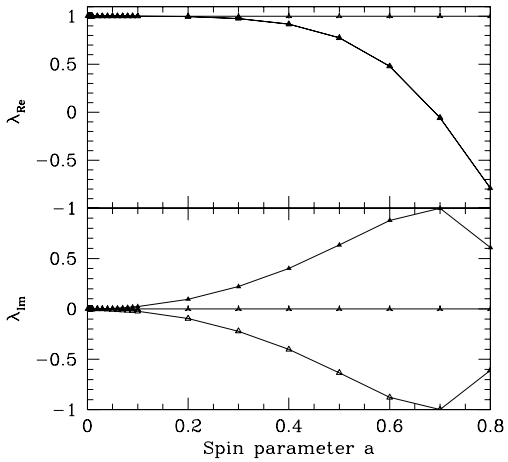

Fig. 3.1. Plots of the real and imaginary parts of the eigenvalues of the matrix **M** (defined in eqn. (3.15)) versus a large range of the spin parameter a.

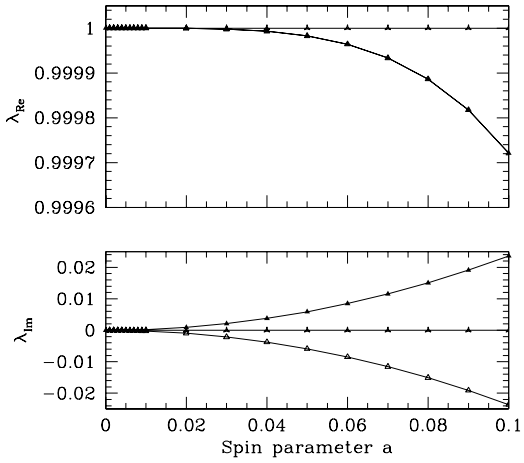

Fig. 3.2. Plots of the real and imaginary parts of the eigenvalues of the matrix **M** versus the spin parameter a, when a is small.

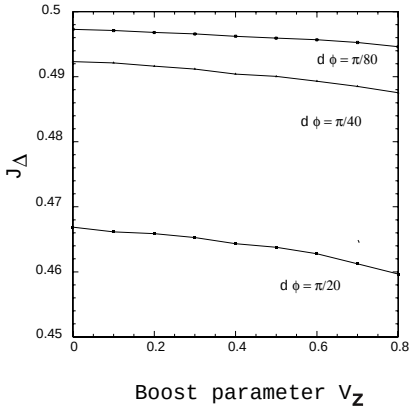

Fig. 3.3. The numerically computed angular momentum of the black hole at different boosts for a black hole with mass $M = 1$ and spin $a = 1/2$. Three different resolutions $d\phi$ are shown.

Table 3.1. Various parameter values for the boost and spin considered in the text

Scenario	M	a	v_x	v_z
I	1	0	0	0
II	1	1/2	0	0
III	1	1/2	1/2	0
IV	1	1/2	0	1/2

were performed with three resolutions: 1. $dx = 1/4$, $d\phi = 10^\circ$; 2. $dx = 1/8$, $d\phi = 5^\circ$; 3. $dx = 1/16$, $d\phi = 2.5^\circ$. Figure 3.4 shows J_Δ versus resolution, and figure 3.5 displays M_Δ versus resolution, showing second-order convergence to the known solutions for each of the cases described in table 3.1. In addition to J_Δ and M_Δ, we also monitor how well we converge to a truly isolated horizon, one in which the shear σ is zero. Figure 3.6 plots the value of σ versus resolution and demonstrates second-order convergence toward zero. As expected due to additional errors, the convergence factors are not as good as in the case of analytic data; but are still acceptable for second order convergence.

3.4 Comparison With Other Methods

In this section we want to compare our method of finding the mass and angular momentum of a black hole in a numerical simulation with other methods that are commonly used.

Note that the method proposed in this paper has three advantages: (i) it is not tied to a particular geometry (like the Kerr geometry), (ii) it is completely coordinate independent, and (iii) it only requires data that is intrinsic to the apparent horizon. The commonly used alternatives for calculating mass and angular momentum do not share all three of these features.

Owing to the uniqueness theorems of classical general relativity, it is commonly believed that a black hole that has been created in a violent event will radiate away all its higher multipole moments and settle down to form a Kerr black hole near the horizon. One strategy for assigning a mass and an angular momentum to a black hole is then to identify the member of the Kerr family one is dealing with and to read off the corresponding mass and angular momentum parameters.

While this strategy is physically well motivated, and one does expect the final black hole to be close to Kerr in some sense, we can refine this strategy considerably. The main difficulty with this method is that there are many subtleties and open questions regarding the issue of uniqueness of the final black hole. To briefly illustrate this point, let us consider the isolated horizon describing the final black hole. The intrinsic geometry of the horizon is, by definition, time independent. However, it is not necessary that *four dimensional* quantities evaluated at the horizon must also be time independent. For instance, using the Einstein equations at the isolated horizon, it turns out that the expansion and shear of the inward pointing normal n^a may not be time independent;

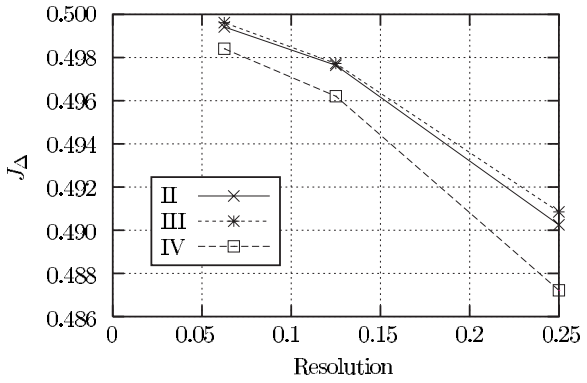

Fig. 3.4. Resolution tests for the angular momentum J_Δ of the horizon. The scenarios II – IV are explained in table 3.1.

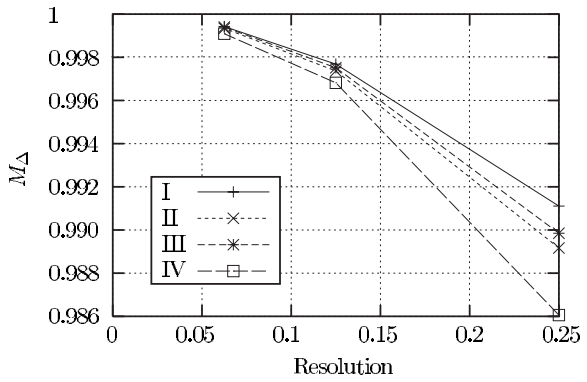

Fig. 3.5. Resolution test for the mass M_Δ of the horizon. The scenarios II – IV are explained in table 3.1.

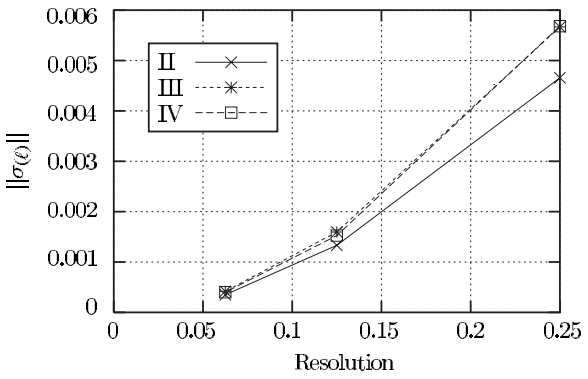

Fig. 3.6. This graph shows the L_2 norm of $\sigma_{(\ell)}$. We see that it converges to zero, indicating that the horizon is isolated. The scenarios II – IV are explained in table 3.1.

these quantities decay exponentially [5] (see eqn. (4.11)). This means that the four-geometry in the vicinity of the horizon is generically not time independent, and hence may not be isometric to a Kerr solution. It is also not clear whether the four geometry tends to the Kerr geometry as we approach future time like infinity. Clearly, what we need is an analog of the black hole uniqueness theorems, which have so far only been proven for stationary spacetimes. To answer these important questions, it is imperative that one does not assume a Kerr geometry from the beginning. In particular, it is desirable that we not use the Kerr geometry to calculate angular momentum and mass.

If one nevertheless makes the assumption that the final black hole is described by a Kerr geometry, one has to find a way to identify the particular member in the Kerr family. The method that is most commonly used is the *great circle method* which is based on properties of the Kerr horizon found by Smarr [16]. It can be described as follows:

In the usual coordinates, let L_e be the length of the equator and L_p the length of a polar meridian. Here the equator is the great circle of maximum length and a polar meridian is a great circle of minimum length. The distortion parameter δ is then defined to be $(L_e - L_p)/L_e$. Smarr then showed that the knowledge of δ, together with one other quantity like area, L_e, or L_p, is sufficient to find the parameters m and a of the Kerr geometry.

The difficulty with this method, apart from relying overly on properties of the Kerr spacetime, is that notions such as great circles, equator or polar meridian etc. are all highly coordinate dependent. If we represent the familiar two-metric on the Kerr horizon in different coordinates, the great circles in one coordinate system will not agree with great circles in the other system. The two coordinate systems will therefore give different answers for M and a as calculated by this method. In certain specific situations where one has a good intuition about the coordinate system being used and the physical situation being modelled, this method might be useful as a quick way of calculating angular momentum, but it is inadequate as a general method.

The problem of coordinate dependence can be dealt with in axisymmetric situations; assume that the coordinate system used in the numerical code is not adapted to the axial symmetry. The idea is to use the orbits of the Killing vector as analogs of the lines of latitude on a metric two-sphere. The analog of the equator is then the orbit of the Killing vector which has maximum proper length. This defines L_e in an invariant way. The north and south poles are the points where the Killing vector vanishes, and the

analog of L_p is the length of a geodesic joining these two points (because of axial symmetry, all geodesics joining the poles will have the same length). Since this geodesic is necessarily perpendicular to the Killing vector, we just need to find the length of a curve which joins the north and south poles and is everywhere perpendicular to the Killing orbits. With L_e and L_p defined in this coordinate invariant way, we can follow the same procedure as in the great circle method to calculate the mass and angular momentum. This method can be called the *generalized* great circle method.

How does the generalized great circle method compare to our method? From a purely practical point of view, note that this method requires us to find the Killing vector, to determine the orbit of the Killing vector with maximum length, and to calculate the length of a curve joining the poles which is orthogonal to the Killing orbits. The first step is the same as in the isolated horizon method presented in this paper. While the next step in the isolated horizon method is simply to integrate a component of the extrinsic curvature on the horizon, this method requires more work, and furthermore, the numerical errors involved are at least as high as in the isolated horizon method. Thus the simplicity of the great circle method is lost when we try to make it coordinate invariant, and it retains the disadvantage of relying heavily on the properties of the Kerr geometry.

It should also be mentioned here that there exist exact solutions to Einstein's equations representing static, non-rotating and axisymmetric black holes. Examples of such solutions are the distorted black hole solutions found by Geroch and Hartle [8] or the solutions representing black holes immersed in electromagnetic fields [17]. The apparent horizons in all these solutions are distorted, and the generalized great circle method will give a non-zero value for the angular momentum. While these solutions are not relevant for numerical simulations of binary black hole collisions, they represent physically interesting situations in which a black hole is surrounded by different kinds of external matter fields which distort the black hole; these black holes may have some relevance astrophysically. These solutions show that the generalized great circle method cannot be correct in general. They also illustrate that the great circle method will in general give results that are different from the ones obtained using Komar integrals. See appendix C for an example of such a distorted black hole.

A completely different approach to finding the mass and angular momentum of a black hole in a numerical solution is to use the concept of a Killing horizon. Since in a numerical simulation one is interested in highly dynamical situations, one can not assume the existence of Killing vectors in the whole spacetime. Instead one assumes that

stationary and axial Killing vectors exist in a neighborhood of the horizon, and then uses appropriate Komar integrals to find the mass and angular momentum.

While this method is coordinate independent and does not rely on a specific metric, it has two disadvantages when compared with the isolated horizon approach. First, it is not a priori clear how the stationary Killing vector is to be normalized if it is only known in a neighborhood of the horizon. Secondly, this method requires the Killing vectors to be known in a whole neighborhood of the horizon. Computationally this is more expensive than finding a Killing vector just on the horizon. Conceptually it is also unclear how big this neighborhood of the horizon should be. Furthermore, at present there is no Hamiltonian framework available in which the boundary condition involves the existence of Killing vectors in a finite neighborhood of the horizon. In a sense, the isolated horizon framework extracts just the minimum amount of information from a Killing horizon in order to carry out the Hamiltonian analysis and define conserved quantities.

Chapter 4

Extracting physics from the strong field region

Thus far, in this thesis we have been mainly concerned with the *intrinsic* geometry of the black hole. It turns out that the isolated horizon framework can also be used to study the near horizon geometry of the black hole [1]. This is potentially a very useful tool in numerical relativity. Section 4.1 explains the general construction and is based on [1]. Section 4.2 gives the basic equation used to restrict the choice of null normals on a weakly isolated horizon (this was derived in [5]). In this section we also give the numerics for implementing these results. This is work in progress carried out in collaboration with Ken Smith. Finally, section 4.3 describes some invariant ways to pick the preferred cross-sections of an isolated horizon which were discovered by Jerzy Lewandowski and Tomasz Pawlowski.

4.1 Near horizon geometry

While the isolated horizon boundary conditions only constrain the intrinsic geometry of an isolated horizon Δ, by a procedure analogous to the one usually carried out at null infinity to construct the Bondi coordinates, we can obtain an invariantly defined coordinate system in a neighborhood of Δ. As we shall explain later in this section, this coordinate system can be used to study the strong field region. Let us first describe the construction.

Assume for now that there is a preferred equivalence class of null normal $[\ell^a]$ and a preferred family of cross sections on a weakly isolated horizon Δ; we shall show in sections 4.2 and 4.3 how this can be accomplished. Using terminology from null infinity, we will refer to the preferred sections of Δ as the *good cuts* on Δ. Assume further that this is a non-extremal horizon, i.e. $\kappa_{(\ell)} \neq 0$. Pick a null normal ℓ^a from the equivalence class $[\ell^a]$; this can be done e.g. by choosing a value for surface gravity. Let n_a be the unique one-form satisfying $\ell^a n_a \triangleq -1$ and which is orthogonal to the good cuts. Let (v, θ, ϕ) be coordinates on Δ such that v is an affine parameter along ℓ^a: $\ell = \partial_v$, the good cuts are given by surfaces of constant v and θ and ϕ are coordinates on the good cut satisfying $\mathcal{L}_\ell \theta \triangleq 0$ and $\mathcal{L}_\ell \phi \triangleq 0$.

Consider now past null geodesics emanating from the good cuts with $-n^a$ as their initial tangent vector (the index of n_a is raised using the four metric). Let the null geodesics be affinely parameterized and let the affine parameter be caller r and set $r = r_0$ on Δ. Lie drag the coordinates (v, θ, ϕ) along the null geodesics. This leads to a set of coordinates (r, v, θ, ϕ) in a *neighborhood* of the horizon. This coordinate system will break down when the null geodesics start to cross. The only arbitrariness in this coordinate system is in the choice of (θ, ϕ) on one good cut and the choice of r_0.

We can also define a null tetrad in the neighborhood in a similar fashion. Let m^a be an arbitrary complex vector tangent to the good cuts such that $(\ell, n, m, \overline{m})$ is a null tetrad on Δ. Using parallel transport along the null geodesics, we can define a null tetrad in the neighborhood. This tetrad is unique upto the spin rotations of m: $m \to e^{2i\theta} m$. This construction is shown in figure 4.1.

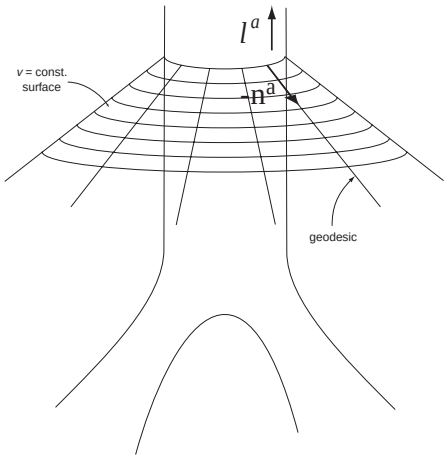

Fig. 4.1. Bondi-like coordinates in a neighborhood of Δ.

This invariantly defined coordinate system and null tetrad can be used to address some issues in numerical relativity. For example, the aim of many numerical simulations is to extract the gravitational waveforms produced say, during a binary black hole collision. The Weyl tensor component Ψ_4 (see appendix A) will contain information about

the waveform. The null tetrad presented above can be used to calculate Ψ_4 invariantly. By expressing all quantities in the preferred coordinates and basis, this will also enable us to compare different the results of different simulations which may use very different coordinates, initial conditions etc. The past null cone of a good cut at a sufficiently late time can be used as an approximate null infinity. This will enable us to calculate dynamical quantities such as the analog of the Bondi mass, rate of energy loss from the black hole etc.

4.2 Finding the preferred null normal

The construction described in the previous section has the following essential ingredients:

1. Finding a preferred null normal ℓ^a.
2. Locating the good cuts of the isolated horizon.
3. Integrating the null geodesics emanating from the good cuts.

In this thesis we will consider the first two steps. The integration of the null geodesics will be discussed elsewhere. In this section we show how a preferred ℓ can be found numerically. We refer the reader to [5] for further details about the geometry of isolated horizons.

4.2.1 Constraint equation on a WIH

Our condition for picking out the preferred null normal is based on putting restrictions on the expansion $\theta_{(n)}$ of the ingoing null normal n^a. We will first find the restrictions placed on the time derivative of $\theta_{(n)}$ by the Einstein equations. Since time evolution here corresponds to motion along ℓ which is tangent to Δ, this amounts to finding a constraint on the WIH data $([\ell], q_{ab}, \mathcal{D}_a)$.

We begin by recalling some notation. Let $(\Delta, [\ell])$ be a WIH and let S be a cross-section of Δ. Denote the one-form normal to S by n_a; we choose n so that it satisfies $\ell^a n_a \triangleq -1$, $dn \triangleq 0$ and $\mathcal{L}_\ell n_a \triangleq 0$. Let $\underline{n}_a$ be an extension of n_a to the full spacetime: $\underline{n}_{\underleftarrow{a}} \triangleq n_a$; we are free to add any multiple of ℓ_a to $\underline{n}_a$. As usual, let ∇_a be the four dimensional derivative operator compatible with the four-metric g_{ab}, q_{ab} the induced metric on Δ, $\mathcal{D}_a$ the induced derivative operator on Δ (see eqn. (2.20)); $\widetilde{q}_{ab}$ is the Riemannian two-metric on S and $\widetilde{\mathcal{D}}_a$ the unique derivative operator on S compatible

with $\widetilde{q}_{ab}$. The tensor $\widetilde{q}_a{}^b := q_a^b + n_a\ell^b + \ell_a n^b$ is the projection operator for the surface S. Following [5], we also define the quantities $S_{ab} = S_{(ab)} := \mathcal{D}_a n_b$ and $\widetilde{S}_{ab} := \widetilde{q}_a^c \widetilde{q}_b^d \mathcal{D}_c n_d$. The trace of $\widetilde{S}_{ab}$ gives the expansion $\theta_{(n)}$ while the trace free part gives the shear $\sigma_{(n)}$. The geometry of a WIH is completely specified by $([\ell], q_{ab}, \mathcal{D}_a)$. We shall only consider non-extremal horizons, i.e. we shall only consider those null normals for which surface gravity is non-zero. The extremal case is discussed in [5].

From the definition of the four-dimensional Riemann tensor

$$2\nabla_{[a}\nabla_{b]}\underline{n}_c \triangleq R_{abc}{}^d \underline{n}_d \,. \tag{4.1}$$

Pulling back all covariant indices in this equation to Δ and contracting both sides with ℓ^a we obtain

$$\ell^a \left(\mathcal{D}_a\mathcal{D}_b - \mathcal{D}_b\mathcal{D}_a\right) n_c \triangleq R_{a\underset{\leftarrow}{bc}d}\ell^a n^d \tag{4.2}$$

where n^a is a null vector satisfying $g_{ab}n^b = \underline{n}_a$. Note that we are free to change $\underline{n}_a \to \underline{n}_a + h\ell_a$ for any smooth function h; however, due to the properties of the Weyl tensor and eqn. (2.25), the above equation is insensitive to this ambiguity. For a given ℓ^a, the vector n^a in uniquely determined by the requiring it to be null and to satisfy $\ell_a n^a \triangleq -1$ and $g_{\underset{\leftarrow}{a}b}n^b = n_a$. Using the definition of the Lie derivative and symmetrizing on the indices b and c, the above equation can be written as

$$\mathcal{L}_\ell S_{bc} \triangleq \mathcal{D}_{(b}\omega_{c)} + \omega_{(b}\omega_{c)} + R_{a\underset{\leftarrow}{(bc)}d}\ell^a n^d \tag{4.3}$$

where we have also used the definition of ω_a (see eqn. (2.5)). The antisymmetric part of this equation is equivalent to eqn. (2.28). Finally, projecting to S we get

$$\mathcal{L}_\ell \widetilde{S}_{ab} \triangleq -\kappa_{(\ell)}\widetilde{S}_{ab} + \widetilde{\mathcal{D}}_{(a}\widetilde{\omega}_{b)} + \widetilde{\omega}_a\widetilde{\omega}_b + \widetilde{q}^p{}_a\widetilde{q}^q{}_b R_{c\underset{\leftarrow}{(pq)}d}\ell^a n^d \,. \tag{4.4}$$

The Riemann tensor term can be conveniently written as

$$\widetilde{q}_a{}^p\widetilde{q}_b{}^q R_{c\underset{\leftarrow}{(pq)}d}\ell^a n^d = -\frac{1}{2}\widetilde{\mathcal{R}}_{ab} + \frac{1}{2}\widetilde{q}_a{}^p\widetilde{q}_b{}^q R_{pq} \tag{4.5}$$

where $\widetilde{\mathcal{R}}_{ab}$ is the intrinsic Ricci tensor of S. To prove this, note that the surface S has codimension 2 if it is considered to be embedded in the four-dimensional spacetime. Furthermore, ℓ^a and n^a span the directions orthogonal to S whence it follows that the

second fundamental form of S is characterized by *two* extrinsic curvatures

$$K^{(\ell)}_{ab} := \widetilde{q}_a{}^p \widetilde{q}_b{}^q \nabla_p \ell_q \qquad \text{and} \qquad K^{(n)}_{ab} := \widetilde{q}_a{}^p \widetilde{q}_b{}^q \nabla_p \vec{n}_q \,. \tag{4.6}$$

With these definitions, it is easy to prove the following relation between the two-dimensional and four-dimensional curvature tensors:

$$\widetilde{\mathcal{R}}_{abcd} = \widetilde{q}_a{}^p \widetilde{q}_b{}^q \widetilde{q}_c{}^r \widetilde{q}_d{}^s R_{pqrs} - 2K^{(n)}_{c[a} K^{(\ell)}_{b]d} - 2K^{(\ell)}_{c[a} K^{(n)}_{b]d} \,. \tag{4.7}$$

This equation is invariant under boost transformations of ℓ and n and can be viewed as an extension of the usual Gauss-Codazzi equation for a hypersurface of unit codimension. Since $\underset{\leftarrow}{\nabla_a} \ell_b \triangleq 0$ for a WIH, we immediately see that $K^{(\ell)}_{ab} \triangleq 0$ whence it follows that

$$\widetilde{\mathcal{R}}_{abcd} = \widetilde{q}_a{}^p \widetilde{q}_b{}^q \widetilde{q}_c{}^r \widetilde{q}_d{}^s R_{pqrs} \tag{4.8}$$

Contracting both sides with $\widetilde{q}^{bd} = g^{bd} + 2n^{(b}\ell^{d)}$ and using the symmetries of the Riemann tensor yields eqn. (4.5) which is what we wanted to show. Using this result, eqn. (4.4) becomes

$$\mathcal{L}_\ell \widetilde{S}_{ab} \triangleq -\kappa_{(\ell)} \widetilde{S}_{ab} + \widetilde{\mathcal{D}}_{(a}\widetilde{\omega}_{b)} + \widetilde{\omega}_a \widetilde{\omega}_b - \frac{1}{2}\widetilde{\mathcal{R}}_{ab} + \frac{1}{2}\widetilde{q}_a{}^p \widetilde{q}_b{}^q R_{pq} \tag{4.9}$$

This is the key result we were looking for. It relates the time derivative of the expansion and shear of n^a to the matter fields via the four-dimensional Ricci tensor and it tells us that $\theta_{(n)}$ and $\theta_{(\ell)}$ need not be time independent on a WIH. This is in sharp contrast to a Killing horizon on which all geometrical fields are time independent. Apart from the constraint that $\kappa_{(\ell)}$ must be constant, eqn. (4.9) is the only constraint on $([\ell], q_{ab}, \mathcal{D}_a)$. To proceed further, we make the additional assumption that the spacetime Ricci tensor is time independent on Δ:

$$\mathcal{L}_\ell \left(\widetilde{q}_a{}^p \widetilde{q}_b{}^q R_{pq} \right) \triangleq 0 \,. \tag{4.10}$$

This condition is independent of the choice of ℓ on Δ considered as a NEH. Typical numerical simulations of say, binary black hole mergers focus on vacuum spacetimes where this condition is trivially satisfied. With this assumption, we can solve eqn. (4.9) and obtain the explicit time dependence of $\widetilde{S}_{ab}$:

$$\widetilde{S}_{ab} = e^{-\kappa_{(\ell)} v} \widetilde{S}^{(0)}_{ab} + \frac{1}{\kappa_{(\ell)}} \left(\widetilde{\mathcal{D}}_{(a}\widetilde{\omega}_{b)} + \widetilde{\omega}_a \widetilde{\omega}_b - \frac{1}{2}\widetilde{\mathcal{R}}_{ab} + \frac{1}{2}\widetilde{q}_a{}^p \widetilde{q}_b{}^q R_{pq} \right) \tag{4.11}$$

where v is the affine parameter along ℓ^a ($\ell^a = \partial_v$ and we have used the fact that the only time dependence in eqn. (4.9) is in $\widetilde{S}_{ab}$. This tells us that $\widetilde{S}_{ab}$ (and hence $\theta_{(\ell)}$ and $\sigma_{(\ell)}$) approach their equilibrium values *exponentially*.

4.2.2 Elliptic equation for finding the preferred null normal

With eqn. (4.9) at hand, we are now ready to describe the method used to select a preferred null normal. Though it is not difficult to include matter fields, we shall only consider vacuum spacetimes in this section.

The first condition we impose is to require that the surface gravity be constant; this is, of course, just the condition for a non-expanding horizon to be a weakly isolated horizon. However, as discussed in section 2.3, this does not select a unique equivalence class $[\ell]$; given a null normal ℓ^a with constant surface gravity $\kappa_{(\ell)}$, the null normal $\ell'^a = f\ell^a$ has constant surface gravity $\kappa_{(\ell')}$ for any function f of the form

$$f = Be^{-\kappa_{(\ell)}v} + \frac{\kappa_{(\ell')}}{\kappa_{(\ell)}} \tag{4.12}$$

where v satisfies $\mathcal{L}_\ell v = 1$ and B satisfies $\mathcal{L}_\ell B \triangleq 0$. In a *given* equivalence class $[\ell]$, fixing the value of surface gravity enables us to pick out a preferred ℓ, but the above equation shows that there is an infinite number of ways of choosing $[\ell]$.

We will now see that we can indeed pick out a preferred $[\ell]$ by imposing an additional condition on the expansion of the inward pointing null normal. First define the symmetric tensor $N^{(\ell)}_{ab}$, associated to a null normal ℓ, by the following equation:

$$[\mathcal{L}_\ell, \mathcal{D}_a]\,\xi_b \triangleq -N^{(\ell)}_{ab}\ell^c\xi_c \tag{4.13}$$

where ξ_b is an arbitrary one-form intrinsic to Δ. To prove the existence of N_{ab}, we use the fact that there exists a tensor $C_{ab}{}^c$ such that $[\mathcal{L}_\ell, \mathcal{D}_a]\xi_b \triangleq C_{ab}{}^c\xi_c$ and $C_{[ab]}{}^c \triangleq 0$. The existence of $C_{ab}{}^c$ is guaranteed by the properties of the differential operators $\mathcal{L}_\ell$ and $\mathcal{D}_a$. Furthermore, if h_a satisfies $\ell^a h_a \triangleq 0$, then using eqns. (2.25) and (2.5), it can be shown by a direct calculation that $[\mathcal{L}_\ell, \mathcal{D}_a]h_a \triangleq 0$. From this it follows that $C_{ab}{}^c h_c \triangleq 0$ for any h_c orthogonal to ℓ^c, which in turn implies $C_{ab}{}^c = -N^{(\ell)}_{ab}\ell^c$.

The tensor $N^{(\ell)}_{ab}$ is just the time derivative of S_{ab}. To show this, just set $\xi_b \triangleq n_b$ in eqn. (4.13) and obtain $N_{ab} \triangleq \mathcal{L}_\ell S_{ab}$. Furthermore, on weakly isolated horizons, $N^{(\ell)}_{ab}$ is transverse to ℓ. To show this, note that for any vector field X^a tangent to Δ, using

eqn. (4.13) and the Liebnitz rule:

$$[\mathcal{L}_\ell, \mathcal{D}_a]\, X^b \triangleq N^{(\ell)}_{ac} \ell^b X^c \,. \tag{4.14}$$

Setting $X^c \triangleq \ell^c$ leads to

$$N^{(\ell)}_{ab} \ell^b \triangleq \mathcal{L}_\ell \omega^{(\ell)}_a \tag{4.15}$$

which shows that for a WIH, $N^{(\ell)}_{ab} \ell^b \triangleq 0$. Finally, if ℓ^a is rescaled $\ell^a \to \ell'^a \triangleq f\ell^a$, then $N^{(\ell)}_{ab}$ transforms as follows

$$f N^{(\ell')}_{ab} \triangleq f N^{(\ell)}_{ab} + 2\omega^{(\ell)}_{(a} \mathcal{D}_{b)} f + \mathcal{D}_a \mathcal{D}_b f \,. \tag{4.16}$$

This shows that N^{ℓ}_{ab} is a property of the equivalence class $[\ell]$ because $N^{(\ell)}_{ab}$ is unchanged under constant rescalings.

Our condition for selecting a preferred $[\ell]$ is to require that N_{ab} be trace free. Given a WIH $(\Delta, [\ell])$ for which $\widetilde{q}^{ab} N^{(\ell)}_{ab} \neq 0$, we want to find a WIH $(\Delta, [\ell'])$ for which $\widetilde{q}^{ab} N^{(\ell')}_{ab} \triangleq 0$. To do this, first substitute f from eqn. (4.12) into eqn. (4.16) and project onto S using $\widetilde{q}^b_a$ to obtain

$$0 \triangleq f \widetilde{q}^{ab} N^{(\ell')}_{ab} \triangleq f \widetilde{q}^{ab} N^{(\ell)}_{ab} + e^{-\kappa_{(\ell)} v} \left[\widetilde{\mathcal{D}}^2 + 2\widetilde{\omega}^a \mathcal{D}_a + \kappa_{(\ell)} \widetilde{q}^{ab} \widetilde{S}_{ab} \right] B \tag{4.17}$$

where we have set $v = 0$ on the given section s and used $n_a \triangleq -\mathcal{D}_a v$. This is an elliptic equation for the time independent function B. Some of the coefficients of this elliptic equation ($\widetilde{S}_{ab}$, N_{ab} and $e^{-\kappa_{(\ell)} v}$) depend on time and we need to show that this equation admits time independent solutions for B. We have already found the explicit time dependence of $\widetilde{S}_{ab}$ is eqn. (4.11) and we can substitute that result here and use $N_{ab} \triangleq \mathcal{L}_\ell S_{ab}$ to obtain

$$\left[\widetilde{\mathcal{D}}^2 + 2\widetilde{\omega}^a \widetilde{\mathcal{D}}_a + \widetilde{\mathcal{D}}^a \widetilde{\omega}_a - \frac{1}{2}\widetilde{\mathcal{R}} + \frac{1}{2}\widetilde{q}^{ab} R_{ab} \right] B \triangleq \frac{\kappa_{(\ell')}}{\kappa_{(\ell)}} \left(\mathcal{L}_\ell \theta_{(n)} \right)_S \tag{4.18}$$

where we have assumed that the spacetime is vacuum ($R_{ab} = 0$). We have also set

$$\kappa_{(\ell)} \widetilde{S}^{(0)}_{ab} = \left(\mathcal{L}_\ell \widetilde{S}_{ab} \right)_{v=0} \tag{4.19}$$

and the expansion $\theta_{(n)}$ is defined in the usual way: $\theta_{(n)} := \widetilde{q}^{ab}\widetilde{S}_{ab}$. We have to solve eqn. (4.18) in order to find B and thereby fix the null normal ℓ uniquely. There will be a unique solution for B if the elliptic operator on the LHS of eqn. (4.18) is invertible; this will be true in the generic case.

Based on this discussion, we are now ready to list the steps required to find the preferred null normal in a numerical simulation. We assume that we are given data on a spatial slice Σ and that the apparent horizon S on Σ has been located. Denote the canonical outgoing and ingoing null normals to S by $\ell^{(0)}$ and $n^{(0)}$ respectively (see eqn. (2.1) and figure 2.1).

1. First calculate the area A_Δ of S and its angular momentum J_Δ. Here we assume that the horizon is isolated within numerical errors (use eqns. (3.8) and (3.9)) and the fact that the horizon is axisymmetric. The angular momentum is calculated using the method described in chapter 3. Using A_Δ and J_Δ, calculate the canonical value of surface gravity κ_0 using eqn. (2.55).

2. Find *some* null normal ℓ such that its surface gravity is κ_0. In general, it may not even be true that the surface gravity of the canonically defined null normal $\ell^{(0)}$ is constant; we have to find a null normal $\ell = f^{(0)}\ell^{(0)}$ for which $\kappa_{(\ell)}$ is given by eqn. (2.55). Using the transformation property of surface gravity (eqn. (2.8)), we see that the function $f^{(0)}$ is found by numerically solving the following equation

$$\mathcal{L}_\ell f^{(0)} + f\kappa_{(\ell^{(0)})} = \kappa_{(\ell)} = \kappa_0\,. \tag{4.20}$$

   Note that we do not need to solve this equation everywhere on Δ, we only want $f^{(0)}$ on S. Therefore, we only need data on three spatial slices (so that we can take centered differences to approximate time derivatives) in order to solve this equation.

3. If it turns out that $(\mathcal{L}_\ell\theta_{(n)})_S = 0$, then ℓ is the preferred null normal. However, in general, we need to solve eqn. (4.18) to find the function B at all points of S. The preferred null normal ℓ' is then given by $\ell' \triangleq f\ell$ where f is the function

$$f = 1 + Be^{-\kappa_0 v}\,. \tag{4.21}$$

   Here we have used eqn. (4.12) with $\kappa_{(\ell)} = \kappa_0$.

4. Having found ℓ' at points of S, we can then solve the geodesic equation for ℓ' to find the preferred null normal at all points of Δ.

Step 1 has already been numerically implemented in chapter 3. In the rest of this section, we shall focus on step 3 which involves solving an elliptic equation on the apparent horizon. Steps 2 and 4 require us to solve a differential equation along ℓ and have not yet been implemented numerically though we do not see any conceptual difficulties.

In order to solve eqn. (4.18), we need to calculate all the coefficients of the elliptic equation. The one form $\widetilde{\omega}_a$ on S can be calculated from the extrinsic curvature by replacing φ^a in eqn. (2.48) by an arbitrary vector ξ^a tangent to S. We will then obtain the result

$$\xi^a \omega_a \triangleq \xi^a R^b K_{ab} \,. \tag{4.22}$$

where R^b is the spacelike normal to S. This demonstrates that $\widetilde{\omega}_a = K_{\underleftarrow{a}\, b} R^b$. All the other terms on the LHS of eqn. (4.18) are uniquely determined by the two metric $\widetilde{q}_{ab}$. To calculate the RHS of eqn. (4.18), we can either calculate the time derivative of $\theta_{(n)}$ directly or alternatively, we can use eqn. (4.11) with $v = 0$ to calculate $\widetilde{S}^{(0)}_{ab}$ and hence its trace $\widetilde{q}^{\,ab}\widetilde{S}^{(0)}_{ab}$. At present, we have a working code in which all these steps have been implemented.

We want to solve eqn. (4.18) numerically on the apparent horizon assuming that we are given the metric and extrinsic curvature on spatial slices. Note that, except for the spacetime curvature R_{ab}, all other quantities in eq.(4.18) only require data on a *single* spatial slice. In vacuum, we will have $R_{ab} = 0$ so that eq.(4.18) can be solved using only the knowledge of quantities on a single spatial slice. For this purpose, eq.(4.18) can be rewritten as

$$\left[\widetilde{q}^{\,ab}\partial_a\partial_b + X^a\partial_a + F\right] B \triangleq G \tag{4.23}$$

where

$$F = \widetilde{\mathcal{D}}^a\widetilde{\omega}_a - \frac{1}{2}\widetilde{\mathcal{R}}\,, \qquad X^a = -\widetilde{q}^{\,pq}\Gamma^a_{pq} + 2\widetilde{\omega}^a \qquad \text{and} \qquad G = \mathcal{L}_{\,\ell}\theta_{(n)}\,. \tag{4.24}$$

Let us use arbitrary spherical coordinates (θ, φ) on the AH and let ∂_a be the canonical flat derivative operator in these coordinates. Then we can write $\widetilde{\mathcal{D}}_a\xi_b = \partial_a\xi_b - \Gamma^c_{ab}\xi_c$

for any one-form ξ_a and Γ^c_{ab} is uniquely determined by the two-metric $\widetilde{q}_{ab}$. In spherical coordinates, there is the well known coordinate singularity at the poles where the coordinate φ and the vector field ∂_θ are not well defined. To avoid this problem, we introduce a grid which does not include the poles as shown in figure 4.2. If $(\Delta\theta, \Delta\varphi)$ is the grid spacing in the θ and φ directions, then the grid points in the theta direction are $\theta = \Delta\theta/2, 3\Delta\theta/2, \ldots, \pi - \Delta\theta/2$ and grid points in the φ directions are $\varphi = 0, \Delta\varphi, 2\Delta\varphi, \ldots, 2\pi - \Delta\varphi$. Let (θ_j, φ_k) denote an arbitrary grid point. The range of the indices (i, j) are $j = 0 \ldots N_\theta$ and $k = 0 \ldots N_\varphi$ where $N_\theta = \pi/\Delta\theta - 2$ and $N_\varphi = 2\pi/N_\varphi$. Denote the value of any function $f(\theta, \varphi)$ at (θ_k, φ_j) by f_{jk}. We wish to approximate eq.(4.23) on this grid using finite differences.

We impose periodic boundary condition in the φ direction: $B(\theta, 0) = B(\theta, 2\pi)$. For now, exclude the points next to poles and the meridian $\varphi = 0$; consider only the points (j, k) such that $j \neq 0, N_\theta$ and $k \neq 0, N_\varphi$. At these points approximate the partial derivatives as follows:

$$\begin{aligned}
\left(\frac{\partial B}{\partial \theta}\right)_{jk} &= \frac{B_{j+1,k} - B_{j-1,k}}{2\Delta\theta} + \mathcal{O}\left(\Delta\theta^2\right), \\
\left(\frac{\partial B}{\partial \varphi}\right)_{jk} &= \frac{B_{j,k+1} - B_{j,k-1}}{2\Delta\varphi} + \mathcal{O}\left(\Delta\varphi^2\right), \\
\left(\frac{\partial^2 B}{\partial \theta^2}\right)_{jk} &= \frac{B_{j+1,k} + B_{j-1,k} - 2B_{jk}}{\Delta\theta^2} + \mathcal{O}\left(\Delta\theta^2\right), \\
\left(\frac{\partial^2 B}{\partial \varphi^2}\right)_{jk} &= \frac{B_{j,k+1} + B_{j,k-1} - 2B_{jk}}{\Delta\varphi^2} + \mathcal{O}\left(\Delta\varphi^2\right), \\
\left(\frac{\partial^2 B}{\partial \varphi \partial \theta}\right)_{jk} &= \frac{B_{j+1,k+1} + B_{j-1,k-1} - B_{j+1,k-1} - B_{j-1,k+1}}{4\Delta\theta\Delta\varphi} \\
&+ \mathcal{O}\left(\Delta\theta^2\right) + \mathcal{O}\left(\Delta\varphi^2\right).
\end{aligned} \tag{4.25}$$

Substituting these approximations into eqn. (4.23) we obtain the difference equation away from the poles and the meridian $\varphi = 0$. It is very easy to take care of the $\varphi = 0$ curve by imposing the periodic boundary condition

$$B_{j,0} = B_{j,N_\varphi}. \tag{4.26}$$

Using this boundary condition, we obtain analogues of eqn. (4.25) on the meridian $\varphi = 0$.

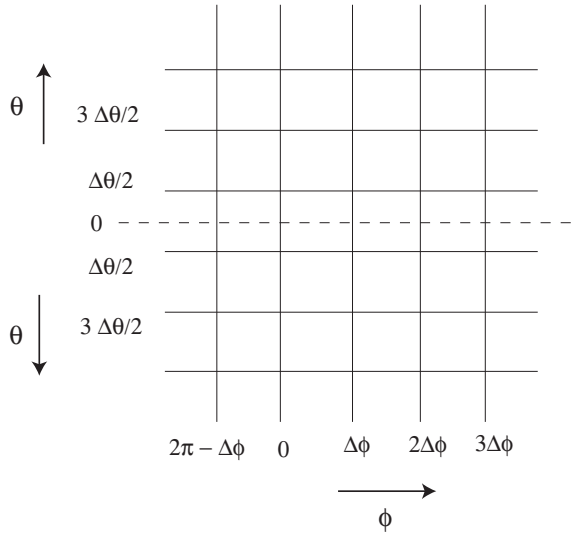

Fig. 4.2. Numerical grid on the apparent horizon used to solve the elliptic equation. In order to avoid the coordinate singularity at the poles, the grid is staggered by an amount $\Delta\theta/2$ so that the poles are not on the grid. This figure shows the grid near the north pole only.

To deal with the points near the poles, we take finite differences *across* the poles. For example:

$$\left(\frac{\partial B}{\partial \theta}\right)_{(\Delta\theta/2,\varphi)} \approx \frac{B(3\Delta\theta/2,\varphi) - B(\Delta\theta/2,\varphi+\pi)}{2\Delta\theta} \tag{4.27}$$

Assuming that N_φ is odd so that we have an even number of grid points in the φ direction, we obtain the following expressions for the partial derivatives at $\theta = \Delta\theta/2$ (we have set $M_\varphi := (N_\varphi + 1)/2$) :

$$\begin{aligned}
\left(\frac{\partial B}{\partial \theta}\right)_{0k} &= \frac{B_{1,k} - B_{0,k+M_\varphi}}{2\Delta\theta} + \mathcal{O}\left(\Delta\theta^2\right) , \\
\left(\frac{\partial B}{\partial \varphi}\right)_{0k} &= \frac{B_{0,k+1} - B_{0,k-1}}{2\Delta\varphi} + \mathcal{O}\left(\Delta\varphi^2\right) , \\
\left(\frac{\partial^2 B}{\partial \theta^2}\right)_{0k} &= \frac{B_{1,k} + B_{0,k+M_\varphi} - 2B_{0,k}}{\Delta\theta^2} + \mathcal{O}\left(\Delta\theta^2\right) , \\
\left(\frac{\partial^2 B}{\partial \varphi^2}\right)_{0k} &= \frac{B_{0,k+1} + B_{0,k-1} - 2B_{0,k}}{\Delta\varphi^2} + \mathcal{O}\left(\Delta\varphi^2\right) , \\
\left(\frac{\partial^2 B}{\partial \varphi \partial \theta}\right)_{0k} &= \frac{B_{1,k+1} + B_{0,k+M_\varphi-1} - B_{0,k-1} - B_{0,k+M_\varphi+1}}{4\Delta\theta\Delta\varphi} \\
&+ \mathcal{O}\left(\Delta\theta^2\right) + \mathcal{O}\left(\Delta\varphi^2\right) .
\end{aligned} \tag{4.28}$$

The approximations at the points $\theta = \pi - \Delta\theta/2$ will be similar and we shall not write them out. Substituting all these finite differences into eqn. (4.23), as for any elliptic equation, we end up with a matrix equation $M_{jk}B_k = G_j$ and the problem has been reduced to the inversion of the matrix M_{jk}. The numerical implementation of this scheme is work in progress and is being carried out in collaboration with Ken Smith.

4.3 Invariant foliations of the horizon

In this section we shall be concerned with the existence of preferred foliations of a non-extremal horizon. As mentioned in section 4.1, this is an important step in constructing the coordinate system in a neighborhood of Δ.

Consider a weakly isolated horizon $(\Delta, [\ell])$. The key relation we need is eqn. (2.26) which relates $d\omega$ to the area two-form ${}^2\epsilon$. In the non-rotating case ($\mathrm{Im}\,[\Psi_2] \triangleq 0$), we have $d\omega \triangleq 0$ whence ω_a is hypersurface orthogonal. Furthermore, since $\ell^a\omega_a = \kappa_{(\ell)} \neq 0$,

the surfaces orthogonal to ω_a are transverse to ℓ and must therefore be topological two-spheres. This gives the foliation in the non-rotating case. In the Schwarzschild horizon, this foliation coincides with the one given by the constant v slices in ingoing Eddington-Finkelstein coordinates.

We are interested in the more general case when $\mathrm{Im}\,[\Psi_2] \neq= 0$. Eqn. (2.26) shows that while ω_a cannot in general be projected to the base space $\widehat{\Delta}$ (see figure 2.2) because $\ell^a\omega_a \neq 0$, its curvature *can* be projected because $\ell^a {}^2\epsilon_{ab} \triangleq 0$ and also $\mathrm{Im}\,[\Psi_2]$ is constant along any $\ell \in [\ell]$. Denote the projection of $d\omega$ by $\widehat{d\omega}$:

$$\widehat{d\omega} := \pi^\star\,(d\omega) = 2\,(\mathrm{Im}\,[\Psi_2])\,{}^2\widehat{\epsilon}\,. \tag{4.29}$$

Our strategy is to now find a one-form $\widehat{\alpha}$ on $\widehat{\Delta}$ which is a potential for $\widehat{d\omega}$:

$$\widehat{d}\,\widehat{\alpha} = 2\,(\mathrm{Im}\,[\Psi_2])\,{}^2\widehat{\epsilon} \tag{4.30}$$

where $\widehat{d}$ is the exterior derivative on $\widehat{\Delta}$. If we can uniquely find $\widehat{\alpha}$, we can then pull it back to Δ to obtain a one-form α on Δ satisfying $\ell^a\alpha_a \triangleq 0$ and $\mathcal{L}_\ell\alpha \triangleq 0$. Most importantly, α and ω have the same curl: $d\omega \triangleq d\alpha$. Thus, if we define $\eta := \omega - \alpha$, then η is hypersurface orthogonal ($d\eta \triangleq 0$) and transverse to ℓ. Thus the leaves of the desired foliation are the surfaces orthogonal to η.

The issue of finding a foliation on Δ has thus been reduced to that of finding a one-form $\widehat{\alpha}$ on $\widehat{\Delta}$. To determine $\widehat{\alpha}$, use the Hodge decomposition:

$$\widehat{\alpha} = \widehat{d}\psi + \hat{\star}\,\widehat{d}\,\beta \tag{4.31}$$

where ψ and β are functions on $\widehat{\Delta}$, and $\hat{\star}$ is the Hodge dual on $\widehat{\Delta}$. In this decomposition we have used the fact that there are no Harmonic one-forms on a two-sphere.

Since the curl of ω is determined by Ψ_2, the function β is determined from eqn. (4.30) by solving a Poisson equation

$$\widehat{d}\,\widehat{\alpha} = \mathrm{div}\beta = 2\,(\mathrm{Im}\,[\Psi_2])\;{}^2\widehat{\epsilon}\,. \tag{4.32}$$

In order to determine ψ and thereby fix $\widehat{\alpha}$ uniquely, we need to impose an additional gauge condition on the divergence of $\widehat{\alpha}$

$$\widehat{d}^{\,\dagger}\widehat{\alpha} = \mathrm{div}\psi\,. \tag{4.33}$$

We shall now present two such gauge conditions. The first condition which may be called the *natural* gauge condition is to simply set $\widehat{\alpha}$ to be divergence free ($\widehat{d}^{\,\dagger}\widehat{\alpha} = 0$), which implies $\psi = 0$. While this seems to be the most natural thing to do mathematically, unfortunately, it turns out that for the rotating Kerr metric, the foliation obtained by this procedure does *not* coincide with any of the commonly used foliations of Kerr.

There is another gauge condition found by T. Pawlowski which, when applied to the Kerr metric, gives the correct result; we shall call this the *Pawlowski* gauge. To understand this gauge condition, note that there is one situation when ω can be projected to $\widehat{\Delta}$, i.e. in the extremal case when $\ell^a\omega_a \triangleq 0$. It turns out that for the extremal Kerr isolated horizon

$$\mathrm{div}\omega = -\frac{1}{3}\mathrm{div}\ln|\Psi_2|\,. \tag{4.34}$$

We can use this relation as a gauge condition for determining ψ and, remarkably, it turns out that the foliation obtained by this condition agrees with the Kerr-Schild cuts of the horizon. One might worry that if Ψ_2 vanishes at any point, then eqn. (4.34) is ill defined. While this is a valid point, we should point out that if the black hole we are considering is a perturbation of Kerr, it is highly unlikely that Ψ_2 will vanish at any point. Thus, this gauge condition probably satisfactory for most numerical work.

Chapter 5

Application to initial data sets

All numerical evolutions of spacetimes require initial data of some kind; we focus on the $3+1$ formalism wherein initial data is provided on a spacelike hypersurface. The result of the numerical evolution will depend strongly on the initial data used because the radiation present in the initial data will be included in the final gravitational waveform. It is therefore important to choose initial data sets representing astrophysically realistic situations.

One way of comparing different initial data sets is to look at the binding energy. Consider two different data sets representing approximately the same physical situation, i,e. the two black holes are roughly the same distance apart and have the same spins and same orbital angular momentum. The binding energy between the black holes is defined as $E_b = M_{\rm ADM} - M_1 - M_2$ where $M_{\rm ADM}$ is the ADM energy and M_1, M_2 are the individual masses of the black holes. Naively speaking, E_b will be made up of two parts: the first part which we call E_c will consist of the Coulombic interaction between the holes ($E_c$which will be negative) and the energy due to gravitational radiation E_r (which will be positive): $E_b = E_c + E_r$ (in general, E_b will also have a contribution from the Kinetic energy of the black holes but for now we ignore this possibility). We want our initial data to have as little radiation content as possible, therefore we want to make E_b as negative as possible. This provides a way of comparing two different initial data sets: the one with lower E_b represents the 'better' initial data. In fact, this idea has recently been applied in [18]. In this section we want to explore some aspects of binding energy from the perspective of isolated horizons. In particular, we shall use the Brill-Lindquist data as a prototype because it is one of the few situations which can be handled analytically.

5.1 The Brill-Lindquist initial data

The Brill-Lindquist initial data [19] describes a spatial slice containing an arbitrary number of non-rotating black holes. It is easy to motivate by looking at the

Schwarzschild metric in isotropic coordinates (r, θ, φ) for which the three-metric is

$$\gamma_{ab}^{(\text{Sch.})} = \left(1 + \frac{m}{2r}\right)^4 \left(\partial_a r \partial_b r + r^2 (d\Omega^2)_{ab}\right) \tag{5.1}$$

where $(d\Omega^2)_{ab} := \partial_a\theta\partial_b\theta + \sin^2\theta\partial_a\varphi\partial_b\varphi$. The extrinsic curvature of the spatial slice is zero. The topology of the spatial slice is the familiar Schwarzschild wormhole (see figure (5.1)) which is the same as $\mathbb{R}^2$ with one point removed (the puncture). In isotropic coordinates, $r = 0$ at the puncture and $r = \infty$ in the asymptotic region. Even though the metric component in equation (5.1) diverges as $r \to 0$, the coordinate transformation $r \to r' = m^2/4r$ shows that it is asymptotically flat near the puncture. This is to be expected because the puncture is just an asymptotic region in the wormhole picture.

The Brill-Lindquist initial data is a generalization of this. It is still time symmetric ($K_{ab} = 0$) and conformally flat ($\gamma_{ab} = \phi^4\delta_{ab}$ where $\delta_{ab} = \partial_a r\partial_b r + (d\Omega^2)_{ab}$). The number of punctures is equal to the number of black holes we want. In this thesis, we shall be interested in the case of two black holes. For now, let us assume that the spacetime is vacuum.

The constraint equations reduce to a Laplace equation for the function $\phi(r, \theta)$: $\nabla^2\phi = 0$ where ∇^2 is the laplacian of the flat background metric δ_{ab}. The solution to this equation is

$$\phi = 1 + \frac{\alpha_1}{|\vec{r} - \vec{r}_1|} + \frac{\alpha_2}{|\vec{r} - \vec{r}_2|} \tag{5.2}$$

where α_i $(i = 1, 2)$ are constants, $\vec{r}_i$ is the vector representing the location of the i^{th} puncture; $|\vec{r} - \vec{r}_1|$ is the Euclidean distance between a point $\vec{r}$ and the i^{th} puncture. The generalization for arbitrary number of black holes is obvious. The topology of the initial data surface consists of two separate wormholes connecting two different asymptotic regions to a common asymptotic region (see figure (5.2). For our purposes, it is more useful to think of this three-surface as $\mathbb{R}^3$ with two punctures at $\vec{r}_1$ and $\vec{r}_2$. It is convenient to put the black holes along the z-axis and to set and to introduce a new parameter $d := |\vec{r}_1 - \vec{r}_2|$. We choose to put the first black hole at the origin and the second black hole at $z = d$ on the z-axis (see figure (5.3). With these conventions, the metric with two punctures can be written as

$$\gamma_{ab} = \left(1 + \frac{\alpha_1}{r_1} + \frac{\alpha_2}{r_2}\right)^4 \left(\partial_a r \partial_b r + r^2 (d\Omega^2)_{ab}\right) \tag{5.3}$$

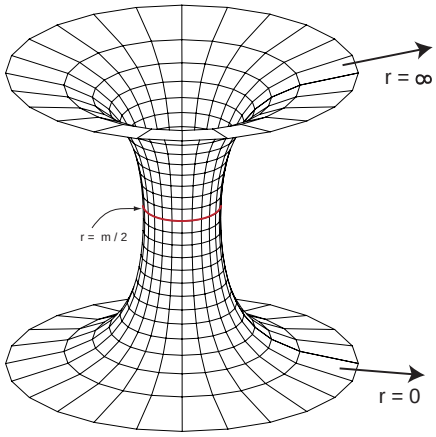

Fig. 5.1. Topology of a spatial slice in Schwarzschild spacetime; r is the radial isotropic coordinate.

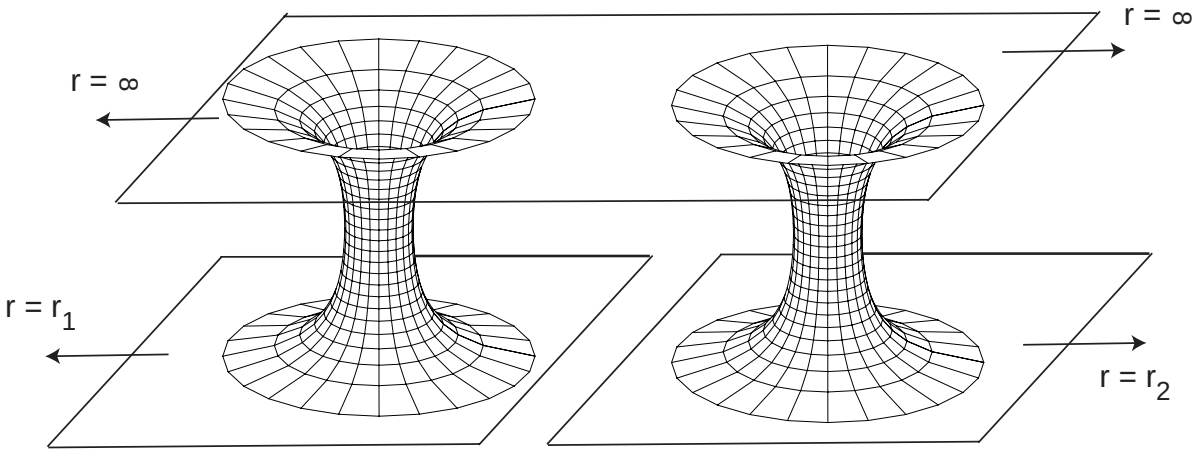

Fig. 5.2. Topology of the spatial slice in the Brill-Lindquist data with two black holes.

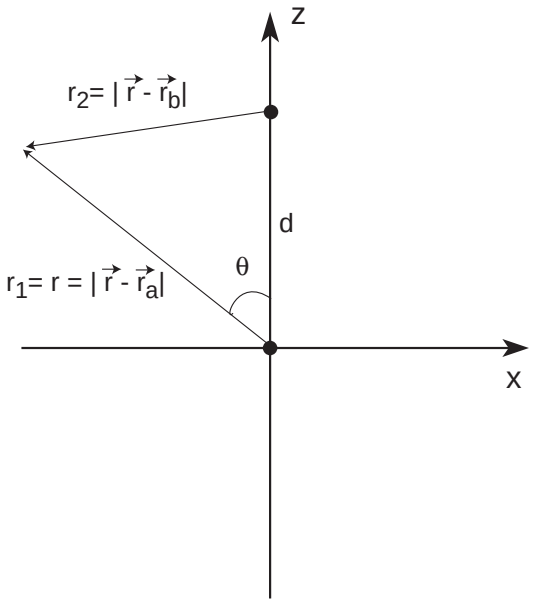

Fig. 5.3. Diagram showing the two punctures on the z-axis.

where

$$r_1 = r \qquad \text{and} \qquad r_2 = \sqrt{r^2 + d^2 - 2dr\cos\theta}\,. \tag{5.4}$$

5.2 Binding energy

5.2.1 The original Brill-Lindquist calculation

We now explore various properties of the Brill-Lindquist data. In particular, we are interested in the interaction energy between the two black holes. Let us first review the original calculation of Brill and Lindquist [19].

The first important step in this calculation is to assign a value of mass to each individual black hole. The proposal in [19] is to use the ADM mass calculated on the individual asymptotic regions as the mass $m^{(i)}_{\rm ADM}$ $(i = 1, 2)$ of the individual black holes and the ADM mass on the common asymptotic region as the total mass $M_{\rm ADM}$. Conceptually, this means that we are associating the punctures (or the asymptotic regions) with the black hole. The interaction energy is then defined to be

$$E_b := M_{\rm ADM} - m^{(1)}_{\rm ADM} - m^{(2)}_{\rm ADM}\,. \tag{5.5}$$

All these quantities can be calculated *exactly* for the metric in equation (5.3):

$$\begin{aligned} m^{(1)}_{\rm ADM} &= 2\alpha_1 + \frac{2\alpha_1\alpha_2}{d}\,, \qquad m^{(2)}_{\rm ADM} = 2\alpha_2 + \frac{2\alpha_1\alpha_2}{d}\,, \\ M_{\rm ADM} &= 2\alpha_1 + 2\alpha_2\,. \end{aligned} \tag{5.6}$$

We shall mostly focus on the case when

$$\epsilon_1 := \frac{\alpha_1}{d} \ll 1 \qquad \text{and} \qquad \epsilon_2 := \frac{\alpha_2}{d} \ll 1\,. \tag{5.7}$$

The notation $\mathcal{O}(\epsilon^n)$ will be used to denote terms which are n^{th} order in ϵ_1 and ϵ_2. Eqn. (5.6) then leads to following expression for E_b in the limit when d is large compared to both α_1 and α_2:

$$E_b = -\frac{4\alpha_1\alpha_2}{d} = -\frac{m_1 m_2}{d} + \mathcal{O}\left(\epsilon^2\right)\,. \tag{5.8}$$

The leading term reproduces the Newtonian result and the higher order terms give the relativistic corrections. It is not difficult to obtain the exact expression for E_b, but for now we only need the leading order term.

This calculation can also be repeated for the case when the black holes have charge and we obtain the result

$$E_b = -\frac{m_1 m_2}{d} + \frac{q_1 q_2}{d} + \mathcal{O}\left(\epsilon^2\right) \tag{5.9}$$

where q_i is the charge of the individual black holes calculated at infinity in the appropriate asymptotic regions. This calculation again reproduces the expected non-relativistic result.

5.2.2 The isolated horizon calculation

While the calculation presented above reproduces the Newtonian result in the correct limit, there remain some open questions in this approach:

1. The parameter d is the distance between the two punctures measured in the fictitious flat background metric. The *physical* distance between the two punctures measured using the actual three-metric in equation (5.3) is infinite because the conformal factor diverges at the punctures. We expect the distance between the black holes to be finite and to appear in the denominator in the formula for binding energy (equation 5.8). Therefore, it seems inconsistent to take the punctures to represent the black holes.

2. Why should we take the ADM masses m_i to represent the mass of the individual black holes? It is clear that m_1 and m_2, since they are the ADM masses, will include contributions from the radiation present near the punctures. Is this physically correct? It is also worth noting that the result in equation (5.6) is an exact result. It is true for all values of d; in particular it is true even when the two black holes are very close to each other and even when the two punctures are surrounded by a common apparent horizon. Should we be able to assign separate masses to the individual black holes even in such situations?

We would like to see if the isolated horizon framework can help us better understand some aspects of this situation. Since we expect the isolated horizon framework to be valid if the black holes are far apart, we shall again assume that $\epsilon \ll 1$. As discussed in the previous chapter, an isolated horizon is very closely related with the world tube of apparent horizons; in particular, an apparent horizon is a cross-section of a NEH. Therefore, motivated by isolated horizons, we would like to base our calculations on properties of apparent horizons instead of the punctures. One advantage of this is that

there exist initial data sets (e.g. Misner data [20, 21]) in which each black hole does not have separate asymptotic regions; there are only two common asymptotic regions. For these cases, the ADM approach is not sufficient. The apparent horizon approach will still be valid.

Our procedure for calculating binding energy is: (i) verify that the shear of the outward null-normal vanishes upto numerical errors; (ii) If the horizon is isolated, then use the procedure of chapter 3 to calculate J_Δ and M_Δ; (iii) The binding energy is then defined as

$$E_b := M_{\rm ADM} - M_\Delta^{(1)} - M_\Delta^{(2)} \tag{5.10}$$

which is the same definition as used by Brill and Lindquist except that the ADM masses for the individual holes have been replaced by the isolated horizon masses. Before presenting the results of the calculation for the Brill-Lindquist data set, we mention some general issues regarding binding energy between black holes in general relativity.

In the far limit, we expect eqn. (5.10) to reproduce the Newtonian formula (equation (5.8)) with d replaced by the physical distance d_Δ between the two apparent horizons, i.e. the shortest distance between the two apparent horizons as measured by the full three-metric. However, as the following argument shows, while we shall indeed reproduce the Newtonian result, there is really nothing sacrosanct about the $m_1 m_2/d$ form of the binding energy.

Consider a spacetime containing two black holes as shown in figure 5.4. There is now well defined way to assign a value to the distance between the two black holes between in the full spacetime; the metric is Lorentzian so that there is no minimum length geodesic between two points. It is also not clear if there is an invariant way in the full spacetime to demarcate the two black holes in what is, after all, a single smooth surface (the 'pair of pants'). These concepts make sense only for a given spatial surface on which the distance between the black holes is the shortest distance between the apparent horizons. It is immediately clear that the concept of distance between the two black holes is then highly dependent on how we choose the spatial slices. For example, in figure 5.4 we show two spatial surfaces (Σ and Σ') which are the same everywhere except in a small region between the black holes. The distance between the two cross-sections of the horizon is different in the two surfaces. The binding energy defined in equation (5.10) is however the same because Σ and Σ' are the same near the black holes and at infinity whence all the terms in equation (5.10) are the same for the two surfaces.

Another point worth emphasizing again is the conceptual difference between the ADM calculation in equation (5.5) and the isolated horizon calculation in equation (5.10). The isolated horizon calculation, as emphasized earlier, is only valid when the black holes are very far apart. The ADM calculation on the other hand, is valid at all values of d; even when the two punctures are surrounded by a common AH S as in figure 5.5. Each puncture is also surrounded by a outer-marginally-trapped surface S_1 and S_2, i.e. these are surfaces for which the outgoing null normal is expansion free and the ingoing null normal has negative expansion, but it is not the outermost surface with these properties. An observer in region I will see a single black hole and will not be aware of the presence of S_1 and S_2. Such an observer will not assign any binding energy to the system. If the common AH S has small shear, then the isolated horizon formula for M_Δ can be applied. The difference $M_{\rm ADM} - M_\Delta$ will then quantify the amount of radiation present outside S. An observer in region II will be in a very different situation. He or she will observe two trapped surfaces in a very dynamical regime so that the isolated horizon formulae will probably not be applicable. This observer can still calculate $m^{(1)}_{\rm ADM}$ and $m^{(2)}_{\rm ADM}$ and assign a binding energy for the system. This shows that the isolated horizon calculation gives the correct result in the regime where we expect the notion of binding energy to be valid and is not applicable in other regimes. The ADM calculation gives the same result exact in all regimes including those situations where we do not trust the notion of binding energy.

Let us now give the results of the calculation. Our first task is to find the location of the apparent horizons for the Brill-Lindquist data set. The details are given in appendix B; here we shall just quote the result of the calculation. We find that upto third order in α_i/d, the location of the apparent horizon is given by:

$$\begin{aligned} r = h_3(\theta) &= \alpha_1 - \frac{\alpha_1\alpha_2}{d} + \frac{\alpha_1\alpha_2}{d^2}\left(\alpha_2 - \alpha_1\cos\theta\right) \\ &- \frac{\alpha_1\alpha_2}{d^3}\left(\alpha_2^2 - 3\alpha_1\alpha_2\cos\theta + \frac{5}{7}\alpha_1^2 P_2(\cos\theta)\right) . \end{aligned} \tag{5.11}$$

The subscript 3 indicates that the true horizon is located at $r = h(\theta) = h_3(\theta) + \mathcal{O}(\epsilon^4)$.

With the location of the apparent horizon at hand, we can now proceed to calculate the binding energy. First, to check that the black holes are isolated, we must calculate the shear. It turns out that the shear for the surface in equation (5.11) vanishes at least upto $\mathcal{O}(\epsilon^3)$ which means that the shear of the true apparent horizon also

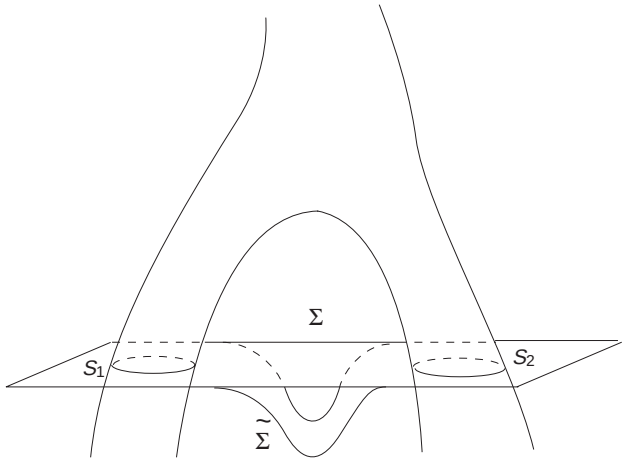

Fig. 5.4. Two different spatial hypersurfaces in a binary black hole collision.

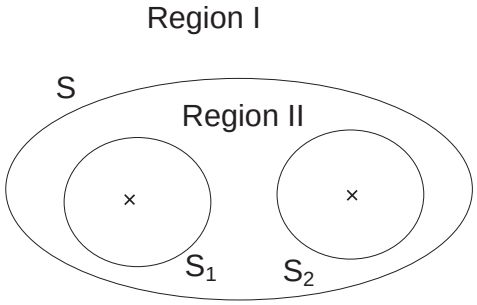

Fig. 5.5. Two punctures surrounded by a common apparent horizon S. Each puncture is also surrounded by a marginally trapped surface S_1 and S_2.

vanishes upto third order:

$$\sigma_{(\ell)} = 0 + \mathcal{O}(\epsilon^4) \tag{5.12}$$

which shows that $s = \mathcal{O}(\epsilon^8)$ (see equation (3.8)); the horizon is (instantaneously) isolated for all practical purposes (upto $\mathcal{O}(\epsilon^7)$). We have not calculated the shear for higher orders and it is possible that it vanishes at higher orders also.

The ADM mass is the same as before : $M_{\rm ADM} = 2\alpha_1 + 2\alpha_2$. The mass $M_\Delta^{(1)}$ is given by the expression

$$M_\Delta^{(1)} = 2\alpha_1 \left(1 + \frac{\alpha_2}{d}\right) + \mathcal{O}\left(\epsilon^4\right) \tag{5.13}$$

and $M_\Delta^{(2)}$ is given by an identical expression with the labels 1 and 2 interchanged. Surprisingly, at this order, $M_\Delta^{(i)}$ is the same as the mass m_i calculated using the ADM definition. The binding energy therefore evaluates to

$$E_b = M_{ADM} - M_\Delta^{(1)} - M_\Delta^{(2)} = -\frac{4\alpha_1\alpha_2}{d} + \mathcal{O}\left(\epsilon^4\right). \tag{5.14}$$

This can also be expressed in terms of $M_\Delta^{(1)}$ and $M_\Delta^{(2)}$:

$$\begin{aligned} E_b = \quad & -\frac{M_\Delta^{(1)} M_\Delta^{(2)}}{d} + \frac{M_\Delta^{(1)} M_\Delta^{(2)}}{2d^2}\left(M_\Delta^{(1)} + M_\Delta^{(2)}\right) \\ & -\frac{M_\Delta^{(1)} M_\Delta^{(2)}}{4d^3}\left((M_\Delta^{(1)})^2 + (M_\Delta^{(2)})^2 + 3M_\Delta^{(1)} M_\Delta^{(2)}\right) + \mathcal{O}\left(\epsilon^4\right). \end{aligned} \tag{5.15}$$

To leading order, this reproduces the Newtonian result. But we are not finished yet. We have to use the physical distance d_Δ between the black holes instead of the parameter d. we can easily calculate d_Δ and hence E_b upto fourth order, but here we only give the following expression:

$$d_\Delta = d\left(1 - 2\epsilon_1 \ln\epsilon_1 - 2\epsilon_2 \ln\epsilon_2 + \mathcal{O}(\epsilon^2 \ln\epsilon)\right) \tag{5.16}$$

which leads to

$$E_b = -\frac{M_\Delta^{(1)} M_\Delta^{(2)}}{d} + \mathcal{O}(\epsilon \ln\epsilon). \tag{5.17}$$

Somewhat surprisingly, the leading order corrections to the Newtonian formula are logarithmic.

Let us summarize the general method for calculating binding energy: (i) check that the shear of the outward normal of the horizons is small enough so that the isolated horizon formulae are applicable, (ii) Calculate the angular momentum using eqn. (2.48) assuming that the horizon is axisymmetric and calculate the mass M_Δ for each black hole using eqn. (2.56), (iii) calculate the ADM mass and finally, (iii) calculate the binding energy $E_b := M_{\rm ADM} - M_1 - M_2$.

5.2.3 The Newtonian force

To further study the interaction between two black holes, we present a possible way of calculation the 'force' between two black holes on a spatial slice. The idea behind this calculation is due to Jorge Pullin.

Just as in Newtonian mechanics, we would like to define the force between two black hole as the rate of change of momentum of the individual holes. We first need a definition of the linear momentum of a black hole and we propose to use the ADM formula applied at the apparent horizon S:

$$P_\Delta = \frac{1}{8\pi} \oint_S (K_{ab} - K\gamma_{ab})\, \xi^a \, d^2S^b \tag{5.18}$$

where ξ^a is a translational vector field on the spatial slice. See section 6.3 for a discussion of this formula.

The force is then defined as the Lie derivative of P_Δ along a time evolution vector field t^a. To calculate $\mathcal{L}_t P_\Delta$, we need equations (6.8) and (6.9) which describe the time evolution of the three metric and extrinsic curvature

Applying these equations to the Brill-Lindquist initial data where $K_{ab} = 0$ we obtain

$$\mathcal{L}_t P_\Delta = \frac{1}{8\pi} \oint_S \left(-N(\mathcal{R}_{ab} - \mathcal{R}\gamma_{ab}) + D_a D_b N - (D_c D^c N)\gamma_{ab}\right) \xi^a \, d^2S^b \tag{5.19}$$

The force is then defined to be $F := \mathcal{L}_t P_\Delta$. The important issues for making this calculation meaningful are (i) the choice of the lapse function N and (ii) the choice of ξ^a.

The various possible choices for ξ^a are discussed in section 6.3. There are also various possibilities for choosing N. The most naive choice would be to choose $N = 1$ but other choices are also possible. For example, we could choose N to be the 'background' value of the lapse, i.e. choose N assuming that only one black hole is present. The three

metric in the vicinity of one of the apparent horizons is then viewed as a perturbation of the three metric of a single black hole. Since the Brill-Lindquist data is motivated by the Schwarzschild metric in isotropic coordinates, the background lapse can be taken to be $N = (2r - M_\Delta)/(2r + M_\Delta)$.

Let us now give the results of the calculations. All th echoices mentioned above generically give a result of the form

$$F = k\frac{M_\Delta^{(1)} M_\Delta^{(2)}}{d} + \mathcal{O}\left(\frac{1}{d^2}\right) \tag{5.20}$$

where k is a numerical constant. Somewhat surprisingly, the choice $N = 1$ and $\xi^a = z^a$ ($z^a = (\partial_z)^a$ is just the translational Killing vector of the flat background metric) reproduces the Newtonian result ($k = 1$) at leading order. This is especially surprising because z^a is not even tangent to the inner boundary S. The other choices all lead to values of k different from unity. In particular, choosing ξ^a to be tangent to the apparent horizon leads to $k = 0$. At present, we do not know if these results are significant or whether we get similar results for other data sets.

Chapter 6

Dynamical horizons

In this chapter study generalizations of the isolated horizon framework by allowing matter fields to fall into the black hole. Our method is based on the fact that the world tube of apparent horizons is a spacelike surface in the dynamical regime and therefore the usual Hamiltonian and momentum constraints must hold on this surface. This chapter is also influenced by the work of Sean Hayward [13] who introduced the notion of *trapping horizons* for studying black hole physics. Since we rely heavily on the constraint equations, section 6.1 briefly reviews the standard initial value formulation of general relativity. Section 6.2 briefly describes the Hamiltonian methods used to derive the ADM formulae for mass and angular momentum. We point out the similarities of this method with the analysis of isolated horizon mechanics described in the earlier chapters and we also describe some subtleties regarding the ADM angular momentum [22]. These subtleties may be important in numerical computations of the ADM quantities. Section 6.3 describes the application of the initial value formulation to dynamical black holes. In particular, we discuss angular momentum, linear momentum and mass and we also obtain balance laws relating the flux of matter and radiation to change in angular momentum and mass.

6.1 The initial value formulation

This section briefly summarizes the initial value formulation of general relativity (see e.g. [23]) for the case when there are no internal boundaries. Let the spacetime $(\mathcal{M}, g_{ab})$ be foliated by spacelike three-surfaces so that it is topologically $\Sigma \times \mathbb{R}$. Let T^a denote the unit timelike normal to the surface $\Sigma_t \subset$ which represents a generic spatial slice. A general tensor $T_{a_1 \ldots a_n}{}^{b_1 \ldots b_m}$ will be said to be spatial we get zero when any of its indices is contracted with T_a or T^a. Let t^a be a time evolution vector field which is future directed and timelike (or at least transverse to Σ_t). Denote the induced metric on Σ_t by

$$\gamma_{ab} := g_{ab} + T_a T_b \tag{6.1}$$

and the extrinsic curvature K_{ab} of Σ_t by

$$K_{ab} := \gamma_a{}^c \gamma_b{}^d \nabla_c T_d \tag{6.2}$$

where ∇_a is the unique torsion-free four-dimensional derivative operator compatible with g_{ab}. In this $3+1$ decomposition, the basic variables will be γ_{ab} and K_{ab}. The induced derivative operator D_a on Σ_t compatible with q_{ab} is defined by

$$D_a \alpha_b := \gamma_a{}^c \gamma_b{}^d \nabla_c \alpha_d \tag{6.3}$$

for any spatial α_a. The Liebniz rule is then used to define the action of D_a on all other spatial tensors.

Let R_{abcd} be the four-dimensional Riemann curvature tensor: $2\nabla_{[a}\nabla_{b]}\eta_c = R_{abc}{}^d \eta_d$ for any η_c, and let R_{abcd} be the three-dimensional curvature tensor: $2D_{[a}D_{b]}\alpha_c = \mathsf{R}_{abc}{}^d \alpha_d$ for all spatial α_c. The Ricci tensors and Ricci scalars are defined in the usual way: $R_{ab} := R_{acb}{}^c$, $R := g^{ab}R_{ab}$ and similar definitions for the three-dimensional quantities R_{ab} and R. The relation between the different curvature tensors is given by the well known Gauss-Codazzi relation:

$$\mathsf{R}_{abcd} = \gamma_a{}^p \gamma_b{}^q \gamma_c{}^r \gamma_d{}^s R_{pqrs} - K_{ca}K_{bd} + K_{cb}K_{ad}\,. \tag{6.4}$$

The Einstein tensor is defined as

$$G_{ab} := R_{ab} - \frac{1}{2} R g_{ab} \tag{6.5}$$

and it is related to the stress energy tensor T_{ab} by the Einstein equation $G_{ab} = 8\pi T_{ab}$. The following important geometric identities are easily derived using the Gauss-Codazzi equation, the definition of G_{ab} and the Einstein equation:

$$\mathsf{R} + K^2 - K^{ab}K_{ab} = 16\pi T_{ab}T^a T^b =: 16\pi\rho \tag{6.6}$$

$$D^a\left(K_{ab} - K\gamma_{ab}\right) = 8\pi T_{ac}T^a q^c{}_b =: 8\pi j_b\,. \tag{6.7}$$

These equations do not contain any time derivatives and therefore constrain the three metric and extrinsic curvature of the spatial slice. Equation (6.6) is the Hamiltonian constraint while equation (6.7) is the momentum constraint. Any valid initial data set (γ_{ab}, K_{ab}) must satisfy these constraints. The constraints constitute four of the ten

Einstein equations. The remaining six equations are the evolution equations for γ_{ab} and K_{ab} which can be written in the form

$$\begin{aligned} \pounds_t \gamma_{ab} &= 2NK_{ab} + \pounds_{\vec{N}} \gamma_{ab} && (6.8) \\ \pounds_t K_{ab} &= N\gamma_a{}^m \gamma_b{}^n R_{ab} - N\mathsf{R}_{ab} + 2NK_a{}^m K_{mb} - NKK_{ab} \\ &\quad + D_a D_b N + \pounds_{\vec{N}} K_{ab} && (6.9) \end{aligned}$$

The quantities N and N^a are the lapse and shift respectively and determine the projections of the time evolution vector field t^a along the directions perpendicular and tangent to the spatial slice: $t^a = NT^a + N^a$.

6.2 The ADM mass and angular momentum

In this section we digress from the discussion of black holes and discuss the derivation of the ADM mass $M_{\rm ADM}$ and angular momentum $J_{\rm ADM}$. One reason for doing this is to again highlight how the derivation of M_Δ and J_Δ in the isolated horizon framework (section 2.4) is very similar to the ADM formalism. More importantly, we also wish to point out some subtleties which may be relevant in the numerical computation of $M_{\rm ADM}$ and $J_{\rm ADM}$. These subtleties have to do with the behavior of the expression for $M_{\rm ADM}$ and $J_{\rm ADM}$ under coordinate transformations and the choice of the background flat metric f_{ab}. These results were derived in [22].

Let us first define the phase space of general relativity for the case when no internal boundaries are present. Fix a Euclidean metric f_{ab} outside some compact region of Σ and let r be a radial coordinate of this metric. The configuration space $\mathcal{C}$ is the space of all metrics γ_{ab} which have the following fall-off at infinity:

$$\gamma_{ab} = \left(1 + \frac{M(\theta,\phi)}{r}\right) f_{ab} + \mathcal{O}\left(\frac{1}{r^2}\right) . \qquad (6.10)$$

The momentum conjugate to γ_{ab} is given by

$$p^{ab} = \sqrt{\gamma}\left(K^{ab} - K\gamma^{ab}\right) . \qquad (6.11)$$

In this case, the phase space is the cotangent bundle over the configuration space $\mathcal{C}$ and we must therefore define the action of any p^{ab} on a tangent vector of $\mathcal{C}$. A tangent vector

to $\mathcal{C}$ at any point $\gamma_{ab} \in \mathcal{C}$ is a tensor $\delta\gamma_{ab}$ whose fall off rate at infinity is

$$\delta\gamma_{ab} = \frac{M(\theta,\phi)}{r}\, f_{ab} + \mathcal{O}\left(\frac{1}{r^2}\right) . \tag{6.12}$$

Define the action of p^{ab} on $\delta\gamma_{ab}$ in the obvious way

$$p(\delta\gamma) = \int_\Sigma p^{ab}\delta\gamma_{ab}\, d^3V . \tag{6.13}$$

Using the falloff of γ_{ab}, we see that this integral will converge if

$$p^{ab} f_{ab} = \mathcal{O}\left(\frac{1}{r^3}\right) \qquad \text{and} \qquad p^{ab} - \frac{1}{3} p\, f^{ab} = \mathcal{O}\left(\frac{1}{r^2}\right) . \tag{6.14}$$

This determines the fall-off rate of p^{ab}. Therefore the phase space Γ consists of the pair (γ_{ab}, p^{ab}) satisfying these fall-off conditions. The symplectic structure is then defined as

$$\Omega_{\mathrm{ADM}}(\delta_1,\delta_2) = \frac{1}{16\pi}\int_\Sigma \left(\delta_1 p^{ab}\delta_2\gamma_{ab} - \delta_2 p^{ab}\delta_1\gamma_{ab}\right) d^3V . \tag{6.15}$$

Using this symplectic structure, we can now calculate the Hamiltonians which generate various diffeomorphisms.

Let us begin with diffeomorphisms along vector fields t^a which are asymptotic time translations, i.e. outside a compact region, $t^a = NT^a$. The Hamiltonian is defined via the relation

$$\delta H_N = \Omega_{\mathrm{ADM}}(\delta, \delta_t) \tag{6.16}$$

where δ_t is the vector field on phase space corresponding to diffeomorphisms along t^a. A direct calculation leads to the result

$$H_N(q,p) = \frac{1}{16\pi}\oint_{\partial\Sigma} N(\partial_a\gamma_{bc} - \partial_b\gamma_{ac}) f^{ac}\, dS^b \tag{6.17}$$

where ∂_a is the derivative operator compatible with δ_{ab} and $\partial\Sigma$ is the two-sphere at infinity. The ADM mass is defined to be the value of H_N for $N = 1$. This is the natural normalization at infinity. We were not able to use this procedure at the horizon because there T^a is not tangent to the horizon and therefore does not preserve the phase space; we had to use the null normals to define time evolution. To find the right scaling of the null normals, we had to use a more complicated procedure using the Kerr as reference points in phase space in order to derive equation (2.56) for M_Δ.

In a similar way, we can obtain a formula for the ADM three-momentum if we assume that outside a compact region of Σ, $t^a = \xi^a$ where ξ^a is a translational Killing vector field vector field of f_{ab} and we will get the result

$$P_{\mathrm{ADM}}(\xi) = \frac{1}{8\pi} \oint_{\partial\Sigma} \xi^b (K_{ab} - K\gamma_{ab})\, dS^b \,. \tag{6.18}$$

At this point, one might naively conclude that the formula for ADM angular momentum would be

$$J_{\mathrm{ADM}} = \frac{1}{8\pi} \oint_{\partial\Sigma} \phi^b (K_{ab} - K\gamma_{ab})\, dS^b \tag{6.19}$$

where ϕ^b is an asymptotic rotational Killing vector of f_{ab}: $\partial_{(a}\phi_{b)} = 0$ (but ϕ^a must not be covariantly constant). However, it turns out that equation (6.19) is not correct by itself; certain ambiguities need to be removed which we now describe.

6.2.1 Supertranslation ambiguities in J_Δ

To understand the ambiguities in equation (6.19), note that the construction of the conserved quantities is tied down to a choice of the background flat metric f_{ab}. Let $x^{(i)}$ $(i = 1 \ldots 3)$ be coordinates in the asymptotic region such that f_{ab} is Euclidean

$$f_{ab} = \sum_{i=1}^{3} \partial_a x^{(i)} \partial_b x^{(i)} \,. \tag{6.20}$$

A spatial *super-translation* of these coordinates is a coordinate transformation of the form

$$x^{(i)} \to x'^{(i)} = x^{(i)} + f^{(i)}(\theta, \phi) \,. \tag{6.21}$$

Let f'_{ab} be the Euclidean metric in the new coordinates:

$$f'_{ab} = \sum_{i=1}^{3} \partial_a x'^{(i)} \partial_b x'^{(i)} \,. \tag{6.22}$$

Since the functions $f^{(i)}$ depend only on the angular variables, it is clear that $f'_{ab} - f_{ab} = \mathcal{O}(1/r)$. It follows that if $\gamma_{ab} = f_{ab} + \mathcal{O}(1/r)$ then $\gamma_{ab} = f'_{ab} + \mathcal{O}(1/r)$ and thus f'_{ab} is as good a background flat metric as f_{ab}.

How are the conserved ADM quantities affected by changing f_{ab} to f'_{ab} and ∂_a to ∂'_a? First, M_{ADM} is unaffected because $\partial_a \gamma_{bc}$ falls off as $\mathcal{O}(1/r^2)$ and dS^b diverges as

$\mathcal{O}(r^2)$. Thus changing f^{ab} by $\mathcal{O}(1/r)$ terms will not affect M_Δ. By a similar argument, $P_{\rm ADM}$ is unaffected because a translational vector ξ^a will differ from ξ'^a by $\mathcal{O}(1/r)$ terms. However, it is easy to verify explicitly that, for example, $\partial_\phi - \partial_{\phi'}$ does *not* go to zero when $r \to \infty$. The same is true for the other rotational vector fields. Thus, if there is no preferred rotational Killing vector near infinity (which would be the case, for example, if there were a *global* rotational Killing vector), then, as it stands, equation (6.19) is not well defined.

The problem with defining $J_{\rm ADM}$ arises because there are many flat metrics (or equivalently, many coordinate systems) which can serve as flat backgrounds near spatial infinity. We need to select a preferred family of metrics, related to each other by simple translations, i.e. by transformations with constant $f^{(i)}$ (see eqn. (6.21)). It can be shown [22] that this is possible if the r–θ and r–ϕ components of the three dimensional Ricci tensor R_{ab} fall-off faster than $1/r^3$, i.e.

$$\mathsf{R}_{ab} r^a \tilde{q}^b_m = \mathcal{O}\left(\frac{1}{r^4}\right) \tag{6.23}$$

where r^a is the unit normal to the constant r surfaces and $\tilde{q}^m_b := \gamma_b{}^m - r_b r^m$ is the operator which projects onto the constant r surfaces. This condition has been stated in a particular flat coordinate system for which r is the radial coordinate but it turns out to be independent of this choice: it is super-translation independent.

If equation (6.23) is satisfied, then the prescription for picking the correct family of flat metrics can be stated as follows. For every flat metric we choose, we can define a radial coordinate r and we look at the extrinsic curvature ${}^2K_{ab}$ of the constant r spheres embedded in the spatial slice Σ. In general, this tensor will fall off as

$${}^2K_{ab} = \frac{1}{r}\tilde{q}_{ab} + \mathcal{O}\left(\frac{1}{r^2}\right) . \tag{6.24}$$

The preferred family of flat metrics $\mathcal{F}$ then consists of those flat metrics for which the trace free part of ${}^2K_{ab}$ (i.e. the shear of r^a) has a faster fall-off rate:

$${}^2K_{ab} = \frac{1}{r}\tilde{q}_{ab} + \mathcal{O}\left(\frac{1}{r^3}\right) . \tag{6.25}$$

Different elements of $\mathcal{F}$ are related to each other by simple translations; super-translations would lead to $1/r^2$ terms in the above equation. Such two-spheres can be found if eqn. (6.23) is satisfied.

To summarize, if we wish to calculate the ADM angular momentum using equation (6.19), say in a numerical simulation, we first need to verify that the r–θ and r–ϕ components of the three dimensional Ricci tensor fall off at the appropriate rate (equation (6.23)) and then make sure that the radial coordinate being used is such that equation (6.25) is satisfied. For isolated horizons, since we have no flat background geometry near the horizon, and since the horizon is defined invariantly (so there is no need to find preferred two-surfaces), there are no such ambiguities in M_Δ (eqn. (2.48)).

6.2.2 Other expressions for the ADM mass

Let us now go back to the expression for ADM mass:

$$M_{\rm ADM} = \frac{1}{16\pi} \lim_{r_0 \to \infty} \oint_{r=r_0} (\partial_a \gamma_{bc} - \partial_b \gamma_{ac}) f^{ac}\, dS^b \,. \tag{6.26}$$

Let us go through the commonly used method of computing $M_{\rm ADM}$ numerically. One usually starts with a finite Cartesian grid on a spatial slice and assumes that the flat background metric is Euclidean in these Cartesian coordinates; the partial derivatives in eqn. (6.26) are then the ordinary coordinate derivatives and f^{ab} is $Diag(1,1,1)$. The above equation is then applied on an appropriately chosen spherical surface within the numerical grid.

A potential problem with this is the following: it might happen that the actual three metric on the spatial slice does not approach $Diag(1,1,1)$ but instead approaches some other flat metric, say one with non-zero off-diagonal components and possibly even one for which the metric coefficients are not constants and for which the Christoffel symbols are non-zero. In general, there is no guarantee in a numerical simulation that this will not happen. This procedure might then lead to errors which are bigger than the numerical errors themselves. It can be shown that it is unnecessary to live with such errors and there are alternative expressions for $M_{\rm ADM}$ free of these ambiguities. One such expression involves R_{ab}:

$$M_{\rm ADM} = -\frac{1}{8\pi} \oint_{\partial\Sigma} r \mathsf{R}_{ab} r^a r^b \, d^2A \,. \tag{6.27}$$

To show the equivalence of this equation with eqn. (6.26), express R_{ab} in terms of the derivatives of γ_{ab} and use the fall-off conditions on γ_{ab} and its derivatives [22].

To use this numerically we need the following steps: (i) Choose a large spherical surface S (the surface does not have to be a metric two-sphere, we could choose, say,

ellipsoidal surfaces) within the numerical grid; (ii) Set $r = \sqrt{A/4\pi}$ where A is the area of S; (iii) Calculate R_{ab} at the grid points nearest to S and (iv) Evaluate the above integral with d^2A being the natural volume measure on S. While this method requires more work than the usual procedure for calculating $M_{\rm ADM}$, it might be worthwhile in cases when one does not have very good intuition about the coordinate system being used.

There also exist other expressions for $M_{\rm ADM}$. For example the following equation uses only two-sphere fields and is derived from eqn. (6.27) by using the Gauss-Codazzi equation for the two sphere embedded within Σ:

$$M_{\rm ADM} = \frac{1}{16\pi} \oint_{\partial\Sigma} r \left({}^2R - ({}^2K)^2 + {}^2K_{ab}\, {}^2K^{ab} \right) d^2A \tag{6.28}$$

where ${}^2R$ is the Ricci scalar of the two-metric on the constant r surface and ${}^2K_{ab}$ is, as before, the extrinsic curvature of the two-surface embedded in Σ.

6.3 Application to dynamical horizons

In this section we want to go beyond the isolated horizon framework and discuss dynamical black holes. The basic framework is again to use the world tube H of apparent horizons, but now we are interested in the regime when H is *spacelike*. In this regime, as we showed in section 3.1, the area of the apparent horizons is increasing due to the flux of matter or radiation across H. The properties of H we will need are captured by the following definition of a *dynamical horizon*:

Definition: A smooth three dimensional sub-manifold H of a spacetime $(\mathcal{M}, g_{ab})$ will be said to be a dynamical horizon if

(i) H is topologically $S^2 \times \mathcal{I}$ and spacelike where $\mathcal{I}$ is an interval on the real line.

(ii) There is a preferred foliation of H by two-spheres and each leaf of this foliation is an outer-marginally-trapped-surface; i.e. the expansion $\theta_{(\ell)}$ of any outgoing null normal ℓ^a is identically zero and the expansion $\theta_{(n)}$ of any ingoing null normal n^a is negative.

(iii) All equations of motion hold at H and all matter fields satisfy the condition that $-T^a_b X^b$ is future-directed and causal for any future-directed null vector X^a.

For convenient reference, our notation for physical fields on H is summarized in table 6.1.

While the motivations behind this definition are fairly transparent from the perspective of the world tube of apparent horizons discussed in section 3.1, let us mention a few things to keep in mind. First, while we are more interested in the case when the cross sections of H are apparent horizons, i.e. $\theta(n) < 0$, the results presented below go through with very minor modifications even when $\theta_{(n)} > 0$; we only require that $\theta_{(n)} \neq 0$ on H. Secondly, a dynamical horizon is a special case of a trapping horizon defined by Sean Hayward [13]. In particular, since $\theta_{(n)}$ is negative, H is a *future* trapping horizon. Furthermore, a trapping horizon has additional conditions on the derivative $\mathcal{L}_n \theta_{(\ell)}$. When this quantity is negative (this is called an *outer* trapping horizon), the horizon is spacelike (see section 3.1 for a proof). The reason we defined dynamical horizons above instead of calling it a future-outer-trapping horizon is because we want to collect the properties of H which are important for our purposes.

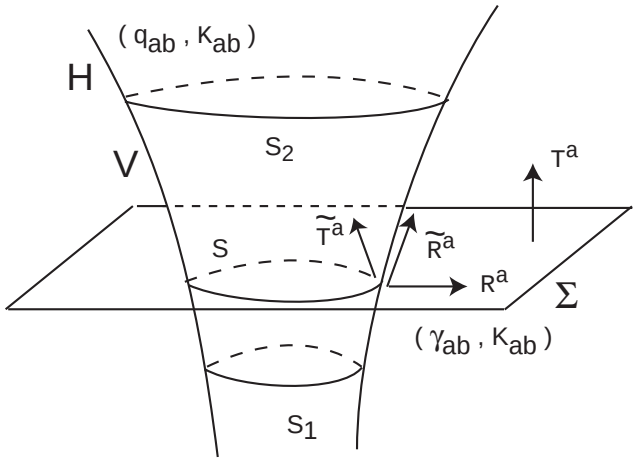

Fig. 6.1. World tube of apparent horizons in the dynamical regime. The various quantities shown here are explained in table 6.1.

Table 6.1. Summary of notation used for dynamical horizons

H	:	Dynamical horizon (world tube of apparent horizons)
S	:	Cross section of H and a member of the preferred foliation
S_1 and S_2	:	Initial and final cross-sections of H
V	:	Portion of H between S_1 and S_2
Σ	:	Spacelike partial cauchy surface ($S = \Sigma \cap H$)
$\widetilde{T}^{\,a}$	:	Unit timelike normal to H
$\widetilde{R}^{\,a}$	:	Unit spacelike vector normal to S and tangent to H
T^a	:	Unit timelike normal to Σ
R^a	:	Unit spacelike vector normal to S and tangent to Σ
ℓ^a	:	Outgoing null-normal to S ($\ell := (\widetilde{T}^{\,a} + \widetilde{R}^{\,a})/\sqrt{2}$)
n^a	:	Ingoing null normal to S ($n := (\widetilde{T}^{\,a} - \widetilde{R}^{\,a})/\sqrt{2}$)
g_{ab}	:	Spacetime four-metric
q_{ab}	:	Riemannian three-metric on H
$\widetilde{q}_{ab}$	:	Riemannian two-metric on S
γ_{ab}	:	Riemannian three-metric on Σ
∇_a	:	Spacetime derivative operator
$\mathcal{D}_a$	:	Derivative operator on H
$\widetilde{\mathcal{D}}_a$	:	Derivative operator on S
D_a	:	Derivative operator on Σ
K_{ab}	:	Extrinsic curvature of Σ
$\mathcal{K}_{ab}$	:	Extrinsic curvature of H
$\mathcal{P}_{ab}$	:	$\sqrt{q}(\mathcal{K}_{ab} - \mathcal{K}q_{ab})$
${}^2\mathcal{K}_{ab}$	:	Extrinsic curvature of S embedded in H
${}^2\sigma_{ab}$	:	Trace-free part of ${}^2\mathcal{K}_{ab}$
$\widetilde{\mathcal{K}}_{ab}$	:	Projection of $\mathcal{K}_{ab}$ onto S ($\widetilde{K}_{ab} := \widetilde{q}_a{}^c \widetilde{q}_b{}^d \mathcal{K}_{cd}$)
$\widetilde{\sigma}_{ab}$	:	Trace-free part of $\widetilde{\mathcal{K}}_{ab}$
W_a	:	Radial–angular component of $\mathcal{K}_{ab}$ ($W_a := \widetilde{q}_a{}^c \mathcal{K}_{cb} \widetilde{R}^{\,b}$)
$\sigma_{(\ell)_{ab}}$	:	Shear of ℓ ($\sigma_{(\ell)_{ab}} = (\widetilde{\sigma}_{ab} + {}^2\sigma_{ab})/\sqrt{2}$)
$\mathcal{R}_{abcd}$	:	Riemann tensor on H
$\mathcal{G}_{ab}$	:	Einstein tensor on H
$\widetilde{\mathcal{R}}_{abcd}$	:	Riemann tensor on S
R_{abcd}	:	Riemann tensor on Σ

For any physical quantity Q such as mass, angular momentum etc., which can be expressed as an integral over a section S of H, our aim is to obtain balance laws of the form

$$Q_2 - Q_1 := \oint_{S_2} (\cdots) - \oint_{S_1} (\cdots) = \int_H (\text{Flux of } Q \text{ across } V)\,. \tag{6.29}$$

The key idea for obtaining these balance equations is to use the fact that H is a spacelike surface and can therefore serve as an initial data surface. This means that just as eqns. (6.6) and (6.7) are satisfied on the Cauchy surface Σ, the following equations will hold on H:

$$\mathcal{R} + \mathcal{K}^2 - \mathcal{K}_{ab}\mathcal{K}^{ab} = 16\pi T_{ab}\widetilde{T}^a\widetilde{T}^b\,, \tag{6.30}$$

$$\mathcal{D}^a\left(\mathcal{K}_{ab} - \mathcal{K}q_{ab}\right) = 8\pi T_{ac}\widetilde{T}^a q_b{}^c\,. \tag{6.31}$$

We would like to use these constraints to obtain expressions for physical quantities relevant to the horizon. An important potential drawback of this approach is the difficulty in making contact with isolated horizons, namely, the case when H is null. This is because, the constraints on a null surface and its geometry are very different from those on a spacelike or timelike surface.

6.3.1 Angular momentum

Fix a vector field φ^a on H which is tangent to the preferred cross-sections of H. Contracting φ^a with the momentum constraint for H (equation (6.31)) and integrating over the region $V \subset H$ which is bounded by S_1 and S_2 we obtain

$$\int_V \varphi_b \mathcal{D}_a \mathcal{P}^{ab}\, d^3V = 8\pi \int_V T_{ab}\widetilde{T}^a\varphi^b\, d^3V \tag{6.32}$$

where, as before, $\mathcal{P}^{ab} := \sqrt{q}(\mathcal{K}^{ab} - \mathcal{K}q^{ab})$. Integrating by parts and using the identity $\mathcal{L}_\varphi q_{ab} = 2\mathcal{D}_{(a}\varphi_{b)}$ we obtain

$$\begin{aligned}\frac{1}{8\pi}\oint_{S_2} \mathcal{K}_{ab}\varphi^a\widetilde{R}^b\, d^2A \;-\; &\frac{1}{8\pi}\oint_{S_1} \mathcal{K}_{ab}\varphi^a\widetilde{R}^b\, d^2A \\ &= \int_V \left(T_{ab}\widetilde{T}^a\varphi^b + \frac{1}{16\pi}\mathcal{L}_\varphi q_{ab}\right) d^3V\,.\end{aligned} \tag{6.33}$$

If we identify the surface integrals with angular momentum then we get the following formula for angular momentum of an apparent horizon

$$J_S = \frac{1}{8\pi} \oint_S \mathcal{K}_{ab}\varphi^a \widetilde{R}^b \, d^2A \,. \tag{6.34}$$

The flux of angular momentum due to matter fields is identified as

$$\mathcal{F}^{(\varphi)}_{\text{matter}} = \int_V \left(T_{ab}\widetilde{T}^a \varphi^b \right) \, d^3V \tag{6.35}$$

while the flux of angular momentum due to gravitational waves is

$$\mathcal{F}^{(\varphi)}_{\text{grav.}} = \frac{1}{16\pi} \int_V \mathcal{L}_{\,\varphi} q_{ab} \, d^3V \tag{6.36}$$

and we get the balance equation

$$J_2 - J_1 = \mathcal{F}^{(\varphi)}_{\text{matter}} + \mathcal{F}^{(\varphi)}_{\text{grav.}} \,. \tag{6.37}$$

How far can we trust this result? While these equations are based upon exact identities, we must make sure that they give physically correct results in known situations. Let us first compare this with the formula for J_Δ, the angular momentum of an isolated horizon given by eqn. (2.48) which we rewrite here:

$$J_\Delta = \frac{1}{8\pi} \oint_S (\varphi^a R^b K_{ab}) \, \mathrm{d}^2V \,. \tag{6.38}$$

The difference between J_Δ and J_S obtained in eqn. (6.34) is that, as written above, J_Δ involves quantities on Σ while J_S involves quantities on H. However, we can show easily that the two are identical:

$$\begin{aligned} \mathcal{K}_{ab}\varphi^a \widetilde{R}^b &= \varphi^a \widetilde{R}^b \nabla_a \widetilde{T}_b = \varphi^a \widetilde{R}^b \nabla_a \left(\widetilde{T}_b + \widetilde{R}_b \right) = \sqrt{2}\varphi^a \widetilde{R}^b \nabla_a \ell_b \\ &= -\varphi^a n^b \nabla_a \ell_b = \varphi^a R^b \nabla_a T_b = K_{ab}\varphi^a R^b \,. \end{aligned} \tag{6.39}$$

Therefore, even though the formula for J_Δ is true when H is null and the formula for J_S is true when H is spacelike, they give the same answer. Based on this result, we can callJ_S the angular momentum of the apparent horizon S when it is axisymmetric. If φ^a is not axisymmetric, there is no reason to identify J_S with angular momentum. For the balance law eqn. (6.37) to hold, it is enough that the initial and final apparent horizons

S_1 and S_2 are axi-symmetric. In the intermediate region, H need not have any axial symmetry vector field.

To conclude this section, it is worth mentioning that, if instead of a rotational vector φ^a, we wanted to calculate the conserved quantity Q^ξ for any other vector field ξ^a, we simply replace φ^a by ξ^a in the calculations presented above:

$$Q^\xi_S = \frac{1}{8\pi} \oint_S \mathcal{P}_{ab} \xi^b \widetilde{R}^a \, d^2V \,. \tag{6.40}$$

In the rest of this chapter, we shall discuss the notions of mass and linear momentum of black holes and isolated horizons. As we shall see, unlike the case of angular momentum, the situation is more complicated for linear momentum and mass. In particular, for the angular momentum analysis, we did not even need to use the fact that H has a preferred foliation of trapped surfaces; the calculation can be carried out for any spacelike three-surface. We shall see below that we do not yet have a good understanding of linear momentum but significant progress can be made for mass and energy.

6.3.2 Linear momentum

Let us now turn our attention to linear momentum. We will first try to define the notion of linear momentum for isolated horizons and later extend it to the dynamical case. It will be useful to first briefly review *boosted black holes*.

Let us begin with the simplest possible case where the concept of a boost is best understood: Minkowski space. A boost in Minkowski space is just a Lorentz transformation of the coordinates: $(x, y, z, t) \to (x', y', z', t')$. For example, a boost in the $z-$direction is given by

$$x' = \gamma(x - Vt) \qquad \text{and} \qquad t' = \gamma(t - Vx) \tag{6.41}$$

where V is the boost parameter ($0 \leq V < 1$) and $\gamma := (1 - V^2)^{-1/2}$. In the original coordinates, it is natural to take surfaces of constant t as the spatial slices while in the boosted coordinates, it is natural to take the constant t' slices (see figure 6.2. Even though the boosted slice looks curved when viewed in the original coordinates (see figure 6.2) using a Penrose diagram, both slices are flat in the sense that the three-dimensional Riemann tensor vanishes in both cases; this will, of course, not be true for general spacelike surfaces and this feature will not be shared in curved spacetimes.

In a curved spacetime, since the only flat background metric available to us in general is the background near infinity, we can only define boosts near infinity in the general case. There is however, at least one notable exception when the metric can be expressed in a Kerr-Schild form: $g_{ab} = \eta_{ab} + 2H\ell_a\ell_b$. Here η_{ab} is a flat metric, H is a smooth function and ℓ^a is a null vector (see e.g. [24] for further details and properties of such spacetimes). If a metric can be written in this form, then we have a flat background metric η_{ab} available to us throughout the entire spacetime; we can then meaningfully talk about boosts everywhere in spacetime and not just at infinity. It is well known that all Kerr metrics can be expressed in this form and therefore we can meaningfully talk about boosting a Kerr black hole. The asymptotic properties of the boosted slices are as expected: the ADM mass of a boosted slice is γM and the magnitude of the ADM momentum is $\gamma V M$. As far as the black hole horizon is concerned, the intersection of a boosted slice with horizon (viewed as an isolated horizon Δ) leads to a different cross section of Δ as compared with the unboosted slices (see figure 6.3).

Consider, as an example, the Schwarzschild black hole in the usual ingoing Eddington-Finkelstein coordinates (v, r, θ, ϕ). It is easy to verify that constant v sections of the horizons correspond to static slices while the boosted slices lead to sections of the horizon given by level surfaces of a function $f(v, \theta, \phi)$. For a black hole with mass M, for a boost in the $z-$direction with boost parameter V_z, the function f is given by $f := f_z = v - 2MV_z \cos\theta$. Boosts in the other direction are given by the other spherical harmonics: $f_x = v - 2MV_x \sin\theta\cos\phi$ and $f_y = v - 2MV_y \sin\theta\sin\phi$.

Can we define the linear momentum of an isolated horizon in such a way that it gives the expected answers for the boosted slices? Let us explore some ideas in this direction. Motivated by the analysis of angular momentum, let us start with the momentum constraint on a spatial slice Σ:

$$D^a \left(K_{ab} - K\gamma_{ab}\right) = 8\pi j_b \tag{6.42}$$

where $j^a = T_{ac}T^a\gamma^c{}_b$ and T^a is the unit timelike normal to Σ. Let ξ^a be a vector field tangent to Σ. We should also require ξ^a to be tangent to the inner boundary $S = \Sigma \cap \Delta$ so that diffeomorphisms generated by the flow of ξ^a preserve the phase space. Contracting

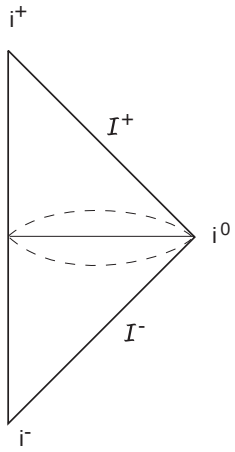

Fig. 6.2. Boosted and un-boosted spatial surfaces in Minkowski space. The solid curve represents the un-boosted slice and each point on this line is a two-sphere. The broken lines represent the boosted slice for various values of the angular coordinates.

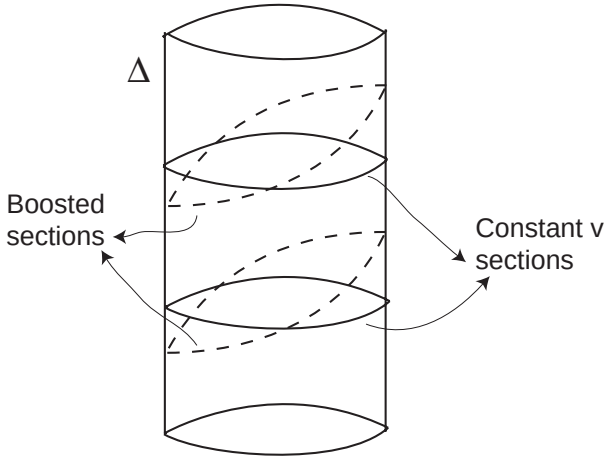

Fig. 6.3. Sections of the Schwarzschild isolated horizon showing the sections corresponding to the boosted and un-boosted slices. The solid curve represents static sections of the horizon while the broken curve represents a boosted cross-section of Δ; v is the affine parameter along ℓ in standard ingoing Eddington-Finkelstein coordinates.

the momentum constraint by ξ^a and integrating by parts, as in eqn. (6.33), we get

$$\begin{aligned}\frac{1}{8\pi}\oint_S P_{ab}\xi^a R^b\, d^2A \;\; - \;\; & \frac{1}{8\pi}\oint_{S_\infty} P_{ab}\xi^a R^b\, d^2A \\ & = \int_\Sigma \left(j_a\varphi^a + \frac{1}{16\pi}\mathcal{L}_\xi \gamma_{ab} \right) d^3V\,. \end{aligned} \tag{6.43}$$

As expected, the surface integral at infinity is the usual ADM momentum and we would like to identify the surface term at S with the linear momentum of the black hole:

$$P_S = \frac{1}{8\pi}\oint_S (K_{ab} - K\gamma_{ab})\,\xi^a\, d^2S^b \tag{6.44}$$

While for angular momentum, using the assumption of axisymmetry, we were able to select a rotational vector field on S, can we do something similar here? Clearly, while we can require a black hole to be axisymmetric, we cannot require it to be invariant under translations. However, if in certain situations, if we have some way of picking a translational vector field z^a on Σ, then we could use the projection of z^a onto S to calculate the momentum. This would happen, for example, if the three metric were conformally flat; we could then take z^a to be one of the three translational Killing vectors of the flat background metric. Alternatively, if S is axisymmetric, then there exists a function h on S such that the rotational Killing vector is given by $\varphi^a = \widetilde{\epsilon}^{ab}\partial_b h$. We can use h to define $\xi^a = \widetilde{q}^{ab}\partial_b h$ which can then be used to calculate linear momentum; this ξ^a can be regarded as a projection of the $z-$direction translational vector field onto S (we are assuming that the black hole's axis of rotation is the $z-$axis). For the Kerr black hole, these two notions give the same result, but this will not be true in general.

The above idea of using the function h to define ξ^a also seems correct from the isolated horizon viewpoint. If S is a cross-section of an isolated horizon, then from a calculation similar to eqn. (2.48) we get

$$\oint_S K_{ab}\xi^a\, d^2S^b = -\oint_S h\widetilde{\mathcal{D}}^{\,a}\widetilde{\omega}_a\, d^2S^b\,. \tag{6.45}$$

The notation used here is the same as in section 4.2. As discussed in section 4.3, we can select preferred foliations of Δ by putting conditions on $\widetilde{\mathcal{D}}^{\,a}\widetilde{\omega}_a$. The most natural condition is to set it equal to zero and the resulting foliation can be said to define the rest frame of the horizon. If S happens to be one of these preferred foliations, then the momentum will be zero as expected. For other generic slices, we will usually get a non-zero result.

While this seems very reasonable, does it give the correct answers for the boosted black holes discussed earlier? For the Schwarzschild black hole, we get $P_\Delta = MV$ for a boosted slice while for the rotating Kerr horizon, for a boost in the $z-$direction, we get $P_\Delta = V_z g(a, M)$ where $g(a, M)$ is a complicated function of the black hole parameters. The fact that we do not reproduce the ADM values is not very surprising because, in eqn. (6.43), the right hand side will not vanish even in vacuum since ξ^a is not a translational Killing vector of the three-metric. For time symmetric initial data ($K_{ab} = 0$), the momentum vanishes identically; this seems reasonable because in time symmetric data, the black holes are momentarily 'at rest'. See section 5.2 for a further test of this definition involving the notion of 'force' between two black holes.

At the present time, this definition of momentum can only be viewed as a tentative proposal. We need to see if it satisfies some of the properties that the momentum of, say a point particle satisfies. For example, we should have $P^2 < M^2$. At present, we have not been able to prove such results.

6.3.3 Dynamical mass

We now turn our attention to the Hamiltonian constraint and obtain a balance law for the energy flux across a black hole horizon. We expect the final result to be similar to the result obtained for the Bondi mass at null infinity [25]. The Bondi mass for a cross-section S of null infinity $\mathcal{I}$ is defined as:

$$M_S^{\rm Bondi} = -\frac{1}{8\pi\sqrt{2}} \oint_S \left(\Psi_2 + \sigma\dot{\bar{\sigma}}\right)\, d^2A \tag{6.46}$$

where σ is the shear of the null normal transverse to $\mathcal{I}$. The shear σ carries information about the flux of gravitational waves across null infinity and there is a balance law for the rate of change of the Bondi mass:

$$\dot{M}_S^{\rm Bondi} = -\frac{1}{8\pi\sqrt{2}} \oint_S (\dot{\sigma}\dot{\bar{\sigma}})\, d^2A\,. \tag{6.47}$$

Thus, the Weyl tensor component Ψ_2 gives the 'static' part of the mass while σ gives the flux of gravitational energy. Returning now to the black hole case, we expect the isolated horizon mass M_Δ calculated for S using eqn. (2.56) to be the static part of the energy analogous to Ψ_2. We expect the flux of energy to be given by the shear of ℓ and n. In addition we also expect matter terms to be present at the horizon.

To obtain such results for dynamical horizons, one possible strategy is to use the Hamiltonian constraint (eqn. (6.30)) on H along with the fact that H is foliated by marginally trapped surfaces (somewhat surprisingly, we did not need to use this fact for studying angular momentum). The analysis of the Hamiltonian constraint is more involved that that for angular momentum and the relevant details follow.

Start by integrating the Hamiltonian constraint on H given in eqn. (6.30):

$$\int_V \left(16\pi N T_{ab}\widetilde{T}^a\widetilde{T}^b\right)\, d^3V = \int_V N\left(\mathcal{R} + \mathcal{K}^2 - \mathcal{K}_{ab}\mathcal{K}^{ab}\right)\, d^3V \tag{6.48}$$

where N is an arbitrary positive function (the lapse) and V is the region on H bounded by S_1 and S_2 (see fig.6.1). Let us now use the fact that H is foliated by two spheres and perform a $2+1$ split of all dynamical fields on H; as before, let S denote a cross-section of H. The two metric on S is $\widetilde{q}_{ab} = q_{ab} + \widetilde{R}_a\widetilde{R}_b$ and the extrinsic curvature of S embedded in H is ${}^2\mathcal{K}_{ab} = \widetilde{q}_a{}^c\widetilde{q}_b{}^d\mathcal{D}_c\widetilde{R}_d$. We want to obtain an expression for $\mathcal{R}$ in terms of quantities on S. The curvature tensor intrinsic to S, ${}^2\mathcal{R}_{abcd}$, is given by the Gauss-Codazzi relation

$$\widetilde{\mathcal{R}}_{abcd} = \widetilde{q}_a{}^p\widetilde{q}_b{}^q\widetilde{q}_c{}^r\widetilde{q}_d{}^s\mathcal{R}_{pqrs} + 2\,{}^2\mathcal{K}_{c[a}{}^2\mathcal{K}_{b]d}\,. \tag{6.49}$$

This leads to the following expression for the scalar curvature $\widetilde{\mathcal{R}}$ on S:

$$\widetilde{\mathcal{R}} = \widetilde{q}^{\,ac}\widetilde{q}^{\,bd}\widetilde{\mathcal{R}}_{abcd} = \mathcal{R} - 2\mathcal{R}_{ab}\widetilde{R}^{\,a}\widetilde{R}^{\,b} + ({}^2\mathcal{K})^2 - {}^2\mathcal{K}_{ab}{}^2\mathcal{K}^{ab} \tag{6.50}$$

which can be rearranged to yield an expression for the Einstein tensor $\mathcal{G}_{ab} := \mathcal{R}_{ab} - \frac{1}{2}\mathcal{R}q_{ab}$ on H:

$$\mathcal{G}_{ab}\widetilde{R}^{\,a}\widetilde{R}^{\,b} = -\frac{1}{2}\left(\widetilde{\mathcal{R}} - ({}^2\mathcal{K})^2 + {}^2\mathcal{K}_{ab}{}^2\mathcal{K}^{ab}\right)\,. \tag{6.51}$$

Furthermore, from the definition of the Riemann tensor, we get

$$\begin{aligned}
\mathcal{R}_{ab}\widetilde{R}^{\,a}\widetilde{R}^{\,b} &= -\widetilde{R}^{\,a}\left(\mathcal{D}_a\mathcal{D}_b - \mathcal{D}_b\mathcal{D}_a\right)\widetilde{R}^{\,b} \\
&= \mathcal{D}_a(\widetilde{R}^{\,b}\mathcal{D}_b\widetilde{R}^{\,a} - \widetilde{R}^{\,a}\mathcal{D}_b\widetilde{R}^{\,b}) + (\mathcal{D}_a\widetilde{R}^{\,a})^2 - (\mathcal{D}_a\widetilde{R}^{\,b})(\mathcal{D}_b\widetilde{R}^{\,a}) \\
&= \mathcal{D}_a\alpha^a + ({}^2\mathcal{K})^2 - {}^2\mathcal{K}_{ab}{}^2\mathcal{K}^{ab}
\end{aligned} \tag{6.52}$$

where we have defined

$$\alpha^a := \widetilde{R}^{\,b}\mathcal{D}_b\widetilde{R}^{\,a} - \widetilde{R}^{\,a}\mathcal{D}_b\widetilde{R}^{\,b}\,. \tag{6.53}$$

Using eqns. (6.51) and (6.52) we finally arrive at the desired expression for $\mathcal{R}$:

$$\mathcal{R} = 2\left(\mathcal{R}_{ab} - \mathcal{G}_{ab}\right)\widetilde{R}^{\,a}\widetilde{R}^{\,b} = \widetilde{\mathcal{R}} + ({}^2\mathcal{K})^2 - {}^2\mathcal{K}_{ab}{}^2\mathcal{K}^{ab} + 2\mathcal{D}_a\alpha^a\,. \tag{6.54}$$

Substituting this result in eqn.(6.48) we get

$$\begin{aligned}&\int_V \left(16\pi N T_{ab}\widetilde{T}^a\widetilde{T}^b\right)\,d^3V\\ &= \int_V N\left(\widetilde{\mathcal{R}} + ({}^2\mathcal{K})^2 - {}^2\mathcal{K}_{ab}{}^2\mathcal{K}^{ab} + \mathcal{K}^2 - \mathcal{K}_{ab}\mathcal{K}^{ab} + 2\mathcal{D}_a\alpha^a\right)\,d^3V\,.\end{aligned} \tag{6.55}$$

This equation relates the flux of energy along the normal to H ($\widetilde{T}^a$) with quantities intrinsic to H. Motivated by isolated horizons, we are more interested in the flux along the outgoing normal ℓ defined in table 6.1. To obtain an expression for this flux, multiply the momentum constraint (eqn. (6.31)) by $2N\widetilde{R}^{\,a}$ and integrate over V:

$$\begin{aligned}\int_V \left(16\pi N T_{ab}\widetilde{T}^{\,a}\widetilde{R}^{\,b}\right)\,d^3V &= \int_V \left(2N\widetilde{R}^{\,b}\mathcal{D}^a(\mathcal{K}_{ab} - \mathcal{K}q_{ab})\right)\,d^3V\\ &= \int_V 2N\left(\mathcal{D}_a\beta^a - \mathcal{P}^{ab}\mathcal{D}_a\widetilde{R}_b\right)\,d^3V\end{aligned} \tag{6.56}$$

where $\beta^a := \mathcal{K}^{ab}\widetilde{R}_b - \mathcal{K}\widetilde{R}^{\,a}$ and, as before, $\mathcal{P}_{ab} = \mathcal{K}_{ab} - \mathcal{K}q_{ab}$. Adding eqns. (6.55) and (6.56) we get

$$\begin{aligned}&16\pi\int_V \left(NT_{ab}\widetilde{T}^a(\widetilde{T}^{\,b} + \widetilde{R}^{\,b})\right)\,d^3V = 16\pi\sqrt{2}\int_V \left(NT_{ab}\widetilde{T}^{\,a}\ell^b\right)\,d^3V\\ &= \int_V N\left(\widetilde{\mathcal{R}} + ({}^2\mathcal{K})^2 - {}^2\mathcal{K}_{ab}{}^2\mathcal{K}^{ab} + \mathcal{K}^2 - \mathcal{K}_{ab}\mathcal{K}^{ab} - 2\mathcal{P}^{ab}\mathcal{D}_a\widetilde{R}_b + 2\mathcal{D}_a\gamma^a\right)\,d^3V\end{aligned} \tag{6.57}$$

where $\gamma^a := \alpha^a + \beta^a$. This is the expression for the flux along ℓ^a that we need. But we are not done yet; we still need to use the fact that S is an outer marginally-trapped surface, i.e. the expansion of ℓ^a vanishes. This leads to the equation

$$0 = \theta_{(\ell)} = \frac{1}{\sqrt{2}}\widetilde{q}^{\,ab}\nabla_a\ell_b = \frac{1}{\sqrt{2}}\left({}^2\mathcal{K} + \mathcal{K} - \mathcal{K}_{ab}\widetilde{R}^{\,a}\widetilde{R}^{\,b}\right) \tag{6.58}$$

which results in the condition

$${}^2\mathcal{K} + \mathcal{K} = \mathcal{K}_{ab}\widetilde{R}^{\,a}\widetilde{R}^{\,b}\,. \tag{6.59}$$

We now have all the basic results we need: eqn. (6.57) is an expression for the energy flux along ℓ and 6.59) expresses the condition that H is foliated by marginally trapped surfaces. No assumption is made about the rest of the spacetime. We need to rewrite these equations to give results which have a clear physical interpretation. Let us first consider the case of spherical symmetry when all fields intrinsic to H are spherically symmetric.

The spherically symmetric case: In the presence of spherical symmetry, we do not expect any flux of gravitational waves across H and the change in the energy should be related only to the flux of matter fields along ℓ^a. We shall see that this is indeed what happens.

When H is spherically symmetric, the extrinsic curvatures $\mathcal{K}_{ab}$ and ${}^2\mathcal{K}_{ab}$ must be of the form

$$ {}^2\mathcal{K}_{ab} = \frac{1}{2}\,({}^2\mathcal{K})\;\widetilde{q}_{ab} \qquad \text{and} \qquad \mathcal{K}_{ab} = A\widetilde{q}_{ab} + B\widetilde{R}_a\widetilde{R}_b \tag{6.60} $$

where A and B are some spherically symmetric functions on H. Eqn. (6.59) leads to the condition ${}^2\mathcal{K} = -2A$. Substituting for the extrinsic curvatures in eqn. (6.57) and using ${}^2\mathcal{K} = -2A$ we get the remarkably simple result

$$ 16\pi\sqrt{2}\int_V N T_{ab}\widetilde{T}^{\,a}\ell^b\; d^3V = \int_V N\widetilde{\mathcal{R}}\; d^2V\,. \tag{6.61} $$

To obtain this result we have also used the fact that $\gamma_a = 0$. To prove this, note that due to spherical symmetry, γ^a must be proportional to $\widetilde{R}^{\,a}$ and it is easy to show $\gamma^a\widetilde{R}_a = 0$. This proves that $\gamma^a = 0$ in the spherically symmetric case.

We can also obtain an energy balance law using eqn. (6.61) by choosing N appropriately. First note that the metric q_{ab} on H can be written in spherical coordinates as

$$ q_{ab} = f^{-2}\mathcal{D}_a r\mathcal{D}_b r + r^2\left(\mathcal{D}_a\theta\;\mathcal{D}_b\theta + \sin^2\theta\;\mathcal{D}_a\phi\;\mathcal{D}_b\phi\right) \tag{6.62} $$

where the coordinate r is defined to be the area radius of the trapped surfaces S ($r := \sqrt{A/4\pi}$ where A is the area of S) and f is a function of r such that $\widetilde{R}_a = f^{-1}\mathcal{D}_a r$. Using the volume measure on H obtained from this metric, the integral of $\widetilde{\mathcal{R}}$ can be written as

$$ \int_V N\widetilde{\mathcal{R}} = \int_{r_1}^{r_2} dr\;\left(Nf^{-1}\oint_S r^2\widetilde{\mathcal{R}}\,d\Omega\right) = 8\pi\int_{r_1}^{r_2} dr\;Nf^{-1} \tag{6.63} $$

where we have used the Gauss-Bonnet theorem in the last step and r_1 and r_2 are the radii of the initial and final cross-sections S_1 and S_2 respectively (see fig.6.1). If we now agree to choose the lapse such that $N = f = ||dr||$, and if we define the mass of S by $M = r/2 = \sqrt{A/16\pi}$, then from eqn. (6.61) we get

$$M_2 - M_1 = \int_V T_{ab}\widetilde{T}^{\,a}\widetilde{\ell}^{\,b}\; d^3V \tag{6.64}$$

where $\widetilde{\ell}^{\,a} := \sqrt{2}N\ell$. This is the balance law we were looking for. It relates the flux of energy across the black hole to the change in mass. The definition of mass $M = \sqrt{A/16\pi}$ agrees with the definition used in non-rotating (and uncharged) isolated horizons (eqn. (2.56). In particular, it agrees with the definition used for the Schwarzschild black hole. In a lot of the numerical relativity literature, $\sqrt{A/16\pi}$ is often called the 'apparent horizon mass'. The analysis presented above justifies this terminology in the dynamical regime for spherically symmetric black holes. However, as we have already seen in section 2.4, this definition is not appropriate if the apparent horizon is a section of an isolated horizon which is not spherically symmetric. Not surprisingly, we shall see below that this is also not the appropriate definition of mass for non-spherically symmetric black holes in the non-isolated case.

The general case: Let us now turn to the general case where we do not assume the existence of any symmetries. As in the spherically symmetric case, we need to decompose the extrinsic curvatures $\mathcal{K}_{ab}$ and ${}^2\mathcal{K}_{ab}$ appropriately. Generalizing eqn. (6.60) we decompose these symmetric tensors in the following manner:

$$\begin{aligned} {}^2\mathcal{K}_{ab} &= \frac{1}{2}\,({}^2\mathcal{K})\;\widetilde{q}_{ab} + {}^2\sigma_{ab}\,, &(6.65)\\ \mathcal{K}_{ab} &= A\widetilde{q}_{ab} + \widetilde{\sigma}_{ab} + 2W_{(a}\widetilde{R}_{b)} + B\widetilde{R}_a\widetilde{R}_b\,. &(6.66) \end{aligned}$$

In these equations, A and B are arbitrary functions on H, ${}^2\sigma_{ab}$ is the trace free part of ${}^2\mathcal{K}_{ab}$, $\widetilde{\sigma}_{ab}$ is the trace free part of the projection of $\mathcal{K}_{ab}$ on S ($\widetilde{\sigma}_{ab} := \widetilde{\mathcal{K}}_{ab} - \frac{1}{2}\widetilde{\mathcal{K}}\widetilde{q}_{ab}$ where $\widetilde{\mathcal{K}}_{ab} := \widetilde{q}_a{}^c\widetilde{q}_b{}^d\mathcal{K}_{cd}$), W_a is the projection of $\mathcal{K}_{ab}\widetilde{R}^{\,b}$ onto S ($W_a := \widetilde{q}_a{}^c\mathcal{K}_{cb}\widetilde{R}^{\,b}$) and finally, as before, $B := \mathcal{K}_{ab}\widetilde{R}^{\,a}\widetilde{R}^{\,b}$. Note that if S were a section of an isolated horizon, W_a would be the projection of the one-form ω_a defined in eqn. (2.5) onto S (see also eqn. (2.48) where it is shown that $\widetilde{\omega}_a = K_{\underleftarrow{a}\,b}R^b$). It is also worth keeping in mind that, in the axisymmetric case, angular momentum is given by the integral of $W_a\varphi^a$ over S (see eqn. (6.34)).

With these decompositions, the following results are very easily verified

$$
\begin{aligned}
{}^2\mathcal{K}_{ab}{}^2\mathcal{K}^{ab} &= \frac{1}{2}({}^2\mathcal{K})^2 + {}^2\sigma_{ab}{}^2\sigma^{ab}\,, && (6.67)\\
\mathcal{K} &= 2A + B\,, && (6.68)\\
\mathcal{K}_{ab}\mathcal{K}^{ab} &= \frac{1}{2}({}^2\mathcal{K})^2 + \widetilde{\sigma}_{ab}\widetilde{\sigma}^{\,ab} + 2W_aW^{\,a} + B^2\,, && (6.69)\\
{}^2\mathcal{K} &= -2A\,. && (6.70)
\end{aligned}
$$

Eqn. (6.70) is a direct consequence of eqn. (6.59). Substituting these expressions in eqn. (6.57) we get the result

$$
\begin{aligned}
&16\pi\sqrt{2}\int_V \left(NT_{ab}\widetilde{T}^{\,a}\ell^b\right)\,d^3V = && (6.71)\\
&\int_V N\left\{\widetilde{\mathcal{R}} - 2\sigma_{(\ell)ab}\sigma^{ab}_{(\ell)} - 2W_aW^{\,a} - 2W^{\,a}\widetilde{R}^{\,b}\mathcal{D}_b\widetilde{R}_a + 2\mathcal{D}_a\gamma^a\right\}\,d^3V
\end{aligned}
$$

where $\sigma_{(\ell)ab} := ({}^2\sigma_{ab} + \widetilde{\sigma}_{ab})/\sqrt{2}$ is the shear of the outgoing null normal $\ell^a = (\widetilde{T}^{\,a} + \widetilde{R}^{\,a})/\sqrt{2}$. Let us first consider the $\mathcal{D}_a\gamma^a$ term. The vector field γ^a is given by

$$
\gamma^a = \alpha^a + \beta^a = \widetilde{R}^{\,b}\mathcal{D}_b\widetilde{R}^{\,a} - \widetilde{R}^{\,a}\mathcal{D}_b\widetilde{R}^{\,b} + \mathcal{K}^{ab}\widetilde{R}_b - \mathcal{K}\widetilde{R}^{\,a}\,. \qquad (6.72)
$$

Note that $\gamma^a\widetilde{R}_a = -{}^2\mathcal{K} + \mathcal{K}_{ab}\widetilde{R}^{\,a}\widetilde{R}^{\,b} - \mathcal{K} = 0$ because of eqn. (6.59). This shows that γ^a is tangential to S; in the spherically symmetric case, this implied that γ^a vanishes identically. In general we get

$$
\gamma^a = \gamma^b\widetilde{q}_b{}^a = \widetilde{R}^{\,b}\mathcal{D}_b\widetilde{R}^{\,a} + W^{\,a}\,. \qquad (6.73)
$$

Substituting this result in eqn. (6.71) and integrating the $\mathcal{D}_a\gamma^a$ term by parts we obtain

$$
\begin{aligned}
&16\pi\sqrt{2}\int_V \left(NT_{ab}\widetilde{T}^{\,a}\ell^b\right)\,d^3V = \int_V\left\{-2W^{\,a}\mathcal{D}_aN - 2\widetilde{R}^{\,b}(\mathcal{D}_b\widetilde{R}^{\,a})(\mathcal{D}_aN)\right\}\,d^3V\\
&+\int_V N\left\{\widetilde{\mathcal{R}} - 2\sigma_{(\ell)ab}\sigma^{ab}_{(\ell)} - 2W_aW^{\,a} - 2W^{\,a}\widetilde{R}^{\,b}\mathcal{D}_b\widetilde{R}_a\right\}\,d^3V\,. \qquad (6.74)
\end{aligned}
$$

Let us define a function h ($\mathcal{D}_ah \neq 0$) on H such that the trapped surfaces are level surfaces of h. Clearly, any smooth monotonic function of h will also suffice for our purposes. In the spherically symmetric case, it was natural to take h to be the area radius of the trapped surfaces but here, in the general case, we shall not make this restriction. There must then exist another function f such that $\widetilde{R}_a = f^{-1}\mathcal{D}_ah$ which

also implies $f = ||dh||$. Using this definition, we can obtain a useful expression for $\widetilde{R}^{\,a}\mathcal{D}_a\widetilde{R}^{\,b}$ as follows:

$$\begin{aligned}\widetilde{\mathcal{D}}_a f &:= \widetilde{q}_a{}^b\mathcal{D}_b f = \widetilde{q}_a{}^b\mathcal{D}_b\left(\mathcal{D}_c h\,\mathcal{D}^c h\right)^{1/2} = f^{-1}\widetilde{q}_a{}^b\left(\mathcal{D}^c h\right)\mathcal{D}_b\mathcal{D}_c h \\ &= f\widetilde{R}^{\,c}\mathcal{D}_c\widetilde{R}_b\,. \end{aligned} \tag{6.75}$$

This immediately gives

$$\widetilde{R}^{\,a}\mathcal{D}_a\widetilde{R}_b = \frac{\widetilde{D}_b f}{f}\,. \tag{6.76}$$

Substituting this result in eqn. (6.74), making the choice $N = f$ and rearranging terms, we finally get the important result

$$\begin{aligned}\int_V 16\pi\sqrt{2}\;NT_{ab}\widetilde{T}^{\,a}\ell^b\,d^3V \;&+\; \int_V N\left\{2\left|\sigma_{(\ell)}\right|^2 + 2\left|W+\widetilde{D}\ln N\right|^2\right\}\,d^3V \\ &= \int_V N\widetilde{\mathcal{R}}\;d^3V \end{aligned} \tag{6.77}$$

where

$$\left|\sigma_{(\ell)}\right|^2 := \sigma_{(\ell)ab}\sigma^{ab}_{(\ell)}\,, \tag{6.78}$$

and

$$\left|W+\widetilde{D}\ln N\right|^2 := \left(W_a+\widetilde{D}_a\ln N\right)\left(W^{\,a}+\widetilde{D}^{\,a}\ln N\right)\,. \tag{6.79}$$

Eqn. (6.77) is the key result of our analysis of dynamical horizons. Each term on the left hand side of this equation is manifestly positive (the T_{ab} term is positive due to the energy condition). The first term is the flux of energy due to matter fields along the outward pointing null normal ℓ^a. Denote this term by $\mathcal{F}^{(\ell)}_{\rm matter}$:

$$\mathcal{F}^{(\ell)}_{\rm matter} := \int_V 16\pi T_{ab}\widetilde{T}^{\,a}\widetilde{\ell}^{\,b}\,d^3V \tag{6.80}$$

where $\widetilde{\ell}^{\,a} := \sqrt{2}N\ell^a$. By analogy with null infinity and motivated by the discussion of section 3.1, the $|\sigma_{(\ell)}|^2$ can be interpreted as the flux of energy due to gravitational radiation. Finally, since W_a is intimately related to angular momentum, the term involving W_a and N may be interpreted as the energy in the angular momentum of the gravitational radiation flowing across the black hole. Denote both these terms together

by $\mathcal{F}^{(\ell)}_{\text{grav.}}$:

$$\begin{aligned}\mathcal{F}^{(\ell)}_{\text{grav.}} : &= \int_V N\left\{2\left|\sigma_{(\ell)}\right|^2 + 2\left|W + \widetilde{D}\ln N\right|^2\right\}\, d^3V \\ &= \int_V N\left\{2\left|\sigma_{(\ell)}\right|^2 + 2\left|\gamma\right|^2\right\}\, d^3V \end{aligned} \tag{6.81}$$

where $|\gamma|^2 := \gamma_a\gamma^a$; we have used eqn. (6.73) along with eqn. (6.76) and $N = f$ to obtain $W_a + \widetilde{D}_a \ln N = \gamma_a$. With this notation, the energy balance equation is

$$\mathcal{F}^{(\ell)}_{\text{matter}} + \mathcal{F}^{(\ell)}_{\text{grav.}} = \int_V N\widetilde{\mathcal{R}}\; d^3V\,. \tag{6.82}$$

The integral of $N\widetilde{\mathcal{R}}$ on the right hand side of this equation contains information about the black hole mass; we need an appropriate definition of mass in order to express this as a difference between the masses of S_1 and S_2.

Since $q_{ab} = \widetilde{q}_{ab} + f^{-2}\mathcal{D}_a h \mathcal{D}_b h$, the volume element d^3V on H obtained from q_{ab} can be written as $d^3V = f^{-1}dh\, d^2A = N^{-1}dh\, d^2A$ where d^2A is the area element on S obtained from $\widetilde{q}_{ab}$. Let h_1 and h_2 be the values of the function h on the initial and final cross sections S_1 and S_2 respectively. The integral of $N\widetilde{\mathcal{R}}$ can therefore be written as

$$\int_V N\widetilde{\mathcal{R}}\; d^3V = \int_{h_1}^{h_2} dr\left(\oint_S \widetilde{\mathcal{R}}\, d^2A\right) = 8\pi\,(h_2 - h_1)\;. \tag{6.83}$$

While this looks very similar to the result obtained in the spherically symmetric case, there is an important difference. While in the spherically symmetric case, we set $h = r$ (and therefore $N = ||dr||$) where r is the area radius of the horizon, we have not made that choice here. There is nothing preventing us from making this choice, and in fact this choice turns eqn. (6.83) into an explicit proof of the area increase law for dynamical horizons. However, we now argue that this is not the appropriate choice for defining black hole mass in the absence of spherical symmetry.

Consider the world tube $\mathcal{H}$ of apparent horizons and look at the general case when a portion (denoted by Δ) of this world tube is null and a part of it (called H) is spacelike; $\mathcal{H} = \Delta \cup H$ and Δ is a closed subset of $\mathcal{H}$ while H is an open subset. This situation will arise, for instance, if a dynamical horizon settles down to an isolated horizon or if matter fields or radiation falls into an isolated horizon. Assume further that this world tube of apparent horizons is axisymmetric. In the null portion, we assume the existence of a rotational vector field φ^a satisfying the conditions given in section 2.4 while in the

spacelike portion, we require the existence of a vector field φ^a which is tangent to the preferred cross-sections and is a Killing vector of the three-metric q_{ab}. Any notion of mass for the dynamical sections must reduce to the isolated horizon mass when applied to an isolated cross section, in fact there must be a smooth transition between the two regimes. In particular, they should give the same answer on the cross-section S_0 defined above. Considered as a cross section of Δ, the mass of S_0 is given by eqn. (2.56) which will not be equal to $r/2$ if the angular momentum is non-zero. This tells us that the mass of cross-sections of H cannot be taken to be $r/2$ if we want a unified description of the whole of $\mathcal{H}$. Note that in the spherically symmetric case, the choice $M = r/2$ works perfectly well for the whole of $\mathcal{H}$.

Let us conclude this chapter by briefly some work in progress describing our strategy for obtaining a mass formula for the axisymmetric case. In order to get a definition of mass we have to know what we mean by time translation at the horizon. Just as in the case of isolated horizons, we want the time translation vector at the horizon to be of the form $A\ell + \Omega\varphi$ where A and Ω are functions on H which are constant on each of the preferred cross-sections; A and Ω are function only of r. We want to choose A and Ω on each cross section such that the mass is given by the isolated horizon formula eqn. (2.56) and the difference between the mass on two infinitesimally separated cross sections is given by the first law. The balance law would then be a 'finite' version of the first law and would also include a contribution due to gravitational radiation.

Chapter 7

Conclusion and future directions

In this thesis we have presented some applications of the isolated horizon framework to numerical relativity. The main motivation behind this work is that numerical simulations of black hole spacetimes are rapidly improving and are dealing with more and more complex situations. In simple cases, very often rough ideas based on intuition gained from idealized situations are satisfactory and lead to excellent physical insight. However, there are many subtleties in the dynamical strong-field regime of general relativity and to extract physical information from numerical simulations, one needs a systematic analytic framework. In this regard, it is important to bridge the gap between the fields of mathematical and numerical relativity.

We have shown that the framework of isolated horizons can be a useful tool for studying the physics in numerical evolutions. This framework is closely related to the commonly used notion of apparent horizons and is therefore directly applicable to numerical situations. In particular, we have presented a method of calculating the mass and angular momentum of an isolated black hole in a coordinate invariant manner. To calculate angular momentum, we need to locate a symmetry vector on the horizon. We present a method for finding Killing vectors and implement it numerically. We have also implemented some ideas which are the first step in studying the local geometry of a black hole based on isolated horizons. In particular, a method for finding the preferred null normal on the horizon has been implemented. Work is in progress to implement the construction of the local coordinate system near the black hole and extract the invariant gravitational waveforms using this coordinate system.

We have applied some of these ideas to study initial data sets. In particular, we show that the isolated horizon formulae are very useful in computation of binding energy between two black holes. This would be useful in, for example, comparing different initial data sets representing roughly the same physical situation. We study the Brill-Lindquist data as a test case since this is one of the few data sets which can be handled analytically.

We have also briefly discussed some issues regarding the ADM quantities at infinity. In particular, the numerical computation of ADM angular momentum involves some subtleties and these may be relevant in numerical computations.

Finally, we have presented some ideas for understanding fully dynamical black holes. While it turns out to be remarkably easy to define angular momentum, issues regarding linear momentum and mass are more complicated. The definition of linear momentum is still unresolved but there are some promising candidates at least in certain special cases. As far as mass and energy are concerned, we have obtained a balance law relating the change in energy of the black hole with the flux of energy due to matter fields and radiation falling into the black hole. This should be useful in practical situations because all quantities in this balance law are not difficult to calculate in typical numerical simulations.

To conclude, we briefly mention another very important potential application of isolated horizons. The isolated horizon framework may also be used to construct initial data representing two (or more) black holes far away from each other. We want to specify the individual black hole spins, velocities and masses in the initial data when the two black holes are very far apart. For this purpose, the formulae for J_Δ and M_Δ would be relevant, and we may assume that the black holes will be isolated at least for a short time and will form an isolated horizon at least for an infinitesimal period of time. The isolated horizon conditions will then yield boundary conditions at the apparent horizon which can be used to solve the constraint equations on the spatial slice. Pioneering work in this direction has already been carried out by Cook [9]. In this work, Cook uses a method of solving the constraints known as the conformal thin-sandwich method. It turns out that the boundary conditions required to solve the constraints in this approach are essentially based on the assumption that the black holes are very far apart and are in equilibrium, at least momentarily. The quasi-equilibrium boundary conditions developed by Cook are identical to the isolated horizon boundary conditions in many ways. It would be interesting to see exactly how Cook's approach is related to the isolated horizon formalism.

Appendix A

Curvature scalars in the Newman-Penrose formalism

In this appendix we summarize the Newman-Penrose formalism relevant for our purposes (see e.g. [26] for a complete account). Apart from the spacetime signature which we take to be $(-,+,+,+)$, we will follow the conventions used in [26]. Consider a tetrad of null vectors n, ℓ, m and $\overline{m}$ (n and ℓ are real while m is complex) which satisfy

$$\begin{array}{rclrclrcl} n.\ell &=& -1 & n.m &=& 0 & n.\overline{m} &=& 0 \\ \ell.m &=& 0 & \ell.\overline{m} &=& 0 & m.\overline{m} &=& 1\,. \end{array} \tag{A.1}$$

The full the information contained in the connection is expressed in terms of twelve complex scalars called the Newman-Penrose spin coefficients defined as follows:

$$\begin{array}{rclrclrcl} \kappa &=& -m^a\ell^b\nabla_b\ell_a & \epsilon &=& \frac{1}{2}(\overline{m}^a\ell^b\nabla_b m_a - n^a\ell^b\nabla_b\ell_a) & \pi &=& \overline{m}^a\ell^b\nabla_b n_a \\ \sigma &=& -m^a m^b\nabla_b\ell_a & \beta &=& \frac{1}{2}(\overline{m}^a m^b\nabla_b m_a - n^a m^b\nabla_b\ell_a) & \mu &=& \overline{m}^a m^b\nabla_b n_a \\ \rho &=& -m^a\overline{m}^b\nabla_b\ell_a & \alpha &=& \frac{1}{2}(\overline{m}^a\overline{m}^b\nabla_b m_a - n^a\overline{m}^b\nabla_b\ell_a) & \lambda &=& \overline{m}^a\overline{m}^b\nabla_b n_a \\ \tau &=& -m^a n^b\nabla_b\ell_a & \gamma &=& \frac{1}{2}(\overline{m}^a n^b\nabla_b m_a - n^a n^b\nabla_b\ell_a) & \nu &=& \overline{m}^a n^b\nabla_b n_a\,. \end{array} \tag{A.2}$$

The ten independent components of the Weyl tensor are expressed in terms of five complex scalars Ψ_0, Ψ_1, Ψ_2, Ψ_3 and Ψ_4. The ten components of the Ricci tensor are defined in terms of four real and three complex scalars Φ_{00}, Φ_{11}, Φ_{22}, Λ, Φ_{10}, Φ_{20} and Φ_{21} . These scalars are defined as follows:

$$\begin{array}{rclrclrcl} \Psi_0 &=& C_{abcd}\ell^a m^b\ell^c m^d & \Phi_{01} &=& \frac{1}{2}R_{ab}\ell^a m^b & \Phi_{10} &=& \frac{1}{2}R_{ab}\ell^a\overline{m}^b \\ \Psi_1 &=& C_{abcd}\ell^a m^b\ell^c n^d & \Phi_{02} &=& \frac{1}{2}R_{ab}m^a m^b & \Phi_{20} &=& \frac{1}{2}R_{ab}\overline{m}^a\overline{m}^b \\ \Psi_2 &=& C_{abcd}\ell^a m^b\overline{m}^c n^d & \Phi_{21} &=& \frac{1}{2}R_{ab}\overline{m}^a n^b & \Phi_{12} &=& \frac{1}{2}R_{ab}m^a n^b \\ \Psi_3 &=& C_{abcd}\ell^a n^b\overline{m}^c n^d & \Phi_{00} &=& \frac{1}{2}R_{ab}\ell^a\ell^b & \Phi_{11} &=& \frac{1}{4}R_{ab}(\ell^a n^b + m^a\overline{m}^b) \\ \Psi_4 &=& C_{abcd}\overline{m}^a n^b\overline{m}^c n^d & \Phi_{22} &=& \frac{1}{2}R_{ab}n^a n^b & \Lambda &=& \frac{R}{24}\,. \end{array} \tag{A.3}$$

The allowed tetrad transformations and the corresponding transformation of the curvature tensors are given below. First consider the *spin-boost* transformation:

$$\ell \to \widetilde{\ell} = a^2 \ell\,, \qquad n \to \widetilde{n} = a^{-2} n \qquad \text{and} \qquad m \to \widetilde{m} = e^{2\imath\theta} m\,. \tag{A.4}$$

Under this transformation, the curvature scalars transform as follows:

$$\begin{array}{lllllllll}
\widetilde{\Phi}_{00} &=& a^4 \Phi_{00} & \widetilde{\Phi}_{01} &=& a^2 e^{2\imath\theta} \Phi_{01} & \widetilde{\Phi}_{02} &=& e^{4\imath\theta} \Phi_{02} \\
\widetilde{\Phi}_{11} &=& \Phi_{11} & \widetilde{\Phi}_{12} &=& a^{-2} e^{2\imath\theta} \Phi_{12} & \widetilde{\Phi}_{22} &=& a^{-4} \Phi_{22} \\
\widetilde{\Psi}_0 &=& a^4 e^{4\imath\theta} \Psi_0 & \widetilde{\Psi}_1 &=& a^2 e^{2\imath\theta} \Psi_1 & \widetilde{\Psi}_2 &=& \Psi_2 \\
\widetilde{\Psi}_3 &=& a^{-2} e^{-2\imath\theta} \Psi_3 & \widetilde{\Psi}_4 &=& a^{-4} e^{-4\imath\theta} \Psi_4\,. & & &
\end{array} \tag{A.5}$$

The *null-rotations* about ℓ are given by

$$\ell \to \widetilde{\ell} = \ell\,, \qquad m \to \widetilde{m} = m + \overline{c}\ell\,, \qquad n \to \widetilde{n} = n + cm + \overline{cm} + c\overline{c}\ell\,. \tag{A.6}$$

Under this transformation, the curvature scalars for the Ricci tensor transform as follows:

$$\begin{aligned}
\widetilde{\Phi}_{00} &= \Phi_{00}\,, \\
\widetilde{\Phi}_{01} &= \Phi_{01} + \overline{c}\Phi_{00}\,, \\
\widetilde{\Phi}_{02} &= \Phi_{02} + 2\overline{c}\Phi_{01} + \overline{c}^2\Phi_{00}\,, \\
\widetilde{\Phi}_{11} &= \Phi_{11} + c\Phi_{01} + \overline{c}\Phi_{10} + c\overline{c}\Phi_{00}\,, \\
\widetilde{\Phi}_{12} &= \Phi_{12} + c\Phi_{02} + 2\overline{c}\Phi_{11} + 2c\overline{c}\Phi_{01} + \overline{c}^2\Phi_{10} + c\overline{c}^2\Phi_{00}\,, \\
\widetilde{\Phi}_{22} &= \Phi_{22} + 2c\Phi_{12} + 2\overline{c}\Phi_{21} + c^2\Phi_{02} + 4c\overline{c}\Phi_{11} + \overline{c}^2\Phi_{20} + \\
&\qquad 2c^2\overline{c}\Phi_{01} + 2c\overline{c}^2\Phi_{10} + c^2\overline{c}^2\Phi_{00}\,.
\end{aligned} \tag{A.7}$$

The Weyl tensor components transform as:

$$\begin{aligned}
\widetilde{\Psi}_0 &= \Psi_0\,, \\
\widetilde{\Psi}_1 &= \Psi_1 + c\Psi_0\,, \\
\widetilde{\Psi}_2 &= \Psi_2 + 2c\Psi_1 + c^2\Psi_0\,, \\
\widetilde{\Psi}_3 &= \Psi_3 + 3c\Psi_2 + 3c^2\Psi_1 + c^3\Psi_0\,, \\
\widetilde{\Psi}_4 &= \Psi_4 + 4c\Psi_3 + 6c^2\Psi_2 + 4c^3\Psi_1 + c^4\Psi_0\,.
\end{aligned} \tag{A.8}$$

Appendix B

Locating the apparent horizon in the Brill-Lindquist data

When the black holes are far apart, each puncture is surrounded by an apparent horizon and when d becomes small enough, there is one common apparent horizon surrounding both punctures. The apparent horizon is defined as the closed two-surface for which the expansion $\theta_{(\ell)}$ of the outward normal ℓ (defined in equation (2.1)) is zero. This leads to the following well known equation which contains only three dimensional quantities:

$$0 = D_a R^a + K - K_{ab} R^a R^b = D_a R^a \tag{B.1}$$

where R^a is the outward normal to the two-surface we are trying to find and we have used the fact that the extrinsic curvature K_{ab} is identically zero for the Brill-Lindquist data.

Thus we have to find a surface whose unit normal is divergence free. We focus on the apparent horizon surrounding the origin. Since the metric is axisymmetric, we may assume that the apparent horizon is axisymmetric as well. Let the surface S be given by a level surface of a function $f(r,\theta) = r - h(\theta)$ and let us also assume without any loss of generality that $f = 0$ at the surface S. The unit normal to S is then

$$R^a = \frac{(df)^a}{||df||} = \frac{r}{\phi^2\sqrt{r^2 + h_\theta^2}} \left(\frac{\partial}{\partial r} - \frac{h_\theta}{r^2} \frac{\partial}{\partial \theta} \right)^a \tag{B.2}$$

where h_θ denotes the derivative of $h(\theta)$ with respect to θ. We can now calculate the divergence of R^a:

$$D_a R^a = \frac{1}{\sqrt{q}} \frac{\partial(\sqrt{q} R^\mu)}{\partial x^\mu} = \frac{1}{\sqrt{q}} \left\{ \frac{\partial}{\partial r} \left(\frac{\phi^4 r^3 \sin\theta}{\sqrt{r^2 + h_\theta^2}} \right) - \frac{\partial}{\partial \theta} \left(\frac{\phi^4 r h_\theta \sin\theta}{\sqrt{r^2 + h_\theta^2}} \right) \right\} .$$

The apparent horizon equation (eq.(B.1)) becomes

$$\frac{\partial}{\partial\theta}\left(\frac{\phi^4 r h_\theta \sin\theta}{\sqrt{r^2+h_\theta^2}}\right)_{r=h(\theta)} = \frac{\partial}{\partial r}\left(\frac{\phi^4 r^3 \sin\theta}{\sqrt{r^2+h_\theta^2}}\right)_{r=h(\theta)} . \tag{B.3}$$

We substitute the condition $r = h(\theta)$ only after all the derivatives are taken. This will lead to a highly non-linear second-order ODE for $h(\theta)$ which will be of the form

$$\frac{d^2h}{d\theta^2} + F(\theta, h, h_\theta; \alpha_1, \alpha_2, d) = 0\,.$$

The function F and thus the equation itself is parameterized by α_1, α_2 and d. We want to find a solution to this equation perturbatively in powers of $1/d$. Strictly speaking, since $1/d$ is not dimensionless, it is not a valid perturbation parameter; we should instead use $\epsilon_1 := \alpha_1/d$ and $\epsilon_2 := \alpha_2/d$. However, just for convenience, we shall continue to use $1/d$ with the understanding that we are actually using ϵ_1 and ϵ_2. It can easily be shown that F does not diverge as $d \to \infty$ and F is analytic in $1/d$:

$$\frac{d^2h}{d\theta^2} + \sum_{n=0}^{n=\infty} \frac{G_n(\theta, h, h_\theta; \alpha_1, \alpha_2)}{d^n} = 0\,. \tag{B.4}$$

We may now truncate the equation at say the i^{th} order

$$\frac{d^2h}{d\theta^2} + F_i(\theta, h, h_\theta; \alpha_1, \alpha_2, d) = 0 \tag{B.5}$$

where

$$F_i = \sum_{n=0}^{n=i} \frac{G_n(\theta, h, h_\theta; \alpha_1, \alpha_2)}{d^n}\,. \tag{B.6}$$

Let us denote the solution to this truncated equation by $\hat{h}_i(\theta)$ and the solution to the full equation (eq.(B.4)) by $h(\theta)$. In general, these solutions may be expanded as

$$h(\theta) = \sum_{n=0}^{n=\infty} \frac{A_n(\theta)}{d^n} \qquad \text{and} \qquad \hat{h}_i(\theta) = \sum_{n=0}^{n=\infty} \frac{A_{i,n}(\theta)}{d^n}\,. \tag{B.7}$$

It is not difficult to see that the truncated solution $\hat{h}_i(\theta)$ will agree with $h(\theta)$ upto the i^{th} order so that $A_{i,n} = A_n$ for $i \le n$. Therefore $h_i = \hat{h}_i + \mathcal{O}(1/d^{i+1})$ where h_i is the

partial sum

$$h_i(\theta) = \sum_{n=0}^{n=i} \frac{A_n(\theta)}{d^n}\,. \tag{B.8}$$

Thus the general solution $h(\theta)$ can be found by solving the truncated equations to find $\hat{h}_i(\theta)$ which we shall now do for $i = 0, 1, 2, 3$. We will need the expansion of $\phi(r, \theta)$:

$$\begin{aligned}\phi(r,\theta) &= 1 + \frac{\alpha_1}{d} + \frac{\alpha_2}{\sqrt{r^2 + d^2 - 2dr\cos\theta}} \\ &= \left(1 + \frac{\alpha_1}{r}\right) + \frac{\alpha_2}{d} + \frac{\alpha_2 r}{d^2}\cos\theta + \frac{\alpha_2 r^2}{2d^3}\left(3\cos^2\theta - 1\right) + \mathcal{O}\left(\frac{1}{d^4}\right)\,. \end{aligned}\tag{B.9}$$

Solution to $\mathcal{O}(1)$: At the lowest order, $\phi = \phi_0 + \mathcal{O}(1/d)$ where $\phi_0(r, \theta) = 1 + \alpha_1/r$ which is spherically symmetric. This implies that the apparent horizon is spherically symmetric at this order i.e. h_0 is independent of θ and we can thus set $h_\theta = 0$ in eq.(B.3) and get

$$\frac{\partial}{\partial r}\left(r^2\phi^4\right)_{r=h_0} = \mathcal{O}\left(\frac{1}{d}\right) \implies \frac{\partial}{\partial r}\left(r\phi_0^2\right)_{r=h_0} = \mathcal{O}\left(\frac{1}{d}\right)\,. \tag{B.10}$$

This leads to

$$0 = \frac{\partial}{\partial r}\left(r\phi_0^2\right)_{r=\hat{h}_0} = \frac{\partial}{\partial r}\left(r\left(1 + \frac{\alpha_1}{r}\right)^2\right)_{r=\hat{h}_0} = 1 - \frac{\alpha_1^2}{(\hat{h}_0)^2} \tag{B.11}$$

which implies that to lowest order, the apparent horizon is at $r = h_0 = \alpha_1$.
Solution to order $\mathcal{O}(1/d)$: At this order, $\phi = \phi_1 + \mathcal{O}(1/d^2)$ where

$$\phi_1(r,\theta) = 1 + \frac{\alpha_1}{r} + \frac{\alpha_2}{d}\,. \tag{B.12}$$

Since $\phi(r, \theta)$ is spherically symmetric at this order, the apparent horizon is spherically symmetric even at $\mathcal{O}(1/d)$ i.e. A_1 is independent of θ. As before, eq.(B.3) reduces to

$$\frac{\partial}{\partial r}\left(r\phi_1^2\right)_{r=h_1} = \mathcal{O}\left(\frac{1}{d^2}\right) \tag{B.13}$$

which, using eq.(B.12), is truncated to

$$0 = \frac{\partial}{\partial r}\left(r\left(1 + 2\frac{\alpha_1}{r} + 2\frac{\alpha_2}{d} + \frac{\alpha_1^2}{r^2} + 2\frac{\alpha_1\alpha_2}{rd}\right)\right)_{r=\hat{h}_1} = 1 + \frac{2\alpha_2}{d} - \frac{\alpha_1^2}{(\hat{h}_1)^2} \tag{B.14}$$

which implies that upto $\mathcal{O}(1/d)$, the apparent horizon is located at

$$r = h_1 = \alpha_1 - \frac{\alpha_1\alpha_2}{d}\,. \tag{B.15}$$

Solution to $\mathcal{O}(1/d^2)$: At this order $\phi = \phi_2 + \mathcal{O}(1/d^3)$ where

$$\phi_2(r,\theta) = 1 + \frac{\alpha_1}{r} + \frac{\alpha_2}{d} + \frac{\alpha_2 r}{d^2}\cos\theta\,. \tag{B.16}$$

Since $\phi_2(r,\theta)$ and therefore the metric is not spherically symmetric at this order, $A_2(\theta)$ will not be independent of θ. Since $h(\theta) = h_2(\theta) + \mathcal{O}(1/d^3)$ and also it is only the $1/d^2$ part of $h_2(\theta)$ which depends on θ, it follows that $h_\theta = \mathcal{O}(1/d^2)$. Therefore, in eq.(B.3) we can neglect the h_θ^2 terms and put $h_\theta = A_2'(\theta)/d^2$ to obtain

$$\frac{1}{d^2}\frac{\partial}{\partial\theta}\left(\phi^4\sin\theta\frac{dA_2}{d\theta}\right)_{r=h_2} = \frac{\partial}{\partial r}\left(r^2\phi^4\sin\theta\right)_{r=h_2} + \mathcal{O}\left(\frac{1}{d^3}\right)\,. \tag{B.17}$$

Since $\phi(r,\theta)$ depends on θ only in the second order, it is clear that we can take $\phi(r,\theta)$ outside the derivative in the LHS of eq.(B.17) and just evaluate it at $r = h_0 = \alpha_1$. Since $\phi(h_1,\theta) = 2 + \mathcal{O}(1/d)$ the equation reduces to

$$\frac{16}{d^2}\frac{1}{\sin\theta}\frac{d}{d\theta}\left(\sin\theta\frac{dA_2}{d\theta}\right) = \frac{\partial}{\partial r}\left(r^2\phi_2^4\right)_{r=h_2} + \mathcal{O}\left(\frac{1}{d^3}\right)\,. \tag{B.18}$$

We now need to evaluate the RHS of this equation

$$\frac{\partial}{\partial r}\left(r^2\phi_2^4\right)_{r=h_2} = \frac{\partial}{\partial r}\left(r^2\phi_2^4\right)_{r=h_1} + (h_2 - h_1)\frac{\partial^2}{\partial r^2}\left(r^2\phi_2^4\right)_{r=h_1}\,. \tag{B.19}$$

It is rather straightforward but somewhat tedious to show

$$\begin{aligned}
\frac{\partial^2}{\partial r^2}\left(r^2\phi_2^4\right)_{r=h_1} &= 16 + \mathcal{O}\left(\frac{1}{d}\right)\,,\\
\frac{\partial}{\partial r}\left(r^2\phi_2^4\right)_{r=h_1} &= \frac{16\alpha_1\alpha_2}{d^2}\left(3\alpha_1\cos\theta - \alpha_2\right) + \mathcal{O}\left(\frac{1}{d^3}\right)\,.
\end{aligned} \tag{B.20}$$

Furthermore, using $h_2 - h_1 = A_2/d^2$, eq.(B.18) is truncated to

$$\frac{1}{\sin\theta}\frac{d}{d\theta}\left(\sin\theta\frac{dA_2}{d\theta}\right) - A_2 = 3\alpha_1^2\alpha_2\cos\theta - \alpha_1\alpha_2^2\,. \tag{B.21}$$

The unique solution to this equation (which is just a inhomogeneous Legendre equation) can be found by putting $A_2(\theta) = B_1 + B_2 \cos\theta$ and solving for the coefficients B_1 and B_2. This leads to the result $A_2(\theta) = \alpha_1\alpha_2(\alpha_2 - \alpha_1\cos\theta)$. Thus to $\mathcal{O}(1/d^2)$, the apparent horizon is located at

$$r = h_2(\theta) = \alpha_1 - \frac{\alpha_1\alpha_2}{d} + \frac{\alpha_1\alpha_2}{d^2}\left(\alpha_2 - \alpha_1\cos\theta\right) . \tag{B.22}$$

Solution to $\mathcal{O}(1/d^3)$: At this order $\phi = \phi_3 + \mathcal{O}(1/d^3)$ where

$$\phi_3(r,\theta) = \left(1 + \frac{\alpha_1}{r}\right) + \frac{\alpha_2}{d} + \frac{\alpha_2 r}{d^2}\cos\theta + \frac{\alpha_2 r^2}{2d^3}\left(3\cos^2\theta - 1\right) . \tag{B.23}$$

Since $h_\theta^2 = \mathcal{O}(1/d^4)$, we can neglect the h_θ^2 terms in eq.(B.3):

$$\frac{1}{\sin\theta}\frac{\partial}{\partial\theta}\left(\phi^4 h_\theta \sin\theta\right)_{r=h_3} = \frac{\partial}{\partial\theta}\left(r^2\phi^4\right)_{r=h_3} + \mathcal{O}\left(\frac{1}{d^4}\right) . \tag{B.24}$$

Since $h_3 = h_2 + A_3/d^3$, we get the following expression for h_θ

$$h_\theta = \frac{\alpha_1^2\alpha_2}{d^2}\sin\theta + \frac{1}{d^3}\frac{dA_3}{d\theta} + \mathcal{O}\left(\frac{1}{d^4}\right) . \tag{B.25}$$

Since $h_\theta = \mathcal{O}(1/d^2)$, we only need ϕ to $\mathcal{O}(1/d)$ in the LHS of eq.(B.24) and we can in fact just evaluate ϕ_1 at $r = h_1 = \alpha_1 - \alpha_1\alpha_2/d$ which yields

$$\phi^4(h_3,\theta) = 16 + \frac{64\alpha_2}{d} + \mathcal{O}\left(\frac{1}{d^2}\right) . \tag{B.26}$$

Thus eq.(B.24) becomes

$$\left(16 + \frac{64\alpha_2}{d}\right)\frac{1}{\sin\theta}\frac{d}{d\theta}\left(\frac{\alpha_1^2\alpha_2}{d^2}\sin^2\theta + \frac{\sin\theta}{d^3}\frac{dA_3}{d\theta}\right) = \frac{\partial}{\partial r}\left(r^2\phi_3^4\right)_{r=h_3} + \mathcal{O}\left(\frac{1}{d^4}\right) . \tag{B.27}$$

It can also be shown that

$$\begin{aligned}\frac{\partial}{\partial\, r}\left(r^2\phi_3^4\right)_{r=h_3} = \quad & \frac{32\alpha_1^2\alpha_2}{d^2}\cos\theta + \frac{16}{d^3}\left(\alpha_1\alpha_2^3 - \alpha_1^2\alpha_2^2\cos\theta + 5\alpha_1^3\alpha_2 P_2(\cos\theta)\right) \\ & + \frac{16A_3}{d^3} + \mathcal{O}\left(\frac{1}{d^4}\right)\end{aligned} \tag{B.28}$$

where $P_2(\cos\theta) = (3\cos^2\theta - 1)/2$ is the second Legendre polynomial. Using this in eq.(B.27) and truncating to $\mathcal{O}(1/d^3)$, we get

$$\frac{1}{\sin\theta}\frac{d}{d\theta}\left(\sin\theta\frac{dA_3}{d\theta}\right) - A_3 = \alpha_1\alpha_2^3 - 9\alpha_1^2\alpha_2^2\cos\theta + 5\alpha_1^3\alpha_2 P_2(\cos\theta)\,. \tag{B.29}$$

The solution of this equation must be of the form $A_3 = B_0 + B_1\cos\theta + B_2 P_2(\cos\theta)$. Substituting this in eq.(B.29) and solving for B_i we get the location of the AH to $\mathcal{O}(1/d^3)$:

$$\begin{aligned} r = h_3(\theta) \;\; &= \;\; \alpha_1 - \frac{\alpha_1\alpha_2}{d} + \frac{\alpha_1\alpha_2}{d^2}\left(\alpha_2 - \alpha_1\cos\theta\right) \\ &\quad -\frac{\alpha_1\alpha_2}{d^3}\left(\alpha_2^2 - 3\alpha_1\alpha_2\cos\theta + \frac{5}{7}\alpha_1^2 P_2(\cos\theta)\right)\,. \end{aligned} \tag{B.30}$$

Appendix C

Schwarzschild black hole in a magnetic field

In this appendix, we want to briefly discuss the effect of magnetic fields on a black hole. We find the value of the magnetic field for which these effects become important and show that the great circle method discussed in section 3.4 gives a non-zero answer for angular momentum for these solutions.

Solutions describing Schwarzschild, Riessner-Nordström and Kerr black holes immersed in magnetic fields were found by Ernst [17]; here we shall only consider the Schwarzschild case. A Schwarzschild black hole in a magnetic field is described by the following static axi-symmetric metric

$$ds^2 = F^2 \left[-(1 - \frac{2M}{r})dt^2 + \frac{dr^2}{(1 - 2M/r)} + r^2\, d\theta^2 \right] + \frac{r^2 \sin^2\theta}{F^2}\, d\phi^2 \qquad \text{(C.1)}$$

where F is a function given by

$$F = 1 + \frac{1}{4} B_0^2 r^2 \sin^2\theta\,. \qquad \text{(C.2)}$$

The constant B_0 is the value of the magnetic field on the north and south poles of the horizon. We recover the Schwarzschild solution for $B_0 = 0$. The horizon is still located at $r = R := 2M$ but the it is no longer a constant curvature two-sphere; it is distorted. The black hole mass is M and the area of the horizon is $A_\Delta = 4\pi R^2 = 16\pi M^2$ which is the same as for the usual Schwarzschild black hole.

To quantify the distortion of the horizon, we use the scalar curvature $\widetilde{\mathcal{R}}$ of the two-metric on the horizon:

$$\widetilde{\mathcal{R}} = \frac{1}{8F^4R^2} \left(16 - 4B_0^4R^4 \cos^2\theta \sin^2\theta - B_0^4R^4 \sin^4\theta + 32B_0^2R^2 \cos^2\theta \right)\,. \qquad \text{(C.3)}$$

Let $\widetilde{\mathcal{R}}_{\max}$ and $\widetilde{\mathcal{R}}_{\min}$ be respectively the maximum and minimum values of $\widetilde{\mathcal{R}}$; define $\delta\widetilde{\mathcal{R}} := \widetilde{\mathcal{R}}_{\max} - \widetilde{\mathcal{R}}_{\min}$. Let $<\widetilde{\mathcal{R}}>$ be the average of $\widetilde{\mathcal{R}}$ over the horizon; from the Gauss-Bonnet theorem, it follows that $<\widetilde{\mathcal{R}}>= 2/R^2$. If the horizon is to be distorted by say

at least $p\%$, we would require

$$\frac{\delta\widetilde{\mathcal{R}}}{<\widetilde{\mathcal{R}}>} \geq \frac{p}{100}\,. \tag{C.4}$$

In the present case, it is easy to see that

$$\begin{aligned} \widetilde{\mathcal{R}}_{\rm max} &= \frac{2}{R^2}\left(1+2B_0^2R^2\right) \\ \widetilde{\mathcal{R}}_{\rm min} &= \frac{2}{R^2}\frac{\left(1-B_0^2R^2/4\right)}{\left(1+B_0R^2/4\right)^3} \end{aligned} \tag{C.5}$$

For general values of B_0, eqn. (C.4) leads to a quartic inequality for B_0. For astrophysical purposes, the case $B_0R \ll 1$ will be the most important case. Assuming this condition, from eqn. (C.4) we get the following inequality which is valid for small values of p:

$$B_0R \leq \frac{\sqrt{p}}{10}\,. \tag{C.6}$$

For comparing with observations, it is useful to rewrite this in c.g.s. units:

$$B_0R \geq \frac{c^2}{\sqrt{G}}\frac{\sqrt{p}}{10} \approx 3.5\times10^{24}\frac{\sqrt{p}}{10}\ \text{Gauss-cm}\,. \tag{C.7}$$

We have used the fact that in the c.g.s. system the magnetic field B_0 has dimensions of $M^{1/2}L^{-1/2}T^{-1}$ and G/c^4 has dimensions of $M^{-1}L^{-1}T^2$. If we divide both sides of eqn. (C.7) by the Schwarzschild radius of the Sun which is approximately 3 km, then we get

$$B_0M \geq \sqrt{p}\times10^{18}\,\text{Gauss} \tag{C.8}$$

where M is the mass of the black hole measured in solar masses. As an example, for a 10 solar mass black hole, a magnetic field of about 3×10^{17} Gauss would be required to distort the black hole by about 10%. We also see from this result that larger black holes are more easily distorted than smaller black holes.

To conclude this appendix, let us apply the great circle method to calculate angular momentum. The proper lengths of the equator (L_e) and the polar meridian (L_p) are

$$L_e = 2\pi R\left(1+B_0^2M^2\right)^{-1} \qquad \text{and} \qquad L_p = \pi R\left(1+B_0^2M^2\right)\,. \tag{C.9}$$

The distortion parameter $\delta = (L_e - L_p)/L_e$ (discussed in section 3.4) for small values of $B_0 M$ is given by

$$\delta = \frac{L_e - L_p}{L_e} \approx -\frac{1}{2} B_0^2 R^2 \approx \frac{1}{2} \frac{p}{100} \tag{C.10}$$

where we have used eqn. (C.7) written in geometrical units. This shows explicitly that the angular momentum calculated by this method will be non-zero for this static axi-symmetric black hole.

References

[1] A. Ashtekar, C. Beetle, O. Dreyer, S. Fairhurst, B. Krishnan, J. Lewandowski, J. Wisniewski. Generic isolated horizons and their applications. *Phys. Rev. Lett.*, 85:3564–3567, 2000.

[2] A. Ashtekar, C. Beetle and S. Fairhurst. Mechanics of isolated horizons. *Class. Quant. Grav.*, 17:253, 2000.

[3] A. Ashtekar, S. Fairhurst and B. Krishnan. Isolated horizons: Hamiltonian evolution and the first law. *Phys. Rev.*, D62:104025, 2000.

[4] A. Ashtekar, C. Beetle and J. Lewandowski. Mechanics of rotating isolated horizons. *Phys. Rev.*, D64:044016, 2001.

[5] A. Ashtekar, C. Beetle and J. Lewandowski. Geometry of generic isolated horizons. *Class. Quant. Grav*, 19.

[6] O. Dreyer, B. Krishnan, E. Schnetter and D. Shoemaker. Introduction to isolated horizons in numerical relativity. *gr-qc/0206008*.

[7] J. L. Friedman, K. Schleich and D. M. Witt. Topological censorship. *Phys. Rev. Lett.*, 71:1486–1489, 1993.

[8] R. Geroch and J.B. Hartle. Distorted black holes. *J. Math. Phys.*, 23(4):680, 1982.

[9] G.B. Cook. Corotating and irrotational binary black holes in quasi-circular orbits. *Phys. Rev.*, D65:084003, 2002.

[10] R. M. Wald. *General Relativity*. University of Chicago Press, 1984.

[11] J. Lee. *Riemannian Geometry*. Graduate texts in mathematics. Springer, 1995.

[12] I. Booth. Metric-based hamiltonians, null boundaries, and isolated horizons. *Class.Quant.Grav.*, 18:4239–4264, 2001.

[13] S. Hayward. General laws of black hole dynamics. *Phys. Rev.*, D49:6467–6474, 1994.

[14] A. Ashtekar and A. Magnon-Ashtekar. A technique for analyzing the structure of isometries. *J. Math. Phys.*, 19(7):1567–1572, 1978.

[15] R. A. Matzner, M. F. Huq, and D. Shoemaker. *Phys. Rev.*, D59:024015, 1999.

[16] L. Smarr. Surface geometry of charged rotating black holes. *Phys. Rev.*, D7:289–295, 1973.

[17] F. J. Ernst. Black holes in a magnetic universe. *J. Math. Phys.*, 17:54–56, 1976.

[18] H.P. Pfeiffer, G.B. Cook and S.A. Teukolsky. Comparing initial-data sets for binary black holes. *gr-qc/0203085*.

[19] D. Brill and R.W. Lindquist. Interaction energy in geometrostatics. *Phys. Rev.*, 131:471–476, 1963.

[20] C.W. Misner. Womhole initial conditions. *Phys. Rev.*, 118(4):1110–1111, 1959.

[21] C.W. Misner. The method of images in geometrostatics. *Ann. Phys.*, 24:102–177, 1963.

[22] A. Ashtekar and A. Magnon. From i^0 to the $3+1$ description of spatial infinity. *J. Math. Phys.*, 25:2682–2690, 1984.

[23] A. Ashtekar. *New perspectives in canonical gravity*. Bibliopolis, 1988.

[24] S. Chandrasekhar. *The Mathematical Theory of Black Holes*. Oxford University Press, 1983.

[25] E.T. Newman and K.P. Tod. Asymptotically flat spacetimes. In A. Held, editor, *General relativity and gravitation*. Plenum, 1980.

[26] J. Stewart. *Advanced General Relativity*. Cambridge University Press, 1991.

Vita

Badri Krishnan was born in New Delhi, India in 1974. He did his undergraduate and masters work at the Indian Institute of Technology (Kanpur) from 1992-97 where he obtained his integrated M.Sc. in physics. In 1997 he joined the Pennsylvania State University as a graduate student and has been a Ph.D candidate in physics for the past five years. His papers include:

A. Ashtekar, S. Fairhurst and B. Krishnan, Isolated Horizons: Hamiltonian Evolution and the First Law, *Phys. Rev.* **D62** 104025 (2000)

A. Ashtekar, C. Beetle, O. Dreyer, S. Fairhurst, B. Krishnan, J. Lewandowski and J. Wisniewski, Generic Isolated Horizons and their Applications, *Phys. Rev. Lett.* **85**, 3564-3567 (2000)

S. Fairhurst and B. Krishnan, Distorted Black Holes with Charge, *Int. J. Mod. Phys.* **D10**, 691-709 (2001)

O. Dreyer, B. Krishnan, E. Schnetter and D. Shoemaker, Isolated Horizons in Numerical Relativity, gr-qc/0206008

O. Dreyer, L. S. Finn, B. Kelly, B. Krishnan, R. Lopez-Aleman, Black Hole Spectroscopy: Testing General Relativity through Gravity Wave Observations, *in preperation*

L.S. Finn, B. Krishnan and P. Sutton, A Figure of Merit for a Gamma–Ray–Burst and Gravitational–Wave–Burst Association, *in preparation*